symmetry

MDPI

Review

Chirality in organic and mineral systems: A review of reactivity and alteration processes relevant to prebiotic chemistry and life detection missions

Carina Lee[1,4*], Jessica M. Weber[2], Laura E. Rodriguez[2], Rachel Y. Sheppard[2], Laura M. Barge[3], Eve L. Berger[3], and Aaron S. Burton[4]

[1] Lunar & Planetary Institute, Universities Space Research Association; carina.h.lee@nasa.gov
[2] NASA Jet Propulsion Laboratory, California Institute of Technology; jessica.weber@jpl.nasa.gov, laura.rodriguez@jpl.nasa.gov, rachel.y.sheppard@jpl.nasa.gov, laura.m.barge@jpl.nasa.gov
[3] Texas State University - Jacobs JETS - NASA Johnson Space Center; eve.l.berger@nasa.gov
[4] NASA Johnson Space Center; aaron.burton@nasa.gov

* Correspondence: carina.h.lee@nasa.gov; Tel.: (+1 281 483 5153)

Abstract: Chirality is a central feature in the evolution of biological systems, but the reason for biology's strong preference for specific chiralities of amino acids, sugars, and other molecules remains a controversial and unanswered question in origins of life research. Biological polymers tend toward homochiral systems, which favor the incorporation of a single enantiomer (molecules with a specific chiral configuration) over the other. There have been numerous investigations into the processes that preferentially enrich one enantiomer to understand the evolution of an early, racemic, prebiotic organic world. Chirality can also be a property of minerals; and their interaction with chiral organics is important for assessing how post-depositional alteration processes could affect the stereochemical configuration of simple and complex organic molecules. In this paper, we review the properties of organic compounds and minerals as well as the physical, chemical, and geological processes that affect organic and mineral chirality during the preservation and detection of organic compounds. We provide perspectives and discussions on the reactions and analytical techniques that can be performed in the laboratory and comment on the state of knowledge of flight-capable technologies in current and future planetary missions with a focus on organics analysis and life detection.

Keywords: chirality; homochirality; origins of life; organics; minerals; biosignatures; life detection; prebiotic chemistry; enantiomeric excess

Citation: Lee, C.; Weber, J.M..; Rodriguez, L.E. Sheppard, R.Y.; Barge, L.M.; Berger, E.L.; Burton, A.S. Chirality in organic and mineral systems: A review of reactivity and alteration processes relevant to prebiotic chemistry and life detection missions *Symmetry* **2022**, *14*, x. https://doi.org/10.3390/xxxxx

Academic Editor: Firstname Lastname

Received: date
Accepted: date
Published: date

1. Review summary

This review article aims to bring together multiple perspectives on research centered around chiral determination in organic and mineral systems with a focus towards prebiotic chemistry and origins of life. *Section 2* provides an introduction to the prebiotic chemistry field to give context and highlight the importance of understanding what chirality is and how it could have played a role in the origins of life. Included in this introduction is a brief summary and overview on the use of enantiomeric excess as a biosignature and the various hypotheses that have been proposed that led to the emergence of homochirality in biological systems.

The next part of the introduction is separated into sections that review chirality in the two systems of focus: 1) organic systems, and 2) mineral systems. *Sections 3 and 4* detail different types of organic chirality that can occur to highlight how chemical structure affects chiral properties and organic reactivity, especially in organic synthesis. This section

draws heavily from examples in the pharmaceutical industry which focuses on organic synthesis/catalysis research into asymmetric reactions. We present some examples of how chirality influences organometallic systems and their relevance to extraterrestrial materials and the origins of life. Also presented in this section is a table that provides examples of enantioselective reactions and asymmetric cross-coupling reactions relevant to various research disciplines. We summarize this section by highlighting the need to consider organic reactions within a geological framework, so that reaction products due to post-depositional geological alteration processes can be properly assessed and contextualized.

Section 5 discusses minerals that are relevant to prebiotic systems in the context of the composition of extraterrestrial bodies that may be explored during life detection missions and presents a table of the mineral and ice composition of major rocky planetary bodies in the Solar System. The chirality of mineral systems and its potential influence on organic systems and driving enantiomeric excess is discussed in *Section 6*. In particular, the section describes how mineral systems display a diverse range of chiral properties and introduces the concepts of enantiomorphic minerals, achiral minerals with chiral faces, local chiral sites, factors that influence a mineral's degree of enantioselectivity, mineral-organic interactions driving enantiomeric excess, as well as future directions for research in this field.

Section 7 of this review takes the geological context further by discussing geochemical processes involved in the preservation, alteration, and detection of organic matter as a primary and robust method for understanding the composition of primitive microorganisms as life began to evolve on Earth. In lieu of macroscopic, fossilized remains in the geological record, the study of early life involves examining molecular compositions, some of which have excellent preservation potential and can be traced back to specific organisms. *Sections 7.1-7.3* detail the reactions and processes that occur during organic preservation and how chirality–particularly the stereochemical configuration of membrane lipids–changes during sequestration into refractory phases that get preserved over geologic time. In addition to terrestrial geochemical alteration processes, in *Section 7.4* we discuss the parent body alteration processes that occur on asteroids and how the composition and chirality of organics are affected.

Section 8 summarizes analytical instrumentation and asymmetric solution phase and solid-state reactions. *Section 8.1* includes a table that documents various separation and analytical methods for determining chirality and which of these has been proposed or flown on spaceflight missions. In the solution phase reactions, we detail three of the relevant reactions to prebiotic chemistry and origins of life: reductive amination (*Section 8.2.1*), Strecker synthesis (*Section 8.2.2*), and the formose reaction (*Section 8.2.3*). In *Section 8.3* we focus on solid-state that are based on mechanochemical reactions, which have been recently shown to be viable options in the study of the origins of life. Additionally, we summarize some experimental studies on impact simulation that are directly related to the synthesis of amino acids, peptides, and molecules of prebiotic interest.

The final section of the review summarizes our recommendations for future research and discusses mission-relevant instrumentation for the analysis of organics and minerals and organic chirality (*Section 9.1*). We highlight the importance of continued instrument development (*Section 9.2*), contamination control (*Section 4.3*), and multidisciplinary collaboration (*Section 9.4*) in order to further the study of chirality in organic and mineral systems that is geared towards understanding the origins and contexts of how life evolved on Earth and where and how to find it elsewhere.

2. Prebiotic chemistry, chirality, and the origins of life

2.1 Chirality, homochirality, and enantiomeric excess

Characterizing the organic chemical composition on planetary bodies is a key component in the search for habitable environments, and evidence of extinct or extant life. The field of prebiotic chemistry focuses on how simple organic precursor compounds could have been synthesized and how they could have evolved into complex, functioning biomolecules such as nucleic acids, peptides, and proteins [1-7]. These building block precursors were likely required to carry out metabolic reactions and information storage and transfer necessary for the maintenance and replication of living organisms [8,9].

Molecules can be arranged in three-dimensional space from a single point source (i.e., at a carbon atom). When a carbon atom has four distinct functional groups attached to it (i.e., is sp^3 hybridized), the molecule can exist as one of two possible three-dimensional shapes, and that carbon atom is termed a "chiral center". Molecular chirality–or handedness–whereby a molecule is not superimposable on its mirror image, is a property that is of great interest in the field of prebiotic chemistry. Chiral molecules are optically active; that is, they rotate plane-polarized light in opposite directions depending on their chirality. Enantiomers of chiral molecules possess identical chemical and physical properties, with the exception of how they interact with other chiral molecules or electromagnetic radiation. Thus, chirality can affect various properties of important molecules such as amino acids and sugars (Figure 1), including: molecular self-assembly, asymmetric reactions/reactivity, molecular recognition and replication, light or spin polarization [10-13].

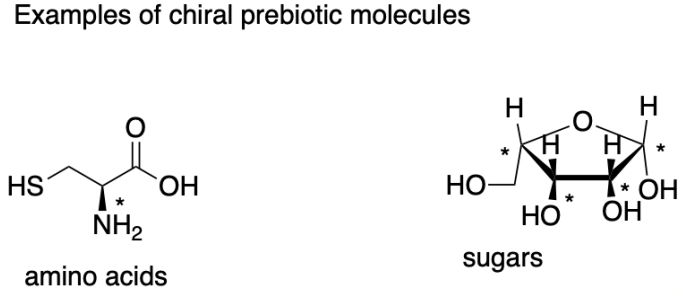

Figure 1. Amino acids and sugars are examples of chiral molecules relevant to prebiotic chemistry. The asterisk indicates the chiral carbon center(s). Left is the amino acid cysteine; right is the sugar ribose.

Homochiral polymers is a result of the preference for one enantiomer over the other; biology on Earth has evolved to use homochiral proteins and nucleic acids, which are made up of L-amino acids and D-sugars, respectively [14,15], although there are rare exceptions [16]. Notably, life generally relies on L-amino acid and D-sugar monomers for metabolic functions as well. L- and D- are stereochemical designations for discerning enantiomeric pairs of amino acids and sugars, and are described in more detail in *Section 3.1*. Without a seed (i.e., a solid catalyst or already chiral reactant) that can induce asymmetry, chemical reactions will synthesize products in racemic mixtures, i.e., an equal mix of both enantiomers. Enantiomeric excess (ee) reflects the abundance of one particular enantiomer over the other and can be determined as a ratio of the observed specific rotation of the mixture over the specific rotation of the pure enantiomer, typically calculated as ee = [(L-D)/(L+D)] x 100 [17]. For example, an enantiopure product will have 100% of one enantiomer and 0% of the other, and racemic mixtures have ee of 0%, since there is no excess of one enantiomer over the other.

2.2 Chirality in a prebiotic context

Before life arose on Earth, nucleosynthetic reactions occurring in the interstellar medium created elements which formed primitive organic compounds [18-22]. These organic compounds can be preserved in asteroids and comets and are delivered to Earth within carbonaceous chondrite meteorites [23]. Homochirality and the amplification of the enantiomeric imbalance resulting in the observed chirality of biological polymers has been hypothesized to have originated from either terrestrial or extraterrestrial processes before abiogenesis (i.e., the origins of life) or afterwards as a consequence of biological evolution [24]. Among the prebiotic hypotheses, there are theories that propose either stand alone or deterministic processes [15]. For example, the autocatalytic mathematical model developed by Frank [25] proposed that homochirality was amplified through the catalysis of a starting compound, which repeatedly synthesizes itself in one structural configuration while excluding the other [26]. Additionally amplification in terrestrial environments of ee could have occurred with the aid of chiral reactants or substrates, as this has been shown to promote the synthesis of specific enantiomers [27-29].

The effect of circularly polarized light and other energy sources such as galactic cosmic rays (GCRs) on the chirality of organics is also well studied [e.g., 14 and references therein, 30-32]. While prebiotic molecules of interest are generally synthesized in racemic mixtures, moderate abiotically-synthesized enantiomeric excesses have been measured in meteorites [14, 17 and references therein]. The organic composition of meteorites, specifically of hydroxy acids [33,34] typically show racemic composition and, in some cases of amino acids and sugar derivatives, meteoritic organics show an enantiomeric excess approaching that observed in biology [35-46].

2.3 Enantiomeric excess as a biosignature

Enantiomeric excess of organic molecules has been proposed as a biosignature based on our observations and knowledge of molecular biochemistry on Earth [17,47-49]. However, it remains to be seen whether enantiomeric excess is a robust indicator of life, given that it is unknown (1) if abiotic processes can generate significant enantiomeric excess such that it would be mistaken for a false positive for life detection; (2) whether the chemical evolution of near-homochiral polymers was required for life to evolve (if not, lack of enantiomeric excess could lead to false negatives); (3) if such chemistry is a requirement for all life or just Earth-like life; or (4) that biological systems always utilize a single enantiomer for building functional polymers. To expand on the fourth point, it remains possible for extraterrestrial life to rely on homochiral polymers of various chiralities; for example, perhaps it could use a protein composed of D-amino acids for one function and another composed of L-amino acids for another. Terrestrial life does this to some extent in that it incorporates only L-amino acids for building proteins, but uses D-amino acid monomers for various functions [50,51]; bacteria also use both D- and L-amino acids for the production of peptidoglycan [52] and some bacterial strains have even been shown to be capable of growing using D-amino acids and L-sugars [53].

Understanding the pathways and environments relevant to chirality is critical to determining how homochiral polymers evolved on Earth and how we can utilize it as a possible biosignature to look for potential life on other planetary bodies. Specifically, the origins of life and astrobiology fields aim to constrain the geochemical conditions under which primitive/abiotic racemic or slightly enantioenriched mixtures of organic molecules could have chemically evolved towards homochiral/near homochiral polymers utilized in life as we know it.

In this paper, we provide a perspective on the interaction between chirality in organic systems with minerals that are relevant in prebiotic environments. We explore geochemical reactions and scenarios, such as the binding and release of organic compounds

from mineral matrices during alteration and preservation, and the astrobiological implications of these phenomena. In the terrestrial context, alteration is defined as any reaction that occurs after the primary deposition of organic matter during sedimentary diagenesis and catagenesis. In the extraterrestrial context, alteration refers to processes occurring on the parent body. Examples include thermal or aqueous processes, shock wave propagation, and brecciation. We also discuss the current state of knowledge regarding the impact of minerals on driving different types of enantiomeric excess and provide some future experimental directions that could address gaps that warrant further study of organic and mineral chirality in the context of prebiotic chemistry and origins of life.

3. Organic chirality

3.1 Point/molecular chirality

There are various types of chirality that organic molecules can possess; some different types are shown in Figure 2 (as illustrated by alanine, Figure 2a). Point or molecular chirality is chirality that is based around an atom such as carbon. Molecules that have atoms where each functional group attached to it is distinct are termed chiral [54]. For carbon, this typically means that the carbon atom has four different groups attached. Compounds that are mirror images of one another but cannot be superimposed through rotation, are termed enantiomers; and those that are non-superimposable, non-mirror images are termed diastereomers (example shown in Figure 2b).

Often enantiomers are described by their absolute configuration as R (rectus, right) or S (sinister, left). The difference between R and S involves assigning priority to the different substituents and determining whether the identified lowest to highest priority groups follows a clockwise direction (designated R) or counterclockwise direction (designated S). This method is also called the Cahn-Ingold-Prelog rules in organic nomenclature [55]. D/L are designations often used for sugars and amino acids; these do not directly line up with the R/S designation. In a Fisher projection of the molecule (for example, a sugar), the second to last carbon determines whether the molecule is D or L. If the hydroxyl is on the left the sugar is L and if the hydroxyl is on the right, the sugar is D. While the majority of chirality discussed in the context of origins of life is point/molecular chirality, there are other types of chirality that organics can possess, including axial, helical, and planar chirality, which we discuss below.

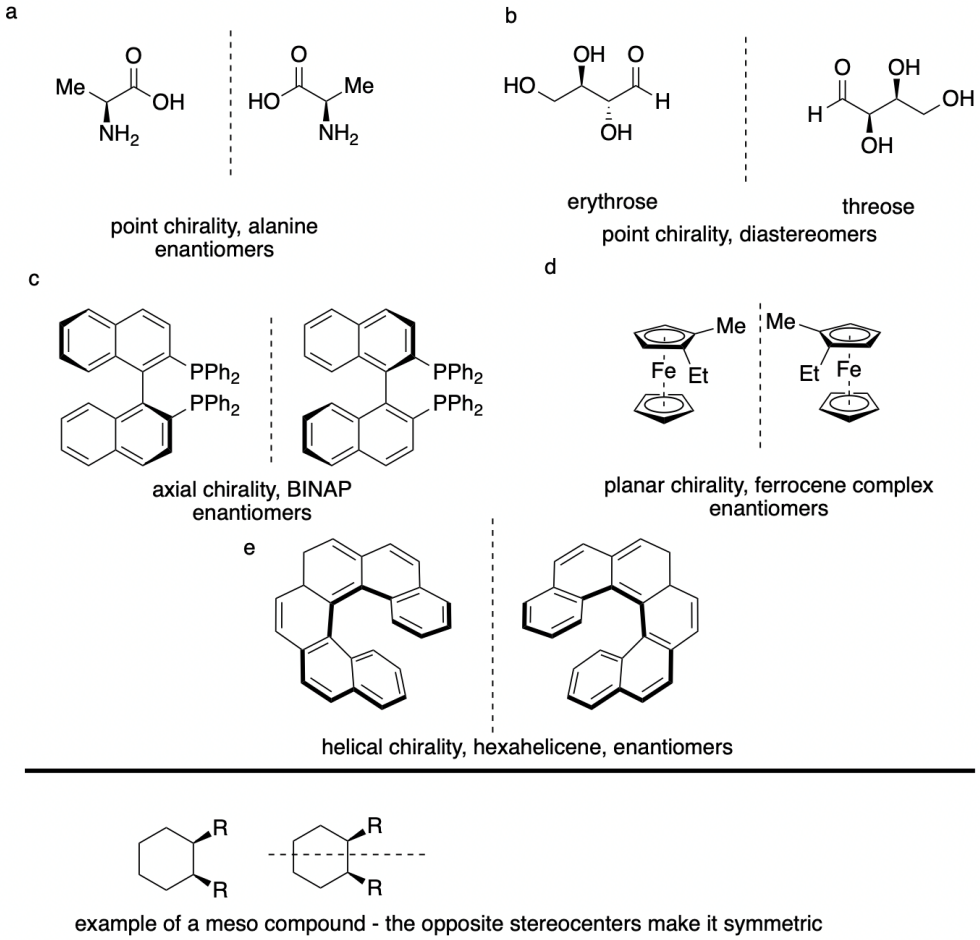

Figure 2. Examples of point/molecular chirality in organic molecules. **a**) Enantiomers of the amino acid alanine. **b**) Diastereomers of erythrose (left) and threose (right). **c**) Axial chirality exhibited by BINAP enantiomers. **d**) Planar chirality of the enantiomers of a ferrocene complex. **e**) Helical chirality of hexahelicene enantiomers. Bottom: generic dialkylcyclohexane as an example of a meso compound with an internal plane of symmetry, which is achiral and does not possess enantiomers.

3.2 Heteroatom chirality

This work will primarily focus on point/molecular chirality relevant to carbon; however, other atoms can be chiral, including P, N, and S, which are common heteroatoms in organic compounds. Additionally, other atoms within the carbon group, e.g., Ge and Si can exhibit chiral structures [56-59]. In the case of heteroatoms; P, N, and S in their neutral form would typically need a lone pair of electrons and three different substituents attached to be considered chiral. A key for maintaining this configuration (i.e., chirality at the heteroatom) is to limit inversion around the lone pair. This is known as pyramidal inversion and, in the specific case of N, it is known as amine inversion. Amine inversion occurs rapidly at and below room temperature, and the N does not exhibit a chiral center. These are known as fluxional reactions and allow the enantiomers to racemize [60] which means pure enantiomers cannot be isolated. During amine inversion, in the transition state there are three substituents arranged in the plane (co-planar) around the N atom, and the lone pair of electrons occupies an out-of-plane p orbital. Therefore, the structures containing chiral heteroatoms are often rigid or bulky, limiting the rate of inversion [61] and giving rise to enantiomers. Phosphine (PH_3) and chiral sulfur-containing compounds such as sulfites, sulfoxides, sulfonium salts, and sulfinic esters, also undergo the same inversion as amines, but the rate at room temperature is much lower [62,63]. Therefore

chiral P-phosphines and appropriately substituted chiral S compounds are optically stable at room temperature [64].

Compounds containing chiral heteroatoms can be used as ligands or reagents in enantioselective reactions and are also used in drugs [65]. Examples of chiral S-based drugs include armodafinil and esomeprazole which, as sulfoxides, always have a stereogenic S center due to the lone pair of electrons [66,67]. These drugs typically have an enantiopure form and a racemic form that display distinct chemical properties and are marketed for different uses. There is also similar research being conducted on P chiral centers [e.g., 68] as well as N [69,70]; however, the stereochemistry of the N atom makes it the most difficult heteroatom to control [70].

3.3 Additional forms of chirality

Molecules possessing features related to axial, helical [71], and planar [72] structure can also impart chirality in compounds that do not possess point chiral or stereogenic centers. Axial chirality is achieved when symmetry exists looking down an axis of a molecule; this commonly occurs in 2,2′-disubstituted biaryls and dissymmetrically substituted allenes. Examples of axial chirality include the organophosphorus compound, 2,2′-bis(diphenylphosphino)-1,1-binaphthyl), or BINAP [73] and 2,2′-dihydroxy-4,4′,6,6′-tetramethylbiphenyl. In both examples, axial chirality is due to restricted rotation as a result of steric hindrance (Figure 2c). Helical chirality is based on twisting in 3D space, as demonstrated in the aromatic compound hexahelicene (Figure 2d). Similar to axial chirality, steric strain promotes the existence of a stereogenic axis, giving rise to chiral forms in helically-chiral structures. Planar chirality is a system where the 2D structures are not superimposable. They contain two dissymmetric, non-coplanar rings that cannot be easily rotated (e.g., metallocenes including ferrocene, Figure 2e).

In addition, not all structures with chiral components are chiral when the structure is examined as a whole. For example, if a meso compound has two or more chiral components (stereogenic centers) they "cancel out" the asymmetry, as the structure contains an internal plane of symmetry (Figure 2). An example of a meso compound is 2,3-dichlorobutane, which is not optically-active nor does it have enantiomers. Achiral structures can also be prochiral, meaning that the addition of a unique functional group to a non-stereogenic center could give rise to chirality, in an asymmetric reaction. For example, in an asymmetric Strecker reaction (see Table 1, entries 2 and 3), the imine group is prochiral. This means that depending on the face (i.e., Re or Si) that the reaction occurs on, different enantiomers (i.e., R and S) can be formed. In these mechanisms, other asymmetric components impart selectivity between the prochiral faces.

Table 1. Examples of enantioselective reactions and the research field(s) they are relevant to. The focus of this review are the reactions relevant to prebiotic chemistry and the origins of life.

Reaction	Starting material	Product	Relevant field(s)	References
Soai	pyrimidine-5-carbaldehyde	pyrimidyl alcohol	Origins of life; autocatalysis	26, 74
Strecker	Aldehyde	Amino acid	Origins of life, Pharmaceutical and natural product synthesis	75

Strecker	Ketone	α,α-disubstituted amino acids	Origins of life, Pharmaceutical and natural product synthesis	76
Reductive amination	Alpha keto acid	Amino acid	Origins of life, Pharmaceutical and natural product synthesis	77, 78
Kiliani–Fischer synthesis	Sugar	Monosaccharide	Origins of life	79,80
Sharpless epoxidation	Allylic alcohols	2,3-epoxyalcohols	Pharmaceutical and natural product synthesis	81
Sharpless bishydroxylation	Alkene	Vicinal diol	Pharmaceutical and natural product synthesis	82
Sharpless oxyamination	Alkene	Vicinal amino diol	Pharmaceutical and natural product synthesis	83
Midland reduction	Carbonyl (ketone)	Alcohol	Pharmaceutical and natural product synthesis	84
Noyori asymmetric hydrogenation	Keto ester	Hydroxy ester	Pharmaceutical and natural product synthesis	85
Corey-Itsuno reduction	Ketone (achiral)	Alcohol (chiral, non-racemic)	Pharmaceutical and natural product synthesis; industrial synthesis	86,87
Asymmetric Diels-Alder	Diene and alkene	Cyclohexene	Pharmaceutical and natural product synthesis industrial synthesis	88-93
Examples of asymmetric cross-coupling reactions				
Suzuki-Miyaura	Alkyl- or arylhalides + organoborates	Alkyl or aryl compounds	Pharmaceutical and natural	13,94,95

			product synthesis; industrial synthesis; catalysis	
Ni/Photoredox dual catalysis	Varied	Varied	Pharmaceutical and natural product synthesis; industrial synthesis; catalysis	96-99
Buckwald-Hartwig amination	Varied	Amine	Pharmaceutical and natural product synthesis; industrial synthesis; catalysis	100-101

3.4 Asymmetric organic synthesis reactions

Asymmetric reactions relevant to the origins of life include reductive amination and Strecker synthesis for synthesizing amino acids and the autocatalytic formose reaction for synthesizing sugars (see *Section 8.2.3* for more details). Asymmetric reactivity is very important in the field of organic chemistry, as it is often a key consideration in pharmaceutical and natural product synthesis [102,103]. Notably the 2021 Nobel Prize in Chemistry was awarded for the discovery of chiral organocatalysis [104]. There are a variety of catalytic methods to create asymmetry in reactions (Table 1). Some examples include organocatalysis that utilize chiral compounds (such as proline) as the catalyst, which then imparts asymmetry [105-107]. For metal-based catalysis, the chiral component can often be the ligand of the metal catalyst; such ligands can include organics with point or axial chirality [108-110]. However, there are other methods to impart chirality with the use of transition metals [111].

There are also chiral pool materials that are enantiopure compounds and readily and naturally available, like amino acids and certain carboxylic acids [e.g., 112,113]. Chiral pool materials are often commercially-available and can be used in total synthesis. Total synthesis–common in organic chemistry–is the complete chemical synthesis of an organic molecule, often a complex natural product such as taxol, strychnine, or a pharmaceutical. In these syntheses, organic chemists need to design enantioselective reactions to access complex chiral products.

In asymmetric organic synthesis reactions, geologic context is not often considered. Instead, considerations for chiral/asymmetric starting materials are often based on availability and yield of product. Ideally, scientists who utilize organic syntheses to impart asymmetry aim to synthesize their natural product with high purity and selectivity, therefore the conditions are often heavily optimized towards achieving those objectives. In the field of prebiotic chemistry, the geologic context is important as yield and/or selectivity are not often the final goal of these projects, but instead to determine the conditions that drive product distribution [5,6]. Below, we describe mineral chirality and how organic reactions can impart chirality in organic-mineral systems in the context of prebiotically-relevant environments.

4. Organometallic systems related to chirality

Organometallic compounds, whereby a carbon atom is covalently bonded to a metal, play important roles in enantioselective organic synthesis and methodology [114,115], industrial synthesis [116], materials science, and nanotechnology [117,118], pharmaceuticals and medicinal research [119,120], and in prebiotic and metabolically-relevant systems [121-123,124 and references therein]. Organometallic reagents can be used in other reactions as reagents e.g., R-MgBr (where R = alkyl, allyl, aryl, or vinyl group) for Grignard reactions [125,126] and catalysts, i.e., Pd and Ni compounds for Heck reactions [127-129]. Cross-coupling reactions are a notable type of organometallic reactions where two organic fragments are coupled together with the use of a metal catalyst, such as the Suzuki reaction [130,131]. Cross-coupling reactions and the use of precatalysts are powerful techniques that can be used to form C-C, C-N, and other C-X bonds [e.g., 132-134] to synthesize materials relevant to all fields of chemistry. While there are a significant number of different cross-coupling techniques, far more often than not, the techniques have not been explored for selectivity. Table 1 lists some of the examples where the reactions are enantioselective. In addition to interest in bioactive starting materials relevant to the pharmaceutical industry, some cross-coupling reactions could have relevance in prebiotic environments. For example, copper-mediated cross-coupling of cyanide and acetylene synthesized the amino acids: arginine, aspartic acid, asparagine, aspartate, glutamine, glutamate, proline [135].

Many proteins are associated with organometallic complexes or metalloenzyme cofactors [136] as they assist with the stabilization of their structure and support other vital biochemical reactions [123 and references therein]. Organometallic compounds have been shown to catalyze the polymerization of peptides and proteins [123,137,138]. The metal ions stabilize spectator ions during peptide formation within their ligands and the amino or carboxyl group of amino acids is protected during peptide synthesis [139,140].

Recently, there have been several reports of metal-organic compounds in meteoritic organic matter that have implications for understanding parent-body interactions with origins of life implications [141-143]. A study by Ruf and colleagues surveyed 61 meteorites over a wide range of petrologic types. They found dihydroxymagnesium carboxylates $[(OH)_2MgO_2CR]^-$ in the soluble organic fraction that could be associated with metamorphic events such as thermal alteration and shock events. These types of organometallic anion complexes had not been identified in meteorites prior to this study. Another study looked at the soluble organic fraction of 44 meteorites and found a novel homologous series of sulfur magnesium carboxylates. They appear to be thermally stable and their abundance was correlated with increasing thermal maturity [143]. Smith and colleagues looked at the origin of cyanide in the CM2 Murchison meteorite and found that it was primarily bound (and subsequently released) as iron cyanocarbonyl ($[Fe^{II}(CN)_5(CO)]^{3-}$ and $[Fe^{II}(CN)_4(CO)_2]^{2-}$) organometallic complexes. These results suggest that cyanide in the form of iron cyanocarbonyl complexes could be a source for free cyanide in delivered by meteorites and potentially be a precursor to catalytic centers of early enzymes such as Fe hydrogenases [142].

5. Minerals relevant to prebiotic chemistry

The composition of planetary surfaces vary based on the planet's histories, including its orbital position during early Solar System development, and subsequent physical, chemical, and space weathering processes (Table 2). Planetary surface minerals can be subdivided into broad categories of primary igneous minerals, secondary minerals produced by processes including impacts, metamorphism, and weathering, and volatile ices. Primary minerals include olivine, pyroxene, quartz, and feldspar. Secondary minerals include phyllosilicates, Fe oxides, carbonates, and sulfates. Common ices of volatile phases are driven by the "frost line" of that volatile phase during the early Solar System, or the

distance at which that phase can condense into liquid form and resist further migration outward by the solar wind [143,144]. The abundance of water, ammonia, and methane ices are relatively low and dependent on regional conditions in the Inner Solar System and more common from the Main Asteroid Belt outwards (Table 2).

Table 2. The surface minerals and ice surface compositions of major rocky bodies in the Solar System.

Planetary body	Major surface minerals	Major ices	References
Mercury	Plagioclase, olivine, pyroxene, sulfide, graphite	Water	145-149
Venus	*Theorized:* Olivine, pyroxene, sulfide, Fe oxides, carbonates, ilmenite, sulfate	None identified to date	150,151
Earth	Olivine, pyroxene, plagioclase, anorthite, quartz, Ca carbonate, phyllosilicates, Fe oxides	Water, lesser methane	152-155
Moon	Anorthite, plagioclase, pyroxene, olivine, ilmenite	Water	146,156,157
Mars	Olivine, pyroxene, phyllosilicates, sulfates, Fe oxides	Water, CO_2, possibly methane	146,158-161
Asteroids, moons, and dwarf planets	Olivine, pyroxene, phyllosilicates, carbonates, Fe oxides	Water, methane, nitrogen, CO_2, CO	162-166

Available surface minerals could have affected prebiotic chemistry in ways that are discernible from mineral records visible today. Because of their long-form structural repetition, available cations, and reactivity, many mineral structures have long been hypothesized to be important in prebiotic chemistry and possible emergence of life [167,168]. Indeed, mineral deposits control the availability of non-volatile bio-essential elements, so distinguishing planetary surface mineral deposits is critical to the question of habitability and preservation in the Solar System [168].

Clay minerals are a commonly cited class of minerals to be relevant to prebiotic chemistry, e.g., montmorillonite is found in carbonaceous chondrite meteorites [169,170]. Fe/Mg-clays are of particular interest when constraining planetary habitability as they tend to be formed in alkaline, reducing environments that some studies propose are favorable for the transition from prebiotic to biotic activity [171-176], and may have even had a role in the origins of life on Earth [177]. The small particle size of clays could have concentrated and protected organic molecules from photolysis [178]. Studies have also suggested that amino acids could be polymerized in aqueous solution in the presence of clay minerals [e.g., montmorillonite, 179]. Illite can promote chain elongation of amino acids [180]. Hydrotalcite can serve to concentrate glycolaldehyde phosphate from dilute solution and thus catalyze condensation of the carbohydrate subunits [181].

Only some of these planetary minerals can structurally have different chiral forms. Mineral chirality is difficult to observe using the surface characterization methods traditional in planetary science, but as mineral chirality could have affected origins of life processes, a review of mineral chirality and how it intersects with prebiotic chemistry is of growing importance.

6. Mineral chirality

Chirality is not just limited to organics; minerals can be intrinsically chiral (e.g., L versus D quartz), be overall achiral, but have chiral faces (e.g., calcite), have local chiral sites, or build chiral macromolecular structures (e.g., carbonate toroidal super structures [182] or spiraling of gastropod shells [183,184]). Mineral chirality is important to understand because interactions of organic molecules with mineral surfaces may also confer a degree of chiral selectivity in abiotic planetary systems.

6.1 Enantiomorphic minerals

Mineral crystals are built from repeated translations of "unit cells," or the smallest repeating pattern of atoms that reflects the symmetry and structure of the entire crystal. Unit cells are classified into one of six geometric crystal families which groups crystals based on a combination of the unit cell's shape (i.e., lattice structure) and the required symmetry of their point groups (i.e., a group that describes the symmetry operations under which the unit cell is invariant). Within each crystal family, the specific geometry and symmetry of a unit cell can be more specifically classified into space groups; thus, every mineral belongs to one of 230 space groups. The space group describes both the specific translational symmetry of the unit cell (i.e., the Bravais lattice, screw axis, and glide planes) and the point group symmetry operations (reflection, rotation, inversion, or rotoinversion). Minerals whose unit cells cannot be superimposed onto their mirror image are considered enantiomorphic (i.e., chiral); thus, asymmetry can be deduced based on the space group of the mineral. In other words, specific space groups are chiral and can be used to identify chiral minerals. Of the 230 possible space groups, 64 (belonging to 11 of the 32 crystal point groups) are chiral (Table 3). A full list of chiral minerals (as identified by their space group) and their chemical formula have been compiled (Table S1) using the mineral database Mindat. Notably, mineral enantiomorphs do not belong to the same space group.

Table 3. A list of chiral minerals organized by their crystal system, class, and space group

Crystal Family	Crystal Class #	Crystal Class	Space Group	Example Mineral	Elemental Formula	Category
Triclinic	1	Pedial	P1	Kaolinite	$Al_2(Si_2O_5)(OH)_4$	Phyllosilicate
				Amesite	$Mg_2Al_2SiO_5(OH)_4$	Phyllosilicate
				Nordstrandite	$Al(OH)_3$	Metal oxide
Monoclinic	2	Sphenoidal	P2, $P2_1$, C2	Buddingtonite	$NH_4AlSi_3O_8$	Tectosilicate
				Bassanite	$Ca(SO_4)\cdot 0.5H_2O$	Sulfate
Orthorhombic	222	Rhombic-disphenoidal	P222, $P222_1$, $P2_12_12$, $P2_12_12_1$, C222, $C222_1$, F222, I222, $I2_12_12_1$	Wülfingite	$Zn(OH)_2$	Metal oxide
				Epsomite	$MgSO_4 \cdot 7H_2O$	Sulfate
				Sanderite	$MgSO_4 \cdot 2H_2O$	Sulfate
				Lecontite	$(NH_4,K)NaSO_4 \cdot 2H_2O$	Sulfate
				Abuite	$CaAl_2(PO_4)_2F_2$	Phosphate
Tetragonal	4	Tetragonal-pyramidal	P4, $P4_1$, $P4_2$, $P4_3$, I4, $I4_1$			
	422	Tetragonal-trapezoidal	P422, $P42_12$, $P4_122$, $P4_12_12$,	Cristobalite	SiO_2	Tectosilicate
				Wardite	$NaAl_3(PO_4)_2(OH)_4\cdot 2(H_2O)$	Phosphate

			$P4_222$, $P4_22_12$, $P4_322$, $P4_32_12$, $I4_122$, $I4_12_12$			
Hexagonal	3	Trigonal-pyramidal	P3, $P3_1$, $P3_2$, R3	Monohydrocalcite	$CaCO_3 \cdot H_2O$	Carbonate
						Phosphate
	32	Trigonal-trapezohedral	P312, $P3_112$, $P3_212c$, $P3_212$, $P3_121$, $P3_221$, R32	Berlinite α-D-quartz α-L-quartz Antarcticite Huntite	$AlPO_4$ SiO_2 SiO2 $CaCl_2 \cdot 6H_2O$ $Mg_3Ca(CO_3)_4$	Tectosilicate Tectosilicate Chloride Carbonate
	6	Hexagonal-pyramidal	P6, $P6_1$, $P6_2$, $P6_3$, $P6_4$, $P6_5$	Trinepheline Kellyite Nagelschmidtite	SiO_2 SiO_2 $KAlSiO_4$ $Mg_4Al_2(OH)_{12}(CO_3) \cdot 3H_2O$	Silicate Phyllosilicate Neosilicate
	622	Hexagonal-trapezohedral	P622, $P6_122$, $P6_222$, $P6_322$, $P6_422$, $P6_522$	β-D-quartz β-L-quartz Kalsilite Quintinite	$(Ni,Fe)_4P$ MnSi FeSi $K_2Mg_2(SO_4)_3$	Tectosilicate Tectosilicate Kalsilite Carbonate
Cubic	23	Tetaroidal	P23, $P2_13$, F23, I23, $I2_13$	Melliniite Brownleeite Naquite Langbeinite	NH_4Cl γ-Fe_2O_3	Phosphide Silicide Silicide Sulfate
	432	Gyroidal	P423, $P4_232$, $P4_332$, $P4_132$, F432, F432, I432, $I4_132$	Salammoniac Maghemite		Chloride Metal oxide

Since larger crystal structures reflect the inherent geometry and symmetry of the unit cell, minerals that are chiral at the unit cell will have crystal faces which are also chiral. Chiral minerals are composed of chiral unit cells which themselves may be made up of achiral subunits. For example, one of the most commonly discussed chiral minerals, α-quartz, is composed of repeated molecules of achiral silicate (SiO_4). It is the arrangement of the silicate molecules into left or right-handed helices that give quartz its chirality (as evidenced by its unit cell and crystal lattice in Figure 3). Consequently, dissolution of chiral minerals will often result in achiral mixtures (e.g., dissolved achiral silicate molecules).

Figure 3. Summary of the variations of chirality of mineral crystals. A) Inherent chirality as observed in the unit cell with quartz as an example. B) Chiral faces of achiral minerals with calcite as the example: The unit cell is achiral as is the crystal lattice; however the crystal habit can have chiral faces as seen with the scalenohedral habit; the rhombohedral habit has no chiral faces. C) Natural minerals have local defects that can result in local chiral centers. Shown are defects typical of a growing crystal structure. D) Macromolecular mineralogical structures can have chirality. Often, precipitated shells of biological organisms have a chiral structure such as the gastropod shells drawn here.

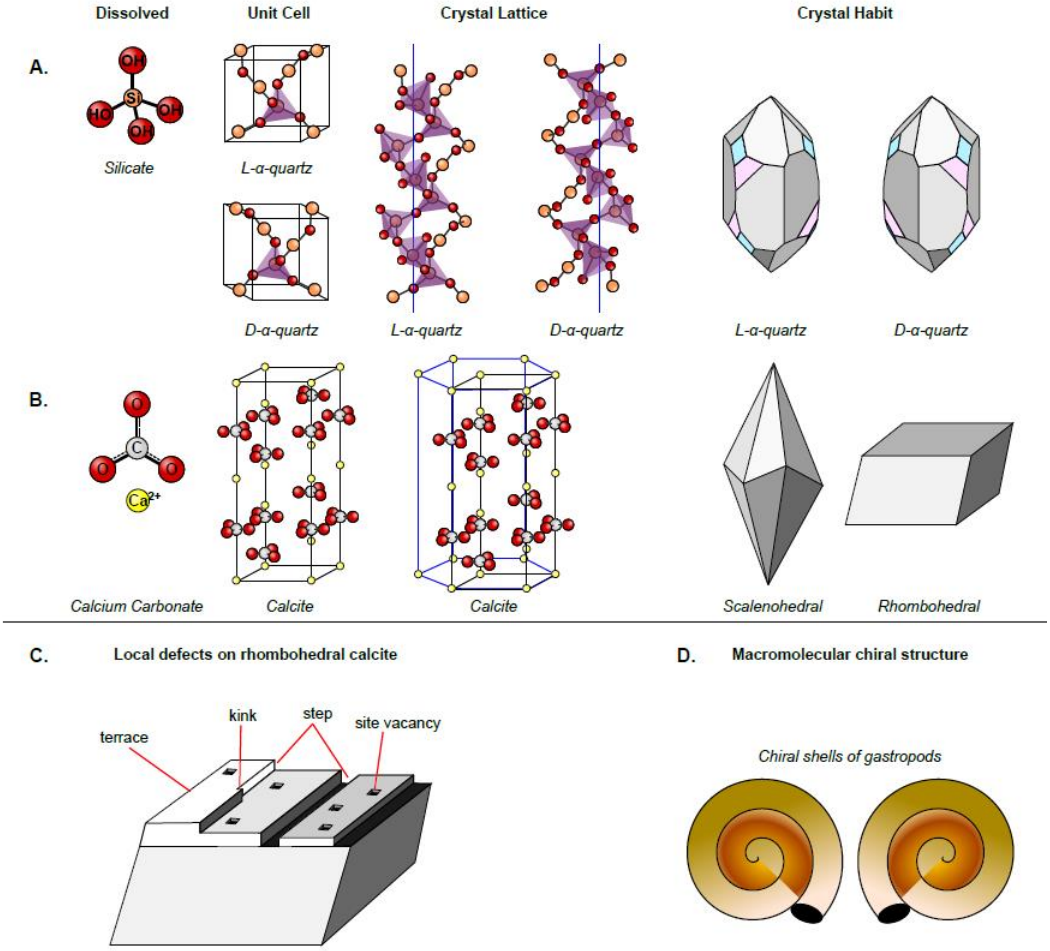

424

6.2 Achiral minerals with chiral faces 425

Depending on the environmental conditions, minerals can form different crystal habits, some of which may have faces that are chiral [185] (Table 4). For example, calcite ($CaCO_3$) is centrosymmetric (i.e., its unit cell is achiral), but it can take on many different forms, the most abundant being scalenohedral (e.g., dog-tooth spar) or rhombohedral; the former has chiral faces {2 1 4} while the latter has faces {1 0 4} that are achiral [186] (Figure 3). The scalenohedral form comes in pairs of chiral faces, but the overall unit cell remains achiral. This is notably distinct from chiral minerals whose faces are not only all chiral, but are either entirely all L or D forms (rather than having a crystal with both) – except for crystals which are internally twinned via the Brazil law. Crystal twinning occurs when a crystal is subjected to an environmental change (usually temperature or pressure) that results in the growth of a different crystal onto a face of the first. This is especially common for minerals which have polymorphs that are favored under different geochemical conditions. There are different types of twinning; for chiral minerals the most relevant is the Brazil law twin which combines right and left-handed crystals within a growing crystal structure. For quartz, Brazil law twinning is common and is almost never reflected in the surface crystal morphology; thus, quartz minerals may appear chiral, but are internally twinned and are thus racemic [187]. Given the potential for an achiral mineral to possess a racemic interior, together with the fact that achiral crystals can possess a set of chiral faces, it has been advocated that chirality studies involving minerals should avoid powdering the mineral of interest (as then chirality information is lost) [188]. Instead, studies should focus on organic adsorption of chiral species on preserved faces of crystals whose chirality can be checked against the resulting enantiomeric excess (if any). 426 427 428 429 430 431 432 433 434 435 436 437 438 439 440 441 442 443 444 445 446 447

Table 4. A list of some achiral minerals with chiral faces

Mineral	Formula	Face {Miller index}	Category
Calcite	$CaCO_3$	(214)	Carbonate
Gypsum	$CaSO_4 \cdot 2H_2O$	(110), (111)	Sulfate
Olivine	$(Mg^{2+}, Fe^{2+})_2SiO_4$	(111)	Silicate
Clinopyroxene	$(Ca,Mg,Fe,Na)(Mg,Fe,Al)(Si,Al)_2O_6$	(110), (111)	Oxide
Clinoamphibole: e.g., hornblende	$(Ca,Na)_{2\text{-}3}(Mg,Fe,Al)_5(Al,Si)_8O_{22}(OH,F)_2$	(110), (011)	Inosilicate

6.3 Local chiral sites

In the natural world, minerals usually form imperfect crystals; that is, their internal structure does not perfectly match that expected from the unit cell. The interruption of the ideal crystal lattice (i.e., crystal defects) can yield local chiral sites on an otherwise achiral mineral or crystal face [185]. Crystal defects are categorized into three groups: point (e.g., vacancies, irregular placement of atoms, substitutions, or kinks), linear (e.g., steps), and plane (e.g., terraces). Since organics adsorb most efficiently at defect sites (ledges, kinks, surface vacancies > terraces), these local chiral centers could provide an efficient means to generate local regions of organic enantiomeric excess [186]. Structural defects are an inherent part of crystal growth; thus, if organics bind to the growing mineral during this process, they can have an impact on the final crystal structure, including the chirality of the mineral [28,182,189]. As every crystal structure will have some crystal defects, local mineral chiral sites may play a bigger role in influencing organic chirality than the inherent chirality of minerals as a whole. In addition to promoting organic adsorption, defect sites are also reactive [190] and can thus serve as an efficient site for further organic reactivity involving the preferentially adsorbed enantiomer.

In addition to local chiral sites existing at mineral surfaces due to structural defects, chiral selectivity can be induced as a result of cooperative effects between chiral organics and the (in)organic analytes that have previously adsorbed at the mineral surface or intercalated (i.e., inserted) between mineral layers. For example, the initial adsorption of one organic enantiomer at the surface could bind in such a way that its orientation further promoted the adsorption of that particular enantiomer. On the other hand, intercalation of other ions/organics could lead to chiral orientations between mineral layers. There are several mechanisms that can induce chirality between layers including partial ion-exchange (e.g., Al^{3+} for Mg^{2+}) which could lead to multiple sites between any mineral layers having different ions that are of various size and possess different binding capabilities for organic enantiomers; alternatively, ion-exchange could also result in site vacancies that are chiral [191]. Another means of inducing chiral selectivity between mineral sheets is due to differences in the binding orientation and exchange kinetics between the mineral layers and organic enantiomers [192,193]. For instance, a study on the intercalation of L- and D- histidine within vermiculite clay found that the two enantiomers had different effects on the osmotic swelling and d-spacing between the mineral layers [194,195].

6.4 Factors that influence a mineral's degree of enantioselectivity

There are inherent factors that influence the degree to which chiral minerals (either via their internal structure or having chiral faces) can drive organic enantiomeric excess: the most notable being the degree to which the mineral enantiomers are structurally different (i.e., the chiral index; [196]) and the degree to which organic enantiomers are sorbed to the mineral surface [e.g., 197].

A chiral index. The degree to which enantiomorphic minerals differ from their mirror counterpart is predicted to impact their organic enantioselective potential and can be described mathematically using the chiral index (a term coined by [196]). Downs and Hazen 2004 proposed a methodology to calculate the chiral index of any mineral, and suggested that this measurement could be used to identify minerals with strong potential for driving organic enantiomeric excess. The basis of their calculations follows the logic used to quantify a similar measurement, the distortion index [198], which quantifies the deviation of a periodic arrangement of atoms from its perfect crystal structure due to imperfections. The chiral index, instead, quantifies the degree of misfit between any two chiral faces or structures. This measurement predicts the potential for mineral faces (e.g., those of calcite) or inherent structure (e.g., quartz) to drive organic enantiomeric excess via mineral-organic interactions. Using this approach, [196] compared the enantioselective potential of the faces of several minerals (calcite, diopside, orthoclase, quartz and copper) and discovered that the calcite (2 1 4) face, and to a lesser extent diopside and copper, had a higher chiral index (and thus larger enantioselective potential) than the mineral with inherent chiral symmetry – quartz. Although this was a computational study, their results are consistent with experimental work that has found that the calcite (2 1 4) face results in larger enantiomeric excess from racemic amino acid mixtures (~10% chiral excess) than quartz (~1% chiral excess; [187,196]). Note that earlier studies may have underestimated the degree of chiral selection on quartz surfaces due to internal Brazil twinning that results in internally racemic quartz crystals [187,199]; although, studies that took care to work with untwinned quartz crystals still found that the degree of chiral selectivity on quartz is modest at best [200-202].

Downs and Hazen (2004) note that their described chiral index does not necessarily capture the degree to which each mineral can drive organic enantiomeric excess (as there are many factors that can impact mineral-organic interactions). Thus, they suggested two additional chiral indices to consider: one that describes the degree of fit between organic enantiomers onto a mineral surface, or a more general approach based on three-point interactions calculated using triangles formed by nearest-neighbor atoms on the mineral surface. To our knowledge a follow-up study to calculate these proposed indices has not been published, nor have there been any efforts to apply the chiral index as previously described [196] to other chiral minerals.

Mineral-organic interactions. Chiral organic molecules have mostly identical physical and chemical properties; however, the difference in their structural arrangement imparts differences in their degree of interaction with any chiral selector, whether it be organic (e.g., proteins) or inorganic (e.g., minerals). Chiral selectors are inorganic or organic materials that form diastereoisomeric complexes with the chiral analyte. Notably, not all chiral organic molecules will form diastereoisomeric complexes with chiral surfaces on minerals; thus, chiral materials are not always enantioselective. Previous work has shown that there must be a minimum of three noncollinear points of interaction between a chiral analyte and chiral selector for there to be any enantioselectivity; this is also referred to as the three-point minimum interaction model [203-205]. This model is consistent with experimental studies which found that chiral surfaces of calcite are enantioselective for only certain amino acids (e.g., aspartate), but not others (e.g., alanine, valine, lysine) [186,188, 206]. Accordingly, computational studies modeling the interactions of alanine and aspartate with calcite surfaces revealed that aspartate was bound to calcite at three binding sites whereas alanine was only bound at two. While the three-point model is a good starting point for assessing the potential enantioselectivity in the binding of molecules, it should be noted that the model has faced scrutiny [207,208] as it has been shown that sometimes four points of interaction are needed [208]; alternatively, with aromatic organic molecules a pseudo-two-point interaction may suffice [207].

If we were to develop an equation that properly predicts the enantioselective potential of a mineral in any given environment, the chiral index [196], which describes the mismatch between any two surface enantiomorphs of a mineral, would only represent one variable. Some of the remaining variables would have to capture some information regarding the chiral analyte of interest, including how it interacts with the mineral surface. As previously discussed, generally three points of interaction are required between the mineral and organic analyte for the mineral to impart chiral selectivity onto the system. At these three points, any molecular interaction will suffice, although the type of molecular interaction will impact the degree to which the mineral can drive organic enantiomeric excess and under which environmental conditions it can do so. Mineral-organic interactions can involve bonding and/or nonbonding interactions (i.e., covalent, H-bonds, steric hindrance, pi-pi, ion-dipole, dipole-dipole, dipole-induced-dipole, and London dispersion or van der Waals [see 209 for a review]) – the relative strength of these interactions (which is dependent on type and environment) impacts the enantioselectivity of the mineral of interest (with stronger bonds increasing enantioselectivity). Thus, an idealized equation for describing the enantioselectivity of a mineral would also include variables that describes the bond type between each organic-mineral interaction, the surrounding environmental conditions (pH, temperature, salinity), and how the organic analyte and mineral surface are expected to change with environmental parameters (e.g., pKa of the organic, point of zero charge for the mineral).

6.5 Mineral-organic interactions for driving enantiomeric excess

Minerals can drive enantiomeric excess (ee) via selective adsorption that facilitates (1) the production of one enantiomer of a chiral compound; (2) the formation of homochiral polymers (e.g., by facilitating polymerization of L-amino acids); (3) solutions with ee (e.g., preferential adsorption of L-sugars generates solutions enriched in R-sugars); and/or (4) the preferential preservation (or degradation) of the adsorbed enantiomer. Notably, the number of studies that have investigated the influence of chiral mineral surfaces on driving enantiomeric excess of organic enantiomers remains limited. In general, these studies have found that minerals only induce minimal to modest enantiomeric selectivity [177,186,200,201,210]. Although over geologic timescales this may result in significant enantiomeric excess, considering that chiral molecules can racemize over time, this may not provide an adequate solution ([211] and references therein). One potential resolution to this conundrum are autocatalytic processes, wherein mineral-organic interactions yield conditions that promote enantioselectivity, and additional mineral-organic interactions in turn further promote enantioselectivity. One of the most notable autocatalytic reactions in organic synthesis is the Soai reaction (Table 1), which produces a near enantiopure solution (>99.5% ee) in high yields (>99%) using 3-pyridylalkanol as an asymmetric autocatalyst [26]. As summarized in the review by [212], the organic autocatalyst of the Soai reaction can be successfully substituted for more prebiotically relevant catalysts, including the minerals quartz, gypsum, retgersite, cinnabar, sodium chlorate, and sodium borate – all of which generated near enantiopure solutions in high yields [27,213-217]. These results demonstrate how minerals can induce significant enantioselectivity when subjected to asymmetric autocatalytic reactions.

Autocatalytic systems can also include the precipitation of enantiopure minerals and/or organic crystals as well as formation of surface defects that further promote mineral-organic enantiospecific reactions. These reactions warrant further studies given that minor enantiomeric excess of either the organic or mineral reagent could lead to near enantiopure solutions or crystals. In fact, even racemic or achiral solutions can produce enantiopure crystals. This was seen in [218], which observed that stirred solutions of sodium chlorate (which is achiral), precipitated chiral crystals all of which had the same handedness; repeated experiments found that the system would consistently produce crystals of

either D or L handedness, although which enantiomorph (D or L) precipitated varied between reactions. Subsequent studies elucidated the mechanism at work: stirring of the solution promoted rapid shearing of the initial crystal that precipitated [15,219]. Thus, if the initial crystal precipitate was of the D form, then shearing (due to mixing) would rapidly break apart the D crystal, producing many smaller D crystals that could then act as nucleation centers for further precipitation of the D enantiomorph. For such reactions, an initial enantiomeric seed was not added to the system, but was a product of random chance.

Although systems that generate enantiopure products from achiral mixtures may have been relevant for the origins of homochiral polymers in biochemistry, the fact that they generate either D or L forms only by chance suggests that overall such systems may have canceled each other out. Alternatively, systems containing a slight excess of an organic and/or mineral enantiomer may result, via positive feedback reactions, in systems with significant enantiomeric excess. One example of such chemistry is that of D and L precipitating tyrosine [220]. Originally, the authors found that D-tyrosine crystallized out of solution much faster than L-tyrosine. These results were replicated by [221] when they used D/L-tyrosine from the same source as [220]; however, when different tyrosine sources were used, the results were not replicated. Accordingly, when [222] repeated the study, they found that D/L-tyrosine had different solubilities only when prepared solutions were not passed through a 0.2 μm filter; when the solutions were filtered, the effect was not observed. Both [221] and [222] concluded that the discrepancy of D/L-tyrosine solubility was due to different contaminants, such as fungal spores, being present in the D/L-tyrosine powders purchased from various vendors. [223] contested this interpretation, arguing that the solubility differences were due to the parity violation energy difference between enantiomers (a topic which falls outside of the scope of this review).

If trace contaminants are responsible for the apparent differences in enantiomeric solubility of tyrosine, then a slight excess of a mineral and/or organic enantiomer could drive the precipitation of chiral structures such as D-tyrosine organic crystals. Alternatively, minor seeds of an organic enantiomer could result in the precipitation of chiral mineral structures that in turn facilitate the adsorption of an organic enantiomer. For example, D/L enantiomers of aspartic acid or glutamic acid present in solutions undergoing $CaCO_3$ precipitation, induced the formation of macro mineral-organic chiral structures [182]. The resulting chiral structure could then promote the adsorption of the seed enantiomer. On the other hand, the presence of organic acids with minor enantiomeric excess can promote the dissolution of the chiral mineral surfaces to which it binds, producing step-like features on the surface [224]. These steps can then enhance organic adsorption onto the corresponding chiral surface, consequently promoting enantioselective adsorption onto that surface and driving enantiomeric excess of the remaining solution [186].

6.6 Future directions

There are many minerals which are inherently chiral (Table 3; Table S1); however, their prevalence on early Earth or other planetary bodies remains understudied and uncertain. Moreover, wide-spread conditions favoring the formation of a particular mineral enantiomorph seem unlikely. For example, on Earth the two quartz enantiomorphs are equally abundant and are often found within the same crystal (i.e., the crystal is internally twinned and thus racemic) [225,226]. Investigations into conditions that could potentially favor the crystallization or preservation of one mineral crystal enantiomorph over the other remains uncertain and largely unexplored. One potential research avenue to explore this question would be to computationally explore whether dissolved achiral contaminants ever preferentially adsorb onto only one of two chiral mineral surfaces, thus promoting the dissolution or precipitation of a particular chiral surface. Alternatively,

circularly polarized light or spin polarized electrons emitted during beta decay of radioactive nuclei, both of which are proposed as a mechanism for ee of L-amino acids in meteorites [227-229; see 14 and references therein], could also impart chirality onto precipitating minerals or preferentially alter the surface of achiral or chiral minerals, producing surface defects that could either serve as additional chiral sites and/or further promote organic adsorption and reactivity [186,190,230-235]. These astrophysical processes could thus serve as a means for generating inorganic chiral seeds that could subsequently trigger asymmetric autocatalytic systems as described in *Section 6.5*.

Prebiotic investigations of the stereoselective effects minerals impart on organic systems and vice versa is relatively limited, with most organic-mineral studies focusing on the adsorption of amino acids on montmorillonite or other clays (see 236 and references therein). However, as shown in Tables 3, 4, and S1, there are many minerals that are either inherently chiral or possess chiral faces that are geologically or chemically relevant; even achiral minerals with achiral faces can possess local chiral sites at the surface or between layers. The most notable minerals with chiral surfaces are those of evaporites, which are especially interesting considering their prevalence on the Martian surface [237,238]. Minerals with inherent chirality and planetary relevance include some phyllosilicates (e.g., kaolinite, a common crustal mineral identified on Mars [239-241]), zeolites (which can act as prebiotic catalysts and has been detected on Mars, [242-245], sulfates (e.g., epsomite, bassanite, and sanderite which are present on the Martian surface and can preserve biosignatures [238,240,246-248]), sal-ammoniac (NH_4Cl) which has been found on the surface of Ceres [249,250], maghemite (a common Fe oxyhydroxide that can form from weathering of magnetite and is also likely on Mars [251-254], phosphates (which could act as a source for organic phosphorylation of chiral compounds), and borates (which are the likely form of boron detected on the Martian surface and have been shown to selectively promote the preservation of ribose [255-260]). Given the planetary and prebiotic relevance of such chiral minerals, additional investigations exploring their enantioselective potential within prebiotic systems is warranted.

As previously discussed, the enantioselective potential of any chiral surface is dependent on its local environment (pH, temperature, salinity, pressure), the organic analyte (pKa, number and types of bonds with the mineral), and its inherent physical properties (point of zero valent charge, degree of mismatch between its two enantiomorphs). [173] calculated a chiral index for several chiral minerals based on the degree of mismatch between their enantiomorphs, and suggested that other chiral indices could be calculated based on the three-point interaction model and the differences between the binding sites of two organic enantiomers onto any chiral surface. This original study was published in 2004, and since then molecular modeling approaches have vastly improved and now provide a facile means to obtain the geometry of the available binding sites on any mineral surface and resulting geometry and bond energies for each of the mineral-organic interactions. These variables could then be used as inputs to calculate a better description of the enantioselective potential of a wide-range of minerals under various geochemical conditions. Such studies are warranted since obtaining enantiopure minerals is challenging (as they may look enantiopure on the outside, but possess internal twinning) and that natural minerals also possess organic contaminants, many of which may be biological and thus have their own asymmetry that could influence the reaction system being studied. In sum, molecular modeling can be a boon to prebiotic studies of enantiomeric excess as it can be leveraged to systematically evaluate a wide-range of minerals and organic-mineral interactions under various geochemical conditions and thus help shed light onto which chiral minerals and mineral surfaces warrant further experimental study.

7. Alteration during geochemical processes

7.1 Terrestrial geochemical alteration and the preservation of organics

If one were to order the classes of organics based on preservation potential and biological specificity, there would be an inverse relationship [261]. While DNA, RNA, and proteins can specifically fingerprint their biological source, they are also the most labile organic compound class [262,263]. Lipids, on the other hand, while present in many living organisms and can have high biological specificity, typically exhibit a broad range of sources. Lipids and their hydrocarbon derivatives are the most recalcitrant class of organic compound; therefore, over geologic time and under suitable conditions, they will be the most likely organic remnants [264,265].

There are some asymmetric reactions that are involved in the synthesis of (phospho)lipid membrane molecules (e.g., [266-269]). Although lipids are considered the most taphonomically-robust to degradation and alteration over long geologic timescales, they are not immediately associated with research into chiral organic compounds. Lipids possess chirality in the way that amino acids and sugars do, and commonly have multiple stereogenic centers leading to many different potential stereoisomers (discussed below). To understand how organics and biosignatures can be detected in samples, it is important to recognize the reactions and conditions that affect their sequestration and preservation. The following sections will describe the processes by which organic compounds are sequestered and preserved in the rock record and the ways in which chiral configurations can be affected by geological alteration.

7.2. Formation of insoluble macromolecular organic matter

On Earth, an average of >99% of organic matter (OM) produced from photosynthesis is rapidly remineralized during early diagenesis by biochemical degradation [270]. As organic matter is sequestered and buried in the sedimentary record, the physical and chemical processes known as diagenesis, catagenesis, and metagenesis take place. Diagenesis occurs during shallow burial at low temperatures, and physical and chemical processes continue to accumulate a small fraction of degradation-resistant OM which is polymerized and crosslinked to form a biomacromolecular matrix known as kerogen. During this process, many lipid components, which can act as biosignatures and are highly resistant to biochemical degradation, are bound within the insoluble organic matter (IOM) matrix [271]. Despite the rapid overturn of organic matter during the early stages of deposition [272] and the specific environmental conditions required for organic preservation [273], kerogen-like macromolecular OM is recovered even during this early phase [274,275] with the proportion of organics bound into the matrix increasing over geological time [275-277]. Catagenesis involves increases in burial temperature and depth over time with a significant component of heating that induces the cracking of the macromolecular structure to liberate shorter-chain hydrocarbons [278]. Metagenesis occurs at higher burial temperatures (low grade metamorphic temperatures, above 200 °C) and depths and involves the cracking of residual hydrocarbon bitumen into dry gas (>98% methane) and solidified pyrobitumen [273,279].

Although the definition of kerogen has evolved over time, traditionally it is operationally defined as the solid residue that remains after organic matter has been extracted with organic solvents [280-282]. For mature, consolidated kerogens, it typically also excludes the acid-digestible and hydrolyzable component containing organics that are associated with the mineral matrix [281]. The remainder of sedimentary organic matter is defined as the component that is readily extractable with organic solvents, known as bitumen. The components of kerogen consist of the sum of the simple organic precursor molecules that were sequestered into the macromolecular structure during sedimentary diagenetic and catagenetic processes.

Mineral substrates and matrices are critically important to the preservation of organic compounds [282-284] as they provide stability and protection to organics not only during deposition and sedimentary alteration, but also against harsh environmental conditions such as radiation (e.g., [285]). The kerogen macromolecular matrix provides long-term preservation of organics by protecting bound molecules from oxidation and degradation [286]. Kerogen is considered an immobile solid matrix; molecules linked within it were deposited synchronously with the host sedimentary rock. Bound lipids released from kerogen are much less prone to organic contamination from migrating fluids relative to their solvent extractable counterparts [287].

Kerogen is the largest sink of organic carbon on Earth [288] and expected to be the dominant mass fraction of preserved organic matter on other planetary bodies [21,289]. Post-depositional alteration processes such as the binding of organics are affected by steric hindrance, especially as the kerogen evolves and becomes more structurally and chemically complex. Hence, stereochemistry is an important consideration for the studies of bound and released organics from mineral and organic matrices. Utilizing techniques that release organic constituents either thermolytically (e.g., heating through pyrolysis) or chemolytically (e.g., selective chemical degradation through chemolysis) significantly enhances the analysis of kerogen, as both processes release products that are amenable to standard chromatographic resolution [287].

7.3 Stereochemistry of lipids in kerogen

The stereochemistry of the organic compounds, specifically the ratio of isomers, that are released through various experimental methods can reveal the thermal maturity conditions during sequestration. An example comes from common microbial cellular membrane lipids, steroids and hopanoids, which are polycyclic biomarker precursors derived primarily from eukaryotes and bacteria, respectively [278]. In the specific case of steroids, the C_{27} steroid (cholesterol) possesses eight asymmetric carbons in its structure, at C-3, 8, 9, 10, 13, 14, 17, and 20 [290]; giving rise to the possibility of numerous stereochemical configurations (Figure 4).

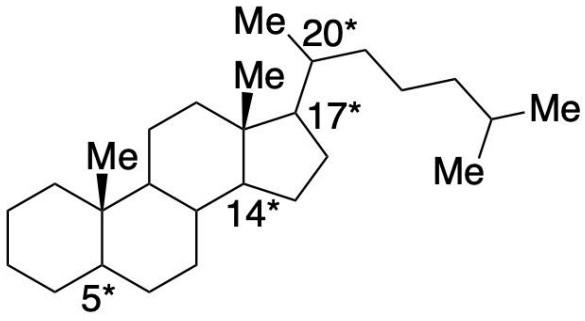

Figure 4. Structure of the C_{27} sterane, cholestane. The asterisk at C-5, C-14, C-17, and C-20 indicate where a H can be in the α- or β- configuration, and the carbon at C-20 can be the R or S enantiomer. The R enantiomer is the biological form, whereas the S enantiomer is the geologically-stable form.

However, only one biological isomer of cholesterol exists due to the high specificity of steroid biosynthesis [291]. The stereochemical configuration of immature/biologically-inherited steroids and hopanoids as their hydrocarbon equivalents are 20R-5α/β(H),14α(H),17α(H)-cholestane (C_{27} sterane) and 17β(H),21β(H)-hopane (C_{30} hopane), respectively. These stereochemical configurations are thermally unstable and they

isomerize to the stable forms of 20S-5α(H),14β(H),17β(H)-cholestane for steranes and 17α(H),21β(H)-hopane for hopanes over geological time, as these molecules relieve ring strain and convert from the flat, planar configuration to a bent configuration [278]. During incorporation into kerogen, the asymmetric centers of steranes and hopanes are protected from further thermal isomerization due to steric hindrance within the matrix [278], although the stereospecificity that is highly conserved in the biological form is often lost, with an array of isomers forming [292].

Isomerization, while primarily due to increases in temperature through thermal alteration, could also be catalyzed by clay minerals [293,294]. It has been demonstrated that mineralogy and salinity can affect oil generation kinetics as well as product composition [295,296]. Experimental techniques for fragmenting kerogen into analyzable components, such as pyrolysis assisted by high pressure hydrogen gas (hydropyrolysis; [287]), releases bound lipids that conserve the original stereochemistry during sequestration [275,297-301]. Thermochemolysis using tetramethylammonium hydroxide (TMAH) compared to standard hydrous pyrolysis shows differences in the stereochemical configuration of released hopanoid products [302], indicating configurational isomerization (epimerization) occurs during the analytical processes. Future experiments that track structural modifications to stereochemistry associated with simulated alteration and/or maturation processes will be critical to understanding the underlying mechanisms and transformation pathways that prevail during natural processes. They will help better identify and optimize the experimental techniques that should be employed to study these chemical reactions.

7.4 Compositional alteration on other planetary bodies

Meteorites can be classified as chondrites; which form from protoplanetary disk material [303,304], and achondrites; which have undergone secondary processes such as melting and differentiation [305,306]. Chondrite meteorites can be separated into ordinary, carbonaceous, Rumuruti, Kakangari, and enstatite chondrites [304,307]. The carbonaceous chondrite group can be further subdivided into eight main groups (Table 5), based on chemical (mineralogy and isotopic) composition and degree of alteration [308,309]. The six petrologic types describe the extent of aqueous (type 1, 2, and 3) and thermal (types 3, 4, 5, and 6) alteration, where type 1 is the most aqueously altered and type 6 is the most thermally altered [310]. Similar to how alteration and structural modifications to chemical composition can occur to organic matter on Earth, alteration can and does occur during the preservation of carbonaceous organic matter on other planetary bodies such as asteroids, comets, and planetary surfaces. These matrices are typically minerals associated with rocky or icy substrates and can occur on the surface regolith or in the parent body interior [311]. Alteration can occur through thermal or aqueous processes, shock wave propagation, and brecciation.

Table 5. Properties of carbonaceous chondrite meteorite groups, including: matrix abundances, chondrule abundances and sizes, refractory component abundances, metallic Fe and Ni abundances, average olivine compositions, and refractory lithophile element abundances. The carbonaceous chondrite meteorite groups are arranged from left to right (CI to CB) in order of decreasing bulk rock oxidation. Table is from [14] and data were compiled from [307,312-314].

Petrologic type	**CI**	**CM**	**CK**	**CV**	**CO**	**CR**	**CH**	**CB**
Petrologic type	1	1-2	3-6	2-3	3	1-2	3	3
Chondrule abundance (vol.%)	$\ll 1^{\dagger}$	$20^{\ddagger}$	15	45	40–48	50–60	~70	20–40
Matrix abundance (vol.%)	$> 99^{\dagger}$	$70^{\ddagger}$	75	40	30–34	30–50	5	< 5

Refractory abundance⧺ (vol.%)	≪ 1	5	4	10	13	0.5	0.1	< 0.1
Metal (Fe,Ni) abundance (vol.%)	≪ 1	0.1	≪ 1	0–5	1–5	5–8	20	60–80
Average chondrule diameter (mm)	n.a.	0.3	0.7–0.8	1.0	0.15	0.7	0.02–0.09	0.2–10
Olivine composition (mol% Fe_2SiO_4; range)	*	*	< 1–47	*	*		< 1–36	2–3
(mol% Fe_2SiO_4; mode)			29–33			1 - 3	2	3
Refractory lithophiles	1.00	1.15	1.21	1.35	1.13	1.03	1.00	1.0–1.4

†Including chondrule fragments and silicate minerals inferred to be chondrule fragments changes matrix and chondrule abundances to > 95 vol.% and < 5 vol. %, respectively.

‡Variable

⧺Calcium Aluminum Inclusions + Amoeboid Olivine Aggregates

*Highly variable and unequilibrated

⧻Mean ratio refractory lithophiles relative to Mg, normalized to CI chondrites

Thermal alteration characterized by increases in temperature can affect the mineralogical composition of chondrites through metamorphic reactions and localized recrystallization but not widespread melting (e.g., [315-319]). CK chondrites are a unique group of carbonaceous chondrites, the only group that has experienced the full range of thermal alteration types [210,320]. Thermal modeling has been used to constrain the cooling histories of different chondrite parent bodies and is often achieved through the use of elemental gradients, trace elemental and isotopic composition, and radiometric ages calculated from the closure temperature of minerals during crystallization [321-325].

Aqueous alteration occurs when water ice in the parent body melts due to heat generated through radioactive decay of elements [326]. Water can alter the primary composition (both mineralogically and isotopically) of parent body materials through dissolution and formation of secondary hydrous phases such as clays, serpentines, carbonates, sulfates, sulfides, halides, oxides, and oxyhydroxides [327]. Aqueous alteration can be determined through petrographic analysis of minerals, stable and radiogenic isotopes [328-332], as well as microtextures [333]. Although most chondrite groups have been affected by aqueous alteration to some degree, there are different types of aqueous alteration. Low temperature hydrothermal alteration occurs at temperatures below 200-300° C [334] and can form mineral phases such as phyllosilicates. At higher temperatures, typically above 300 °C [335], fluid-assisted metamorphism alters mineral composition. At similar temperatures, but in an open system where fluids are flowing through the rock and altering the composition, is referred to as metasomatism [336]. Some recent experimental studies have suggested that the initial parent body composition need not contain water, as heat from impact [337] or organic degradation [338] could induce aqueous alteration on parent bodies.

Alteration to physical and chemical properties by shock is a common and ongoing phenomenon in chondrites; this includes structural changes due to collision with meteorite parent bodies that can be related to pressure and temperature increases [339]. Shock propagation features can be difficult to deconvolve due to the heterogeneous nature of

chondrites [340]. Changes to composition can include localized melting at the site of impact, as well as fracture features.

Formation of meteorite breccias (brecciation) involves the high-speed impact of meteorites that combine with other fragments of parent bodies [341]. Studying meteorite breccias is important for understanding early Solar System processes and combines a variety of the above-mentioned techniques such as shock wave propagation, impact velocities, and textural analysis. Due to the variation in composition of the brecciated fragments, multiple parent body sources may be invoked.

Carbonaceous chondrites and the organic matter contained within them have been subject to thermal and aqueous processing. There are numerous studies that report on the effect of parent body alteration on amino acids, carboxylic acids, and nucleobase compositions [34,40,42,342-346]. The degree to which parent-body processing can affect organic molecule populations is largely dependent on the degree and type of alteration [347]. Petrological type 3 chondrites have undergone little to no thermal or aqueous processing (pristine). Types 1 and 2 have experienced aqueous alteration, while types 4, 5, and 6 have experienced thermal alteration, although not enough to start differentiation. The inventory (specific molecules and abundances) of organics can range markedly across meteorite class and degrees of alteration. For example, [45] reported amino acid distributions in CB and CH chondrites that differed markedly from those reported for type 2 and 3 CM and CR chondrites. The CB and CH chondrites contained beta-, gamma-, and delta-amino acid abundances that were much higher than the relative alpha amino acid abundances, evidencing multiple formation mechanisms. CI chondrites, which are type 1 (highest degree of aqueous alteration), have been reported to contain a higher abundance of beta-alanine relative to alpha-alanine and glycine, which is not the case of CM chondrites [42,348]. This suggests distinct parent bodies for CM and CI chondrites.

8. Laboratory analysis and reactions

8.1 Analytical instrumentation

In laboratory settings, mineral and metal substrates have been shown to be able to mediate different types of organic reactivity. This includes the synthesis of prebiotic materials such as nucleobases and amino acids, as well as promoting metabolically-relevant reactions [3-6,349-353]. In many of these cases, the enantioselectivity of the reaction was not explored. As we are growing to understand these factors, there are several avenues of research that can be explored to answer questions relevant to chirality at the origins of life. Herein, we summarize the alteration processes of minerals as well as relevant organic reactions that could impart asymmetry. We also make recommendations for future research endeavors in this field.

While the focus of this paper is organic reactions relevant to prebiotic chemistry and the origins of life, Table 1 highlights the diverse applications of enantioselective reactions for pharmaceutical, natural product, and other syntheses. Enantioselective synthesis plays a major role in pharmaceutical research, as drug design and testing investigate biological and pharmacological compounds that are chiral and whose chirality has significant implications on their active properties in biological systems [102,354,355]. As a result, there is much research centered around the analysis and detection of chiral compounds, the foremost being separation of enantiomers using chiral column chromatography [356,357]. Chirality can also be distinguished using spectroscopic and calorimetric techniques, and various other separation strategies (Table 6). While enantiomers have the same nuclear magnetic resonance (NMR) spectra, derivatization could allow for visible differences in the NMR by generating diastereomers or employing the use of chiral solvating agents

without the need for diastereomer distinction [358]. Light scattering has been used previously for enantiomeric separation; however, this is extremely sensitive to other materials within the solution [359,360] and is currently not widely used [229].

Table 6. Analytical instrumentation used for separation and detection of racemic mixtures into chiral enantiomers grouped by primary analytical techniques. Included are their relevant fields of application and whether or not the technique used for chiral separation has been proposed or demonstrated in spaceflight.

Instrument	Separation	Detector	Application	Mission Relevance	References
		Chromatography & Spectrometry			
Gas chromatography-Mass spectrometry	GC with a chiral column	MS	Organic chemistry; origins of life	Cometary Sampling and Composition (COSAC) - Rosetta: ***launched March 2004 but sampling unsuccessful*** Sample Analysis at Mars - Mars Science Laboratory: ***in progress, landed August 2012*** Mars Organic Molecule Analyzer (MOMA) - ExoMars: ***planned September 2022 launch***	361-365
Liquid chromatography-Mass spectrometry; high performance LC-MS	(HP)LC with a chiral column	MS (various)	Organic chemistry; origins of life	No	366-368
Sub- and supercritical Fluid Chromatography (SFC)	SF (CO_2 plus polar cosolvent)	Various: UV-Vis, diode-array, evaporative light scattering (ELS) detector, charged-aerosol detection, MS (atmospheric pressure chemical ionization, electrospray ionization)	Organic chemistry; forensics	No	369,370
Capillary Electrophoresis (CE)	CE	Laser-induced fluorescence (LIF)	Origins of life; organic chemistry; instrument development	Proposed	371-373
Capillary electrochromatography (CEC)	CE/HPLC	Various; UV detectors	Organic chemistry	No	374-376

Ligand exchange CE	CE	Various; UV detectors	Organic chemistry	No	377-379
Non-aqueous CE (NACE)	CE	Various detectors; UV, conductivity, MS, LIF	Organic chemistry; medicine	No	380
Ion-Mobility Mass Spectrometry (IM-MS)	Derivatization, chiral neutral gases	IM-MS	Organic chemistry; origins of life	Volatile Organic Analyzer (VOA) on the International Space Station (ISS); for air quality control not enantiomeric separation - ***deployed August 2001***	381-384
Photodissociation	Photodissociation in cold gas phase	Various MS; e.g., ESI	Biochemistry	No	385-387
Matrix-assisted laser desorption ionization (MALDI)-time of flight (TOF) MS	Stereosensitive fragmentation (SF)	MALDI-TOF/TOF MS	Biochemistry	No	388
Spectroscopy					
Nuclear Magnetic Resonance (NMR)	Various, derivatization (typically to form diastereomers)	NMR	Organic chemistry	No	358,389
Ultraviolet (UV)-Visible (Vis) spectrophotometry	Various	UV-Vis	Organic chemistry	No	390,391
Infrared (IR) spectroscopy	Various, e.g., CE, NACE	FT-IR	Organic Chemistry	No	392,393
Optical Rotatory Dispersion (ORD)	Polarized light	Detector	Organic chemistry	No	394,395
Circular Dichroism (CD)	Circularly polarized light	CD detector (various)	Organic chemistry; biochemistry	No	396-398
Femto-second (fs) laser mass spectrometry	fs-laser	MS	Organic chemistry	No	399
Polarimetry	Various; cavity ring-down, near IR	Detector, photodetector	Materials science; origins of life	Proposed	400-402
Optical techniques					

Evaporative Light Scattering (ELS)	Hydrophilic Interaction Chromatography (HILIC)	Light Scattering Detector (LSD)	Organic chemistry	No	403
ELS	High Performance Liquid Chromatography (HPLC)	LSD	Organic chemistry	No	404
Laser	Off-resonant laser beam	Detector	Nanotechnology	No	405
Atomic force microscopy (AFM)	Optical tweezers	Optical and AFM	Nanotechnology; materials science	No	406
Polarization camera	Micropolarizer array	Detector	Origins of life	Proposed	407
Calorimetry					
Differential Scanning Calorimetry (DSC)	Thermal	Calorimeter	Organic chemistry; macromolecules	No	254,408
Separation					
Batch crystallization	Various; e.g., chromatography	Model that calculates the optimal conditions for separation	Organic chemistry	No	409
Diastereoisomeric recrystallization	Crystallization	Various, e.g., MS, DSC, X-ray diffraction (XRD)	Organic chemistry	No	410-412
Kinetic resolution	Various, e.g., chiral catalysts	Various, e.g., HPLC-MS, ESI-MS	Organic chemistry	No	413-415
Labeling					
Fluorescent sensors/dyes	Various dyes, e.g., 5-carboxyfluorescein succinimidyl ester, fluorescamine	Various fluorescence detectors (e.g., confocal fluorescence microscope)	Origins of life; organic chemistry	Proposed	416-420

8.2 Solution phase reactions

For prebiotic chemistry, there are a variety of relevant asymmetric reactions (Table 1). Two important reactions for the synthesis of amino acids are reductive amination and the Strecker synthesis [421; see 422 and references therein]. In addition, the formose reaction [423] is a common reaction cited in prebiotic chemistry for the abiotic synthesis of sugars. In the following sections, we describe these reactions and their relevance to studying the origins of life and prebiotic chemistry.

8.2.1 Reductive amination

Reductive amination is a reaction of a carbonyl species (typically a ketone or aldehyde) with ammonia or an amine to generate an amine or an amino acid. The reaction occurs via synthesis of an imine precursor followed by reduction to access an amine as the final product. Figure 5 illustrates the reductive amination mechanism, indicating the chiral center generated. If the starting carbonyl material is an alpha keto-acid (e.g., pyruvic acid), the resulting product will be an amino acid, making this reaction relevant for the

origins of life. Biologically, amino acid dehydrogenases catalyze such transformations, which are dependent on cofactors like nicotinamide adenine dinucleotide (NADH) and nicotinamide adenine dinucleotide phosphate (NADPH) [424].

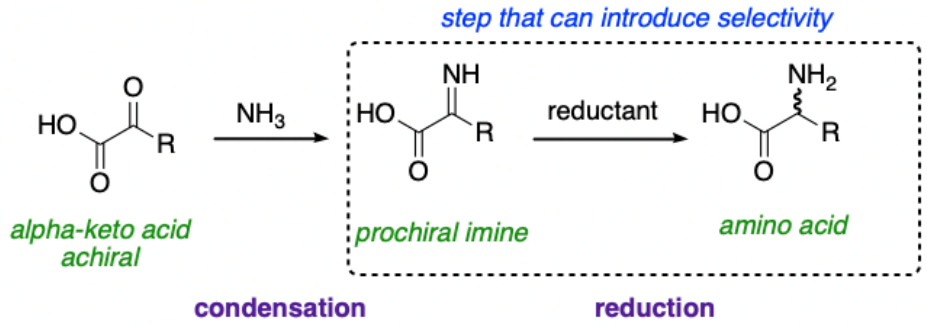

Figure 5. Reaction mechanism of an achiral alpha-keto acid reacting with ammonia to form a prochiral imine intermediate, which is then reduced to an amino acid. If the starting material is an aldehyde, an amine is the reaction product.

This reaction has been demonstrated to occur under geologic conditions [2-6,425] however, these reactions do not give enantiomeric excess and there are limited reports of prebiotic asymmetric reductive amination reactions. Nucleotides have been reported as efficient catalysts for this reaction under prebiotic conditions [426]. In the field of organic chemistry, there are a variety of asymmetric reductive aminations [e.g., 427-429].

8.2.2 Strecker synthesis

Another mechanism for synthesizing amino acids is through Strecker synthesis [75,430-433]. Strecker synthesis is a two-step process that, similar to reductive amination, begins with a carbonyl species like an aldehyde or a ketone. In the presence of ammonia and cyanide ions, it reacts to form an iminium ion intermediate followed by an attack of cyanide to form an α-aminonitrile. This is the selectivity inducing step. The aminonitrile is subsequently hydrolyzed under acidic conditions to form an amino acid (Figure 6). Strecker synthesis of amino acids form racemic products, but asymmetry can be imparted by substituting the ammonia in the reaction with chiral reagents [434-436].

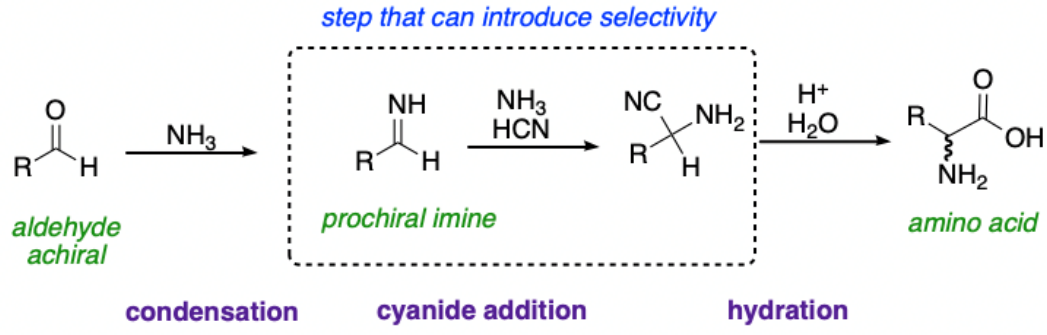

Figure 6. Reaction mechanism of an achiral aldehyde in presence of ammonia and cyanide to form an α-aminonitrile intermediate and an amino acid following hydrolysis.

In comparison to reductive amination, there are more asymmetric Strecker studies directly relevant to prebiotic chemistry. In addition, there are studies of the Strecker

synthesis by using a single crystal face [437]. Depending on the face of the crystal used, L- or D-amino acids can be generated. Relevant to prebiotic chemistry, the Strecker synthesis can also be mediated by ribose [438] to access selective amino acid synthesis.

8.2.3 Formose reaction

The formose reaction begins with formaldehyde, which once it condenses to form glycolaldehyde reacts autocatalytically to form sugars abiotically under alkaline conditions (Figure 7; [439]). Unlike the above examples, this reaction forms a variety of products related to sugars including methanol, formic acid, sugar alcohols, branched sugars, sugar oligomers, sugar acids, and hydroxy acids to name a few [174,440-442]. The formose reaction can be mediated by many different materials, including divalent cations, such as Ca^{2+} [443-446], and silicate minerals [447]. For a detailed review on conditions conducive for the formose reaction see [422] and references therein.

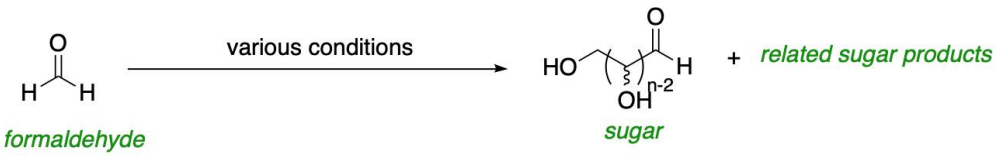

Figure 7. General outline of the formose reaction.

The formose reaction underpins the leading theory for the origin of sugars under prebiotic conditions (although the glyoxylate scenario is a proposed alternative; [448]) and as such, further studies of asymmetric formose reactions are therefore particularly important; especially considering that the formose reaction is autocatalytic and could thus generate large enantiomeric excess if mediated by even scarce amounts of a chiral seed (see *Section 6.5*) Previous work has demonstrated how formose reactions can result in enantiomeric excess of the resulting D-sugars when conducted under conditions such as UV-irradiation [449] or seeded with low concentrations of L-amino acids, namely proline [450,451].

8.3 Solid-state reactions

While many reactions of interest to the prebiotic chemistry field are in the solution phase (homogenous or heterogenous), solid-state chemical reactions could also be relevant to this field. It has been demonstrated that amino acids, nucleotides, nucleosides, peptides, and sugars can be formed under mechanochemical conditions [452-455]. Metal-mediated and metal-catalyzed reactions have been demonstrated under mechanochemical conditions [456]. There are also examples of asymmetric reactions in the solid state [457,458]. Mechanochemical studies utilize mechanical energy to generate reactivity [459]; common examples include ball mill grinding and milling. The advantages associated with mechanochemical synthesis include increased productivity and efficiency [460], as well as resource conservation. These experiments do not require hazardous or expensive solvents and have overall lower energy requirements, vis-a-vis solution reactions [461-463].

While this is used in organic chemistry and materials science [464,465], it is also applicable to planetary science and prebiotic chemistry as a way to mimic bombardment and other interactions. Early prebiotic organics could have been synthesized endogenously or delivered exogenously through impacts via asteroids or comets [466-469]. There is interest in simulating the effect of impacts on the petrologic [470,471] and organic [472-478] composition of prebiotically-relevant materials, through the mechanochemical action of shock-wave propagation. In addition to simulating cometary impact events, there are

impact simulations that investigate the effect of hypervelocity on the breakdown of organic compounds that are relevant for biosignature detection in spaceflight, particularly regarding spacecraft velocity during sampling [479-480].

9. Recommendations for future research

The origin of homochirality of life is a very broad topic; therefore, we recommend that multiple avenues should be explored. This includes experimental conditions/studies that are not directly applicable to prebiotic chemistry on Earth, which could be useful for understanding abiotic sources of organic homochirality and applied to the interpretation of potential biosignatures. We recommend, in the case of mineral-mediated organic reactivity, that the chirality of both the mineral substrate as well as the organic compound be taken into consideration. There has been a significant amount of research exploring mineral-mediated prebiotic reactions and exploring such reactions with chiral mineral mediators would augment understanding.

9.1 Capabilities of flight-ready technology

Significant enantiomeric excess is a potential biosignature [48,481]. As we look to find biosignatures on other planetary bodies, homochirality and organic preservation are two areas that deserve focus. The ability to determine chirality on other planetary bodies is an attractive endeavor, particularly in the astrobiology field. Additionally, organic preservation has been demonstrated to be enhanced by minerals and macromolecular matrices that provide protection against degradation, thus organic-mineral interactions are also an area of importance when looking for potential biosignatures on other planets. There are a variety of instrument technologies that have been proposed and designed for space missions that include a strong focus on colocated mineral and organic detection [482,483] and the separation of chiral organic molecules (e.g., [361,363,364]). The following sections describe the instruments, on three currently active missions (as of this writing), which are focused on the detection of chirality as a potential organic biosignatures.

COSAC on Rosetta's *Philae* lander

The separation of chiral organics via chiral column GC-MS has been proposed and flown on missions to comets [361,484,485] and Mars [363,364]. The European Space Agency (ESA)'s Rosetta mission launched a space probe in March 2004 to investigate the comet 67P/Churyumov-Gerasimenko. The mission consisted of the *Rosetta* spacecraft orbiter and the *Philae* lander. The ten instrument suite on the *Philae* lander was designed to investigate the physical and chemical composition of a cometary nucleus through elemental, isotopic, mineralogical, molecular, surface, subsurface, and structural analysis. The plan was to accomplish these goals via drilling, imagery, spectrometry (gas chromatography and alpha particle X-ray), gas analysis, radio transmission, surface and subsurface sensors, and magnetometry [486].

The chirality experiment involved two instrument subsystems; the sampling system (Sample Drilling and Distribution; SD2) and the GC-TOF-MS (Cometary Sampling and Composition; COSAC). SD2 consisted of a drill that was able to penetrate up to 230 mm into the subsurface to collect samples to deposit into a carousel with 26 ovens. The COSAC GC and TOF-MS had a total of eight GC columns on board, three of which were chiral GC columns (Table 7) with the capability to separate out and analyze amino acid enantiomers. Due to complications that occurred during *Philae's* detachment from the Rosetta spacecraft and landing on the surface of 67P/Churyumov-Gerasimenko in November 2004, the COSAC experiment was not attempted as a sample could not be acquired [365]. Although the chirality experiment was not conducted due to landing issues, COSAC was able to sample

the atmosphere in a passive mode, 25 minutes post-landing. The acquired mass spectrum indicated 16 organic species were present, including four compounds that had not previously been detected in comets [487].

Table 7. Chiral GC columns flown or proposed on missions for enantiomeric separation of organics. ESA–European Space Agency; NASA–National Aeronautics and Space Agency; MSL–Mars Science Laboratory; COSAC–Cometary Sampling and Composition; SAM–Sample Analysis at Mars; MOMA–Mars Organic Molecule Analyzer.

Agency	Mission	Status	Instrument	Total GC columns	Chiral column(s)
ESA	Rosetta	Flown but unsuccessful	COSAC	8	Chirasil Dex CB Chirasil L Val Cyclodextrin G-TA
NASA	MSL	In progress	SAM	6	Chirasil-β Dex CB
ESA/Roscosmos	ExoMars	Planned	MOMA	4	CP Chirasil Dex

SAM on MSL's *Curiosity* rover

The Martian surface and subsurface has long been considered a prime astrobiological life detection target [48,488-490]. Currently, information about the organic inventory and geological context of Mars is sourced from the study of Martian meteorites [491-493] as well as landed spacecraft that have or are currently exploring the Martian surface [494,495]. NASA's Mars Science Laboratory (MSL) *Curiosity* rover landed in Gale crater in August 2012. The instrument payload suite includes the Sample Analysis at Mars (SAM) instrument.

The SAM instrument's primary scientific goals include characterization of the composition of Martian atmosphere and the composition of organics within surface and subsurface sediments [363]. SAM consists of a tunable laser spectrometer (TLS), GC, and a quadrupole mass spectrometer (QMS). The GC has six chemically different 30 m columns for the separation of polar and non-polar organic compounds, one of which is a chiral column intended to separate volatile organic compound enantiomers (Table 7; 363). In a laboratory experiment designed to simulate the flight conditions of the chiral column on the SAM GC, Chirasil-β Dex was used to separate out chlorohydrocarbon compounds at low (35° C) and high (185° C) temperatures. The temperatures were chosen to approximate the dynamic range of temperatures that would be experienced in flight (30 °C and 200 °C are the minimum and maximum GC operating temperatures on SAM, respectively). The results of the experiment showed that 1,2-dichloropropane enantiomers were partially separated at the low temperature, however, at the higher temperature experiment, the enantiomers coeluted [496].

MOMA on ExoMars' *Rosalind Franklin* rover

ESA's and Roscosmos's *Rosalind Franklin* rover, part of the ExoMars mission, is scheduled for launch in September 2022 to land in Oxia Planum, Mars, in June 2023 [497]. The goal of the ExoMars mission is to look for signs of past or present life using an instrument suite that will characterize the geochemical environment contained in the surface and subsurface. With a drill capable of reaching 2 m into the subsurface, samples taken by *Rosalind Franklin* have a higher likelihood of containing sediments that are less affected by radiation and surface oxidation [498].

The Mars Organic Molecule Analyzer (MOMA) consists of a pyrolysis GC-MS and a laser desorption ionization MS (LDI-MS). These two techniques, which ionize samples

thermolytically through pyrolysis and induced by laser ionization, ensure that a wide range of small organic compounds as well as larger refractory phases, will volatilize for spectral analysis. The GC portion of MOMA contains four chemically distinct GC columns, one of which is a chiral column (Table 7), capable of separating enantiomers. Portions of the MOMA payload contain hardware heritage that is similar to the COSAC experiment aboard *Rosetta* and SAM aboard *Curiosity* [364].

Along with the flight models of the instruments discussed above, there exist many brassboard instruments in laboratories that can be used to enhance our knowledge and extend the capabilities of flight technology but with the full range of resources accessible to ground laboratories on Earth (e.g., [499]). We recommend continued testing of analog instruments that are in flight as well as proposed flight-ready instruments at all technology readiness levels (TRLs), along with the traditional techniques used for chiral detection. The generation of extensive datasets from analog and brassboard instruments will help to calibrate and interpret results returned from missions, as well as optimize parameters to be used in new instrument technologies.

9.2 Next generation instrumentation

In addition to existing instruments, the development of new instruments or instrument capabilities to detect chirality in spaceflight is a necessary component in the search for signs of past life. Advancements in the fields of organic separation (e.g., [500-504]) and detection through mass spectrometry [505,506] are needed to enhance the field of chiral separation on spaceflight missions. Refinement of traditional chiral separation and detection methods as well as the development of new analytical strategies to investigate chiral organics [407,420,507-509] and minerals [510] should be prioritized. Analytical advancements, coupled with advances in spaceflight technology, represent an exciting step forward in the study of prebiotic chemistry and the detection of chirality on Earth and other planetary bodies.

9.3 Contamination control

Habitability and life detection missions commonly need to address issues related to contamination and outgassing in accordance with guidelines suggested by the International Committee on Space Research (COSPAR) for planetary protection (e.g., [48,511,512]). Missions and proposed mission concepts that address contamination control issues are typically or wholly concerned with adhering to the requirements set out by planetary protection (PP) guidelines, through verification and quantification of bioburden on instrument and spacecraft surfaces. Bioburden, a quantitative measure of the number of viable microorganisms on any given surface, is not only important to verify from the perspective of PP (so as not to contaminate a planetary body with Earth microorganisms and vice versa), but to ensure that the in situ measurements being made in low biomass environments are genuine, and not a false positive as a result of cross-contamination [513].

Organic contamination in in situ chemical analysis during spaceflight is always a prime concern, particularly given the low threshold of background organic material, which would amplify any detection of trace organic contaminants. Missions focused on life detection and biosignature preservation that target sensitive parameters such as amino acid enantiomeric excess, need to prioritize contamination control not only during spacecraft assembly and testing but also instrument operations and data returned for analysis [514]. When determining chirality in organic compounds during life detection missions, contamination could arise from malfunctioning instrumentation [515], sampling [365], or terrestrial contamination [516]. Strategies employed for dealing with contamination include the use of sterilization procedures, e.g., decontamination heaters, UV

radiation, chemical, and low-heat plasma ([517] and references therein) and limiting the use of solvents and/or derivatization agents [500].

9.4 Future directions

There are many fields that are interested in and actively researching the chirality of organic and mineral systems, as evidenced by the extensive and growing number of enantioselective techniques (reactions and analytical applications) being developed (Tables 1, 6). While research in chirality has been dominated by organic synthesis of natural products and bioactive compounds of interest to the pharmaceutical industry, its relevance and importance continues to grow in the field of life detection and origins of life. Research in combining state-of-the-art separation and detection techniques with analog and laboratory studies to constrain conditions in which asymmetric prebiotic reactions are favored. This would increase our understanding of what life requires, or what conditions should be present for life to be established and to thrive, regardless of whether it is life that is familiar to us or not. In order to address the use of chiral asymmetry as a biosignature, multidisciplinary collaboration is key to facilitating the development of new technology which could lead to new field-defining instrumentation [124,422,518 and references therein].

10. Conclusions

Homochirality is of great interest and importance to prebiotic chemistry as well as those researching the origins of life. Chirality is an important property observed in both organic materials and mineral structures and these structural properties have implications for reactivity and analysis. Understanding both organic and mineral chiral systems is relevant for prebiotic chemistry, as the origins of life had to occur in a geologic context of some kind. We have described asymmetric organic reactions as well as mineral alterations that involve chiral systems to emphasize their relevance to geological processes and highlight the diversity in their applications. Lastly, we recommended some future research directions in the field of chiral organic and mineral systems, in particular, technological and scientific advancements that include: 1) Identifying additional chiral organics and chiral minerals that could be used as biosignatures; 2) Focusing on geologically and astrobiologically-relevant reactions and systems; and 3) Designing instruments that can be modified for spaceflight and remote operation to further the search for life on other planets.

Supplementary Materials: The following supporting information can be downloaded at: www.mdpi.com/xxx/s1, Table S1: List of chiral minerals identified by their space group.

Funding: JMW and LMB were supported by NASA/NSF Ideas Lab for the Origins of Life, "Becoming Biotic: Recapitulating Ancient Cofactor-Mediated Metabolic Pathways on the Early Earth". JMW, LMB, and LER were supported by JPL Strategic Research and Technology Development (R&TD), "Fate of Organics on Ocean Worlds." RYS was supported by a JPL Strategic Research and Technology Development (R&TD), "Experimental Constraints on Groundwater Driven Redox Gradients on Mars."

Data Availability Statement: Not Applicable

Acknowledgments: The authors acknowledge assistant editor Vinky Peng for handling the manuscript and three anonymous reviewers for providing constructive comments that improved the manuscript's final version. Work by JMW, LER, RYS, LMB was carried out at the Jet Propulsion Laboratory, California Institute of Technology, under a contract with the National Aeronautics and Space Administration (80NM0018D0004).

Conflicts of Interest: The authors declare no conflict of interest.

1171

References

1. Cafferty, B.J.; Gállego, I.; Chen, M.C.; Farley, K.I.; Eritja, R.; Hud, N.V. Efficient self-assembly in water of long noncovalent polymers by nucleobase analogues. *J. Am. Chem. Soc.* **2013**, 135(7), 2447-2450. https://doi.org/10.1021/ja312155v
2. Novikov, Y.; Copley, S.D. Reactivity landscape of pyruvate under simulated hydrothermal vent conditions. *Proc Natl Acad Sci U S A* **2013**, 110(33), 13283-13288. https://doi.org/10.1073/pnas.1304923110
3. Muchowska, K.B.; Varma, S.J.; Chevallot-Beroux, E.; Lethuillier-Karl, L.; Li, G.; Moran, J. Metals promote sequences of the reverse Krebs cycle. *Nature Ecology & Evolution* **2017**, 1, 1716-1721. https://doi.org/10.1038/s41559-017-0311-7
4. Muchowska, K.B.; Varma, S.J.; Moran, J. Synthesis and breakdown of universal metabolic precursors promoted by iron. *Nature* **2019**, 569(7754), 104-107. https://doi.org/10.1038/s41586-019-1151-1
5. Barge, L.M.; Flores, E.; Baum, M. M.; VanderVelde, D. G.; Russell, M. J. Redox and pH gradients drive amino acid synthesis in iron oxyhydroxide mineral systems. *Proc Natl Acad Sci U S A* **2019**, 116(11), 4828-4833. https://doi.org/10.1073/pnas.1812098116
6. Barge, L.M.; Flores, E.; VanderVelde, D.G.; Weber, J.M.; Baum, M.M.; Castonguay, A. Effects of geochemical and environmental parameters on abiotic organic chemistry driven by iron hydroxide minerals. *JGR: Planets* **2020**, 125(11), e2020JE006423. https://doi.org/10.1029/2020JE006423
7. Kitadai, N.; Nakamura, R.; Yamamoto, M.; Takai, K.; Yoshida, N.; Oono, Y. Metals likely promoted protometabolism in early ocean alkaline hydrothermal systems. *Sci. Adv.* **2019**, 5(6), eaav7848. https://doi.org/10.1126/sciadv.aav7848
8. Fani, R. The origin and evolution of metabolic pathways: Why and how did primordial cells construct metabolic routes? *Evolution: Education and Outreach* **2012**, 5, 367-381. https://doi.org/10.1007/s12052-012-0439-5
9. Preiner, M.; Xavier, J.C.; do Nascimento Vieria, A.; Kleinermanns, K.; Allen, J.F.; Martin, W.F. Catalysts, autocatalysis and the origin of metabolism. *Interface Focus* **2019**, 20190027 http://doi.org/10.1098/rsfs.2019.0072
10. Vogt, P.F.; Miller, M.J. Development and applications of amino acid-derived chiral acylnitroso hetero Diels-Alder reactions. *Tetrahedron* **1998**, 54(8), 1317-1348. https://doi.org/10.1016/S0040-4020(97)10072-2
11. Zhou, J.; Tang, Y. The development and application of chiral trisoxazolines in asymmetric catalysis and molecular recognition. *Chem Soc Rev 2005*, 34, 664-676. https://doi.org/10.1039/B408712G
12. Smith, D.K. Lost in translation? Chirality effects in the self-assembly of nanostructured gel-phase materials. *Chem Soc Rev* **2009**, 38, 684-694. https://doi.org/10.1039/B800409A
13. Li, Y.; Pan, B.; He, X.; Xia, W.; Zhang, Y.; Liang, H.; Subba Reddy, C.V.; Cao, R.; Qiu, L. Pd-catalyzed asymmetric Suzuki–Miyaura coupling reactions for the synthesis of chiral biaryl compounds with a large steric substituent at the 2-position. Beilstein J. Org. Chem. 2020, 16, 966–973. https://doi.org/10.3762/bjoc.16.85
14. Burton, A.S.; Berger, E.L. Insights into abiotically-generated amino acid enantiomeric excesses found in meteorites. *Life* **2018**, 8, 14. http://doi.org/10.3390/life8020014
15. Blackmond, D.G. The origin of biological homochirality. *Cold Spring Harb. Perspect. Biol*. **2019**, 11, a032540. https://doi.org/10.1101/cshperspect.a032540
16. Sczepanski, J.T.; Joyce, G.F. A cross-chiral RNA polymerase ribozyme. *Nature* **2014**, 515(7527), 440-442. https://doi.org/10.1038/nature13900
17. Glavin, D.P.; Burton, A.S.; Elsila, J.E.; Aponte, J.C.; Dworkin, J.P. The search for chiral asymmetry as a potential biosignature in our Solar System. *Chem. Rev.* **2020a**, 120(11), 4660-4689. https://doi.org/10.1021/acs.chemrev.9b00474
18. Ehrenfreund, P.; Irvine, W.; Becker, L., Blank, J.; Brucato, J.R.; Colangeli, L.; Derenne, S.; Despois, D.; Dutrey, A.; Fraaije, H. Astrophysical and astrochemical insights into the origin of life. *Reports on Progress in Physics* **2002**, 65(10), 1427. https://doi.org/10.1088/0034-4885/65/10/202
19. Kwok, S. The synthesis of organic and inorganic compounds in evolved stars. *Nature* **2004**, 430, 985-991. https://doi.org/10.1038/nature02862
20. Kwok, S. Organic matter in space: from star dust to the Solar System. *Astrophysics and Space Science* **2008**, 319, 5-21. https://doi.org/10.1007/s10509-008-9965-6
21. Kwok, S. Complex organics in space from Solar System to distant galaxies. *The Astronomy and Astrophysics Review* **2016**, 24, 8. https://doi.org/10.1007/s00159-016-0093-y
22. Ehrenfreund, P.; Cami, J. Cosmic carbon chemistry: From the interstellar medium to the early Earth. *Cold Spring Harb Perspect Biol.* **2010**, 2(12), a002097. https://doi.org/10.1101/cshperspect.a002097
23. Ehrenfreund, P.; Charnley, S.B. Organic molecules in the interstellar medium, comets, and meteorites: A voyage from dark clouds to the Early Earth. *Annual Review of Astronomy and Astrophysics* **2000**, 38(1), 427-483. https://doi.org/10.1146/annurev.astro.38.1.427
24. Brandenburg A. Homochirality: A prerequisite or consequence of life? In *Prebiotic Chemistry and the Origin of Life. Advances in Astrobiology and Biogeophysics*; Neubeck A., McMahon S. Eds.; Springer: Cham, 2021. https://doi.org/10.1007/978-3-030-81039-9_4
25. Frank, F.C. 1953. On spontaneous asymmetric synthesis. *Biochimica et Biophysica Acta* **1953**, 11, 459-463. https://doi.org/10.1016/0006-3002(53)90082-1
26. Soai, K.; Shibata, T.; Morioka, H.; Choji, K. Asymmetric autocatalysis and amplification of enantiomeric excess of a chiral molecule. *Nature* **1995**, 378, 767-768. https://doi.org/10.1038/378767a0

27. Soai, K.; Osanai, S.; Kadowaki, K.; Yonekubo, S.; Shibata, T.; Sato, I. d- and l-quartz-promoted highly enantioselective synthesis of a chiral organic compound. *J. Am. Chem. Soc.* **1999**, 121(48), 11235-11236. https://doi.org/10.1021/ja993128t
28. Orme, C.A.; Noy, A.; Wierzbicki, A.; McBride, M.T.; Grantham, M.; Teng, H.H.; Dove, P.M.; DeYoreo, J.J. Formation of chiral morphologies through selective binding of amino acids to calcite surface steps. *Nature* **2001**, 411, 775-779. https://doi.org/10.1038/35081034
29. Wagner, A.J.; Zubarev, D.Y.; Aspuru-Guzik, A.; Blackmond, D.G. Chiral sugars drive enantioenrichment in prebiotic amino acid synthesis. *ACS Cent Sci* **2017**, 3(4), 322-328. https://doi.org/10.1021/acscentsci.7b00085
30. Flores, J.J.; Bonner, W.A.; Massey, G.A. Asymmetric photolysis of (RS)-leucine with circularly polarized ultraviolet light. *J. Am. Chem. Soc.* **1977**, 99(11), 3622-3625. https://doi.org/10.1021/ja00453a018
31. Takano, Y.; Takahashi, J.; Kaneko, T.; Marumo, K.; Kobayashi, K. Asymmetric synthesis of amino acid precursors in interstellar complex organics by circularly polarized light. *Earth and Planetary Science Letters* **2007**, 254(1-2), 106-114. https://doi.org/10.1016/j.epsl.2006.11.030
32. Modica, P.; Meinert, C.; de Marcellus, P.; Nahon, L.; Meierhenrich, U.J.; Le Sargent d'Hendecourt, L. Enantiomeric excesses induced in amino acids by ultraviolet circularly polarized light irradiation of extraterrestrial ice analogs: A possible source of asymmetry for prebiotic chemistry. *The Astrophysical Journal* **2014**, 788(1), 79. https://doi.org/10.1088/0004-637X/788/1/79
33. Pizzarello, S.; Wang, Y.; Chaban, G.M. A comparative study of the hydroxy acids from the Murchison, GRA 95229 and LAP 02342 meteorites. *Geochimica et Cosmochimica Acta* **2010**, 74(21), 6206-6217. https://doi.org/10.1016/j.gca.2010.08.013
34. Aponte, J.C.; Elsila, J.E.; Hein, J.E.; Dworkin, J.P.; Glavin, D.P.; McLain, H.L.; Parker, E.T.; Cao, T.; Berger, E.L.; Burton, A.S. Analysis of amino acids, hydroxy acids, and amines in CR chondrites. *Meteorit Planet Sci*. **2020**, 55(11), 2422-2439. https://doi.org/10.1111/maps.13586
35. Cronin, J.R.; Pizzarello, S. Enantiomeric excesses in meteoritic amino acids. *Science* **1997**, 275(5302), 951-959. https://doi.org/10.1126/science.275.5302.951
36. Engel, M.H.; Macko, S.A. Isotopic evidence for extraterrestrial non- racemic amino acids in the Murchison meteorite. *Nature* **1997**, 389, 265-268. https://doi.org/10.1038/38460
37. Pizzarello, S.; Cronin, J.R. Alanine enantiomers in the Murchison meteorite. *Nature* **1998**, 394, 236. https://doi.org/10.1038/28306
38. Pizzarello, S.; Cronin, J.R. Non-racemic amino acids in the Murray and Murchison meteorites. *Geochimica et Cosmochimica Acta* **2000**, 64(2), 329-338. https://doi.org/10.1016/S0016-7037(99)00280-X
39. Pizzarello, S.; Zolensky, M.; Turk, K.A. Nonracemic isovaline in the Murchison meteorite: chiral distribution and mineral association. *Geochimica et Cosmochimica Acta* **2003**, 67(8), 1589-1595. https://doi.org/10.1016/S0016-7037(02)01283-8
40. Glavin, D.P.; Dworkin, J.P. Enrichment of the amino acid l-isovaline by aqueous alteration on CI and CM meteorite parent bodies. *Proceedings of the National Academy of Sciences of the United States of America* **2009**, 106(14), 5487-5492. https://doi.org/10.1073/pnas.0811618106
41. Herd, C.D.K.; Blinova, A.; Simkus, D.N.; Huang, Y.; Tarozo, R.; Alexander, C.M.O'D.; Gyngard, F.; Nittler, L.R.; Cody, G.D.; Fogel, M.L.; Kebukawa, Y.; Kilcoyne, A.L.D.; Hilts, R.W.; Slater, G.F.; Glavin, D.P.; Dworkin, J.P.; Callahan, M.P.; Elsila, J.E.; de Gregorio, B.T.; Stroud, R.M. Origin and evolution of prebiotic organic matter as inferred from the Tagish Lake meteorite. *Science* **2011**, 332(6035), 1304-1307. https://doi.org/10.1126/science.1203290
42. Glavin, D.P.; Callahan, M.P.; Dworkin, J.P.; Elsila, J.E. The effects of parent body processes on amino acids in carbonaceous chondrites. *Meteoritics & Planetary Science* **2010** 45(12), 1948-1972. https://doi.org/10.1111/j.1945-5100.2010.01132.x
43. Glavin, D.P.; Elsila, J.E.; Burton, A.S.; Callahan, M.P.; Dworkin, J.P.; Hilts, R.W.; Herd, C.K. Unusual nonterrestrial L-proteinogenic amino acid excesses in the Tagish Lake meteorite. *Meteoritics & Planetary Science* **2012**, 47(8), 1347-1364. https://doi.org/10.1111/j.1945-5100.2012.01400.x
44. Pizzarello, S.; Schrader, D.L.; Monroe, A.A.; Lauretta, D.S. Large enantiomeric excesses in primitive meteorites and the diverse effects of water in cosmochemical evolution. *Proc Natl Acad Sci U S A* **2012**, 109(30), 11945-11954. https://doi.org/10.1073/pnas.1204865109
45. Burton, A.S.; Elsila, J.E.; Hein, J.E.; Glavin, D.P.; Dworkin, J.P. Extraterrestrial amino acids identified in metal-rich CH and CB carbonaceous chondrites from Antarctica. *Meteoritics & Planetary Science* **2013**, 48(3), 390-402. https://doi.org/10.1111/maps.12063
46. Cooper, G.; Rios, A.C. Enantiomer excesses of rare and common sugar derivatives in carbonaceous meteorites. *Proc Natl Acad Sci U S A* **2016**, 113(24), E3322-E3331. https://doi.org/10.1073/pnas.1603030113
47. Thiemann, W. Life and chirality beyond the earth. *Origins Life Evol Biosph.* **1975**, 6, 475–481. https://doi.org/10.1007/BF00928896
48. Neveu, M.; Hays, L.E.; Voytek, M.A.; New, M.H.; Schulte, M.D. The ladder of life detection. *Astrobiology* **2018**, 18(11), 1375-1402. https://doi.org/10.1089/ast.2017.1773
49. Avnir, D. Critical review of chirality indicators of extraterrestrial life. *New Astronomy Reviews* **2021**, 92, 101596. https://doi.org/10.1016/j.newar.2020.101596
50. Aliashkevich, A; Alvarez, L; Cava, F. New insights into the mechanisms and biological roles of D-amino acids in complex ecosystems. *Front. Microbiol*. **2018**, 9, 683. https://doi.org/10.3389/fmicb.2018.00683
51. Sasabe, J.; Suzuki, M. Emerging role of D-amino acid metabolism in the innate defense. *Front. Microbiol.* **2018**, 9, 933. https://doi.org/10.3389/fmicb.2018.00933
52. Hu, Y.; Zheng, Q.; Zhang, S.; Noll, L.; Wanek, W. Significant release and microbial utilization of amino sugars and D-amino acid enantiomers from microbial cell wall decomposition in soils. *Soil Biol Biochem.* **2018**, 23, 115-125. https://doi.org/10.1016/j.soilbio.2018.04.024

53. Pikuta, E.V.; Hoover, R.B.; Klyce, B.; Davies, P.C.W.; Davies, P. Bacterial utilization of L-sugars and D-amino acids. Proc. SPIE 6309, Instruments, Methods, and Missions for Astrobiology IX 2006, 63090A. https://doi.org/10.1117/12.690434
54. Clayden, J.; Geeves, N.; Warren, S. *Organic Chemistry*, 2nd ed.; Oxford University Press: Oxford, United Kingdom, 2012.
55. Cross, L.C.; Klyne, W. Rules for the nomenclature of organic chemistry. Section E: Stereochemistry. *Pure & Applied Chemistry* **1974**, 45, 11-30. https://doi.org/10.1515/iupac.45.0002
56. Gualtieri, G.; Geib, S.J.; Curran, D.P. A new class of chiral organogermanes derived from C2-symmetric dithiols: synthesis, characterization and stereoselective free radical reactions. *J. Org. Chem* **2003**, 68(13), 5013-5019. https://doi.org/10.1021/jo026625s
57. Böhme, U.; Wiesner, S.; Günther, B. Easy access to chiral penta- and hexacoordinate silicon compounds. *Inorganic Chemistry Communications* **2006**, 9(8), 806-809. https://doi.org/10.1016/j.inoche.2006.05.002
58. Koga, S.; Ueki, S.; Shimada, M.; Ishii, R.; Kurihara, Y.; Yamanoi, Y.; Yuasa, J.; Kawai, T.; Uchida, T.; Iwamura, M.; Nozaki, K.; Nishihara, H. Access to chiral silicon centers for application to circularly polarized luminescence materials. *J. Org. Chem* **2017**, 82(12), 6108-6117. https://doi.org/10.1021/acs.joc.7b00583
59. Xu, L-W. Chapter 4 - Chiral organosilicon compounds. *Organosilicon compounds: Theory and experiment (Synthesis)* 2017, 145-194. https://doi.org/10.1016/B978-0-12-801981-8.00004-6
60. Montgomery, C.D. Factors affecting energy barriers for pyramidal inversion in amines and phosphines: A computational chemistry lab exercise. *J. Chem. Educ* **2013**, 90(5), 661-664. https://doi.org/10.1021/ed300527t
61. Mandal, N.; Pal, A.K.; Gain, P.; Zohaib, A.; Datta, A. Transition-state-like planar structures for amine inversion with ultralong C–C bonds in diamino-o-carborane and diamino-o-dodecahedron. *J. Am. Chem. Soc* **2020**, 142(11), 5331-5337. https://doi.org/10.1021/jacs.0c00181
62. Kölmel, C.; Ochsenfeld, C.; Ahlrichs, R. An ab initio investigation of structure and inversion barrier of triisopropylamine and related amines and phosphines. *Theoretica Chimica Acta* **1992**, 82, 271-284. https://doi.org/10.1007/BF01113258
63. Marom, H.; Biedermann, U.; Agranat, I. Pyramidal inversion mechanism of simple chiral and achiral sulfoxides: A theoretical study. *Chirality* **2007**, 19(7), 559-569. https://doi.org/10.1002/chir.20417
64. Xiao, Y.; Sun, Z.; Guo, H.; Kwon, O. Chiral phosphines in nucleophilic organocatalysis. *Beilstein J Org Chem*. **2014**, 10, 2089-2121. https://doi.org/10.3762/bjoc.10.218
65. Scott, K.A.; Njardarson, J.T. Analysis of US FDA-approved drugs containing sulfur atoms. *Top Curr Chem* **2018**, 376, 5. https://doi.org/10.1007/s41061-018-0184-5
66. Bentley, R. Role of sulfur chirality in the chemical processes of biology. *Chem Soc Rev* **2005**, 34(7), 609-624. https://doi.org/10.1039/b418284g
67. Wang, W.; Xiang, S.; Zhou, X.; Ji, Y.; Xiang, B. Enantiomeric separation and determination of the enantiomeric impurity of armodafinil by capillary electrophoresis with sulfobutyl ether-β-cyclodextrin as chiral selector. *Molecules* **2012**, 17(1), 303-314. https://doi.org/10.3390/molecules17010303
68. Lemouzy, S.; Giordano, L.; Hérault, D.; Buono, G. Introducing chirality at phosphorus atoms: An update on the recent synthetic strategies for the preparation of optically pure P-stereogenic molecules. *European Journal of Organic Chemistry* **2020**, 2020(13), 3351-3366. https://doi.org/10.1002/ejoc.202000406
69. Feng, H-X.; Tan, R.; Liu, Y-K. An efficient one-pot approach to the construction of chiral nitrogen-containing heterocycles under mild conditions. *Org. Lett.* **2015**, 17(15), 3794-3797. https://doi.org/10.1021/acs.orglett.5b01772
70. Walsh, M.P.; Phelps, J.M.; Lennon, M.E.; Yufit, D.S.; Kitching, M.O. Enantioselective synthesis of ammonium cations. *Nature* **2021**, 597, 70-76. https://doi.org/10.1038/s41586-021-03735-5
71. Rickhaus, M.; Mayor, M.; Juríček, M. Strain-induced helical chirality in polyaromatic systems. *Chem. Soc. Rev*. **2016**. 45, 1542-1556. https://doi.org/10.1039/C5CS00620A
72. Hassan, Z.; Spuling, E.; Knoll, D.M.; Lahann, J.; Bräse, S. Planar chiral [2.2]paracyclophanes: from synthetic curiosity to applications in asymmetric synthesis and materials. *Chem. Soc. Rev*. **2018**, 47(18), 6947-6963. https://doi.org/10.1039/C7CS00803A
73. Noyori, R.; Takaya, H.; Sayo, N.; Kumobayashi, H.; Akutagawa, S. Asymmetric hydrogenation of β-keto carboxylic esters. A practical, purely chemical access to β-hydroxy esters in high enantiomeric purity. *J. Am. Chem. Soc.* **1987**, 109(19), 5856-5858. https://doi.org/10.1021/ja00253a051
74. Welch, C.J.; Biba, M.; Sajonz, P. Fast methods of enantiopurity determination for the Soai reaction: Towards a general enantioenrichment detector? *Chirality* **2007**, 19(1), 34-43. https://doi.org/10.1002/chir.20336
75. Wang, J.; Liu, X.; Feng, X. Asymmetric Strecker reactions. *Chem. Rev.* **2011**, 111(11), 6947-6983. https://doi.org/10.1021/cr200057t
76. Ma, D.; Tian, H.; Zou, G. Asymmetric Strecker-type reaction of α-aryl ketones. Synthesis of (S)-αM4CPG, (S)-MPPG, (S)-AIDA, and (S)-APICA, the antagonists of metabotropic glutamate receptors. *J. Org. Chem.* **1999**, 64(1), 120-125. https://doi.org/10.1021/jo981297a
77. Wang, C.; Xiao, J. Asymmetric reductive amination. *Top. Curr. Chem.* **2014**, 343, 261-282. https://doi.org/10.1007/128_2013_484
78. Tian, Y.; Hu, L.; Wang, Y-Z.; Zhang, X.; Yin, Q. Recent advances on transition-metal-catalysed asymmetric reductive amination. *Organic Chemistry Frontiers* **2021**, 8, 2328-2342. https://doi.org/10.1039/D1QO00300C
79. Ritson, D.; Sutherland, J. Prebiotic synthesis of simple sugars by photoredox systems chemistry. *Nature Chemistry* **2012**, 4(11), 895-899. https://doi.org/10.1038/nchem.1467
80. Stick, R.V.; Williams, S.J. The reactions of monosaccharides. In *Carbohydrates: The essential molecules of life*, 2nd ed.; Elsevier Science, 2009, pp. 75-131. https://doi.org/10.1016/B978-0-240-52118-3.X0001-4

81. Katsuki, T.; Sharpless, K.B. The first practical method for asymmetric epoxidation. *J. Am. Chem. Soc.* **1980**, 102(18), 5974-5976. https://doi.org/10.1021/ja00538a077
82. Jacobsen, E.N.; Marko, I.; Mungall, W.S.; Schroeder, G.; Sharpless, K.B. Asymmetric dihydroxylation via ligand-accelerated catalysis. *J. Am. Chem. Soc.* **1988**, 110(6), 1968-1970. https://doi.org/10.1021/ja00214a053
83. Sharp, T.G.; DeCarli, P.S. Shock effects in meteorites. In *Meteorites and the early Solar System II*, Lauretta, D.S., McSween Jr., H.Y., Eds.; University of Arizona Press: Arizona, United States, 2006, pp. 653-677.
84. Midland, M.M.; Lee, P.E. Efficient asymmetric reduction of acyl cyanides with B-3-pinanyl 9-BBN (Alpine-borane). *J. Org. Chem.* **1985**, 50(17), 3237-3239. https://doi.org/10.1021/jo00217a053
85. Noyori, R.; Takaya, H.; Sayo, N.; Kumobayashi, H.; Akutagawa, S. Asymmetric hydrogenation of β-keto carboxylic esters. A practical, purely chemical access to β-hydroxy esters in high enantiomeric purity. *J. Am. Chem. Soc.* **1987**, 109(19), 5856-5858. https://doi.org/10.1021/ja00253a051
86. Hirao, A.; Itsuno, S.; Nakahama, S.; Yamazaki, N. Asymmetric reduction of aromatic ketones with chiral alkoxy-amineborane complexes. *Journal of the Chemical Society, Chemical Communications* **1981**, 7, 315-317. https://doi.org/10.1039/C39810000315
87. Corey, E.J.; Bakshi, R.K.; Shibata, S. Highly enantioselective borane reduction of ketones catalyzed by chiral oxazaborolidines. Mechanism and synthetic implications. *J. Am. Chem. Soc.* **1987**, 109(18), 5551-5553. https://doi.org/10.1021/ja00252a056
88. Corey, E.J. Catalytic enantioselective Diels–Alder reactions: Methods, mechanistic fundamentals, pathways, and applications. *Angew. Chem. Int. Ed.* **2002**, 41, 1650-1667. https://doi.org/10.1002/1521-3773(20020517)41:10<1650::AID-ANIE1650>3.0.CO;2-B
89. Evans, D.A.; Chapman, K.T.; Bisaha, J. New asymmetric Diels-Alder cycloaddition reactions. Chiral .alpha.,.beta.-unsaturated carboximides as practical chiral acrylate and crotonate dienophile synthons. *J. Am. Chem. Soc.* **1984**, 106, 4261-4263. https://doi.org/10.1021/ja00327a031
90. Kozmin, S.A.; Rawal, V.H. Chiral amino siloxy dienes in the Diels−Alder reaction: Applications to the asymmetric synthesis of 4-substituted and 4,5-disubstituted cyclohexenones and the total synthesis of (−)-α-elemene. *J. Am. Chem. Soc.* **1999**, 121, 9562-9573. https://doi.org/10.1021/ja9921930
91. Hashimoto, S.; Komeshima, N.; Koga, K. Asymmetric Diels–Alder reaction catalysed by chiral alkoxyaluminium dichloride. *J. Chem. Soc., Chem. Commun*. **1979**, 10, 437-438. https://doi.org/10.1039/C39790000437
92. Corey, E.J.; Imwinkelried, R.; Pikul, S.; Xiang, Y. Practical enantioselective Diels-Alder and aldol reactions using a new chiral controller system. *J. Am. Chem. Soc.* **1989**, 111, 5493-5495. https://doi.org/10.1021/ja00196a081
93. Kagan, H.B.; Riant, O. Catalytic asymmetric Diels Alder reactions. *Chemical Reviews* **1992**, 92(5), 1007-1019. https://doi.org/10.1021/cr00013a013
94. Cammidge, A.N.; Crépy, K.V.L. The first asymmetric Suzuki cross-coupling reaction. *Chemical Communications* **2000**, 18, 1723-1724. https://doi.org/10.1039/B004513F
95. Schäfer, P.; Palacin, T.; Sidera, M.; Fletcher, S.P. Asymmetric Suzuki-Miyaura coupling of heterocycles via rhodium-catalysed allylic arylation of racemates. *Nature Communications* **2017**, 8, 15762. https://doi.org/10.1038/ncomms15762
96. Yuan, Y.; Yang, J.; Lei, A. Recent advances in electrochemical oxidative cross-coupling with hydrogen evolution involving radicals. *Chem. Soc. Rev.* **2021**, 50(18),10058-10086. https://doi.org/10.1039/D1CS00150G
97. Zheng, P.; Zhou, P.; Wang, D.; Xu, W.; Wang, H.; Xu, T. Dual Ni/photoredox-catalyzed asymmetric cross-coupling to access chiral benzylic boronic esters. *Nature Communications* **2021**, 12, 1646. https://doi.org/10.1038/s41467-021-21947-1
98. Lautens, M.; Loup, J. Asymmetric reductive cross-coupling of aryl iodides with α-chloroboranes by nickel/photoredox catalysis. *Synfacts* **2021**, 17(06), 0657. https://doi.org/10.1055/s-0040-1720645
99. Yuan, M.; Gutierrez, O. Mechanisms, challenges, and opportunities of dual Ni/photoredox-catalyzed C (sp2)–C (sp3) cross-couplings. *Wiley Interdisciplinary Reviews: Computational Molecular Science* **2021**, e1573. https://doi.org/10.1002/wcms.1573
100. Cosgrove, S.C.; Thompson, M.P.; Ahmed, S.T.; Parmeggiani, F.; Turner, N.J. One-pot synthesis of chiral N-arylamines by combining biocatalytic aminations with Buchwald–Hartwig N-arylation. *Angew. Chem. Int. Ed.* **2020**, 59(41), 18156-18160.https://doi.org/10.1002/anie.202006246
101. Zhang, P.; Wang, X-M.; Xu, Q.; Guo, C-Q.; Wang, P.; Lu, C-J. Enantioselective synthesis of atropisomeric biaryls by Pd-catalyzed asymmetric Buchwald–Hartwig amination. *Angewandte Chemie International Edition* **2021**, 60(40), 21718-21722. https://doi.org/10.1002/anie.202108747
102. Brooks, W.H.; Guida, W.C.; Daniel, K.G. The significance of chirality in drug design and development. *Current Topics in Medicinal Chemistry* **2011**, 11(7), 760-770. https://doi.org/10.2174/156802611795165098
103. Wang, Z. Advances in the asymmetric total synthesis of natural products ssing chiral secondary amine catalyzed reactions of α,β-unsaturated aldehydes. *Molecules* **2019**, 24(18), 3412. https://doi.org/10.3390/molecules24183412
104. MacMillan, D.W.C. – Facts – 2021. NobelPrize.org. Nobel Prize Outreach AB 2021. URL: https://www.nobelprize.org/prizes/chemistry/2021/macmillan/facts/ Accessed 30 November 2021.
105. Ahrendt, K.A.; Borths, C.J.; MacMillan, D.W.C. New strategies for organic catalysis: The first highly enantioselective organocatalytic Diels−Alder reaction. *J. Am. Chem. Soc.* **2000**, 122(17), 4243-4244. https://doi.org/10.1021/ja000092s
106. List, B., Lerner, R.A.; Barbas, C.F. Proline-catalyzed direct asymmetric Aldol reactions. *J. Am. Chem. Soc.* **2000**, 122(10), 2395-2396. https://doi.org/10.1021/ja994280y
107. Jacobsen, E.N.; MacMillan, D.W.C. Organocatalysis. *Proceedings of the National Academy of Sciences of the United States of America* **2010**, 107(48), 20618-20619. https://doi.org/10.1073/pnas.1016087107

108. Zhou, Q-L. Privileged chiral ligands and catalysts. Wiley-VCH Verlag GmbH & Co. KGaA: 2011. https://doi.org/10.1002/9783527635207
109. Reetz, M.T.; Sell, T.; Meiswinkel, A.; Mehler, G. A new principle in combinatorial asymmetric transition-metal catalysis: Mixtures of chiral monodentate P ligands. Angew. *Chem. Int. Ed*. **2003**, 42(7), 790-793. https://doi.org/10.1002/anie.200390209
110. Yang, H.; Tang, W. Efficient enantioselective syntheses of chiral natural products facilitated by ligand design. *Chemical Record* **2020**, 20(1), 23-40. https://doi.org/10.1002/tcr.201900003
111. Hamilton, G.L.; Kang, E.J.; Mba, M.; Toste, F.D. A powerful chiral counterion strategy for asymmetric transition metal catalysis. *Science* **2017**, 317(5837), 496-499. https://doi.org/10.1126/science.1145229
112. Herdeis, C.; Hubmann, H.P.; Lotter, H. Chiral pool synthesis of trans-(2S3S)-3-hydroxyproline and castanodiol from S-pyroglutamic acid. *Tetrahedron: Asymmetry* **1994**, 5(1), 119-128. https://doi.org/10.1016/S0957-4166(00)80492-9
113. Brill, Z.G.; Condakes, M.L.; Ting, C.P.; Maimone, T.J. Navigating the chiral pool in the total synthesis of complex terpene natural products. *Chem. Rev*. **2017**, 117(18), 11753-11795. https://doi.org/10.1021/acs.chemrev.6b00834
114. Cherney, A.H.; Kadunce, N.T.; Reisman, S.E. Enantioselective and enantiospecific transition-metal-catalyzed cross-coupling reactions of organometallic reagents to construct C–C bonds. *Chem. Rev*. **2015**, 115(17), 9587-9652. https://doi.org/10.1021/acs.chemrev.5b00162
115. Toste, F.D.; You, S-L. Asymmetric synthesis enabled by organometallic complexes. *Organometallics* **2019**, 38(20), 3899-3901. https://doi.org/10.1021/acs.organomet.9b00627
116. Parshall, G.W. Trends and opportunities for organometallic chemistry in industry. *Organometallics* **1987**, 6(4), 687-692. https://doi.org/10.1021/om00147a001
117. Tang, J.; Redl, F.; Zhu, Y.; Siegrist, T.; Brus, L.E.; Steigerwald, M.L. An organometallic synthesis of TiO2 nanoparticles. *Nano Lett.* **2005**, 5(3), 543-548. https://doi.org/10.1021/nl047992h
118. Amiens, C.; Chaudret, B.; Ciuculescu-Pradines, D.; Collière, V.; Fajerwerg, K.; Fau, P.; Kahn, M.; Maisonnat, A.; Soulantica, K.; Phillipot, K. Organometallic approach for the synthesis of nanostructures. New Journal of Chemistry 2013, 37, 3374-3401. https://doi.org/10.1039/C3NJ00650F
119. Martins, P.; Marques, M.; Coito, L.; Pombeiro, A.J.L.; Baptista, P.V.; Fernandes, A.R. Organometallic compounds in cancer therapy: Past lessons and future directions. *Anticancer Agents Med Chem*. **2014**, 14(9), 1199-1212. https://doi.org/10.2174/1871520614666140829124925
120. Campeau, L-C.; Fogg, D.E. The roles of organometallic chemistry in pharmaceutical research and development. *Organometallics* **2019**, 38(1), 1-2. https://doi.org/10.1021/acs.organomet.8b00918
121. Kumar, A.; Sharma, R.; Kamaluddin, M.R. Formamide-based synthesis of nucleobases by metal(II) octacyanomolybdate(IV): implication in prebiotic chemistry. *Astrobiology* **2014**, 14(9), 769-779. https://doi.org/10.1089/ast.2014.1187
122. Fioroni, M. Transition metal organometallic/metallorganic chemistry: Its role in prebiotic chemistry and life's origin. In *Prebiotic chemistry and the origin of life. Advances in Astrobiology and Biogeophysics*; Neubeck, A.; McMahon, S., Eds.; Springer, Cham. pp. 1-41. https://doi.org/10.1007/978-3-030-81039-9_1
123. Frenkel-Pinter, M.; Sargon, A.B.; Glass, J.B.; Hud, N.V.; Williams, L.D. Transition metals enhance prebiotic depsipeptide oligomerization reactions involving histidine. *RSC Adv* **2021**, 11, 3534-3538. https://doi.org/10.1039/D0RA07965K
124. Barge, L.M.; Rodriguez, L.E.; Weber, J.M.; Theiling, B. Determining the "biosignature threshold" for life detection on biotic, abiotic, or prebiotic worlds. *Astrobiology* **2021**, https://doi.org/10.1089/ast.2021.0079
125. Kharasch, M.S.; Reynolds, W.B. Factors determining the course and mechanisms of Grignard reactions. X. The oxidation of Grignard reagents—Effect of metallic catalysts. *J. Am. Chem. Soc.* **1943**, 65(4), 501-504. https://doi.org/10.1021/ja01244a005
126. Bäckvall, J.E.; Sellen, M.; Grant, B. Regiocontrol in copper-catalyzed Grignard reactions with allylic substrates. *J. Am. Chem. Soc.* **1990**, 112(18), 6615-6621. https://doi.org/10.1021/ja00174a024
127. Herrmann, W.A.; Brossmer, C.; Reisinger, C-P.; Riermeier, T.H. Öfele, K.; Beller, M. Palladacycles: Efficient new catalysts for the Heck vinylation of aryl halides. *Chemistry A European Journal* **1997**, 3(8), 1357-1364. https://doi.org/10.1002/chem.19970030823
128. Martin, W.B.; Kateley, L.J. The Heck reaction: A microscale synthesis using a palladium catalyst. J. Chem. Educ. 2000, 77(6), 757. https://doi.org/10.1021/ed077p757
129. Bhakta, S.; Ghosh, T. Emerging nickel catalysis in Heck reactions: Recent developments. *Advanced Catalysis & Synthesis* **2020**, 362(23), 5257-5274. https://doi.org/10.1002/adsc.202000820
130. Phan, N.T.S.; Van Der Sluys, M.; Jones, C.W. On the nature of the active species in palladium catalyzed Mizoroki–Heck and Suzuki–Miyaura couplings–homogeneous or heterogeneous catalysis, a critical review. *Advanced Synthesis & Catalysis* **2006**, 348(6), 609-679. https://doi.org/10.1002/adsc.200505473
131. Martin, R.; Buchwald, S.L. Palladium-catalyzed Suzuki-Miyaura cross-coupling reactions employing dialkylbiaryl phosphine ligands. *Acc Chem Res* **2008**, 41(11), 1461-1473. https://doi.org/10.1021/ar800036s
132. Percival, W.C.; Wagner, R.B.; Cook, N.C. Grignard reactions. XXI. The synthesis of aliphatic ketones. *J. Am. Chem. Soc*. **1953**, 75(15), 3731-3734. https://doi.org/10.1021/ja01111a036
133. Hazari, N.; Melvin, P.R.; Beromi, M.M. Well-defined nickel and palladium precatalysts for cross-coupling. *Nat Rev Chem* **2017**, 1, 0025. https://doi.org/10.1038/s41570-017-0025
134. Weber, J.M.; Longstreet, A.R.; Jamison, T.F. Bench-stable nickel precatalysts with Heck-type activation. *Organometallics* **2018**, 37(16), 2716-2722. https://doi.org/10.1021/acs.organomet.8b00351

135. Patel, B.H.; Percivalle, C.; Ritson, D.J.; Duffy, C.D.; Sutherland, J.D. Common origins of RNA, protein and lipid precursors in a cyanosulfidic protometabolism. *Nature Chemistry* **2015**, 7, 301-307. https://doi.org/10.1038/nchem.2202
136. Bartnikas, T.B.; Gitlin, J.D. How to make a metalloprotein. *Nature Structural & Molecular Biology* **2001**, 8, 733-734. https://doi.org/10.1038/nsb0901-733
137. Messina, M.S.; Stauber, J.M.; Waddington, M.A.; Rheingold, A.L.; Maynard, H.D.; Spokoyny, A.M. Organometallic gold(III) reagents for cysteine arylation. *J. Am. Chem. Soc.* **2018**, 140(23), 7065-7069. https://doi.org/10.1021/jacs.8b04115
138. Kamo, N.; Kujirai, T.; Kurumizaka, H.; Murakami, H.; Hayashi, G.; Okamoto, A. Organoruthenium-catalyzed chemical protein synthesis to elucidate the functions of epigenetic modifications on heterochromatin factors. Chem Sci. 2021, 12, 5926-5937. https://doi.org/10.1039/D1SC00731A
139. Isied, S.; Lyon, J.; Vassilian, A. Peptide formation in the presence of metal ion protecting groups. II. Determination of the optical purity of amino acids and peptides bound to pentaamine cobalt (III). *Int J Pept Protein Res*. **1982**, 19(4), 354-360.
140. Arbo, B.E.; Isied, S. Solid-phase synthesis of protected peptides using new cobalt(III) ammine linkers. *Int J Pept Protein Res*. **1993**, 42(2), 138-154. https://doi.org/10.1111/j.1399-3011.1993.tb00490.x
141. Ruf, A.; Kanawati, B.; Hertkorn, N.; Yin, Q-Z.; Moritz, F.; Harir, M.; Lucio, M.; Michalke, B.; Wimpenny, J.; Shilobreeva, S.; Bronsky, B.; Saraykin, V.; Gabelica, Z.; Gougeon, R.D.; Quirico, E.; Ralew, S.; Jakubowski, T.; Haack, H.; Gonsior, M.; Jenniskens, P.; Hinman, N.W.; Schmitt-Kopplin, P. Previously unknown class of metalorganic compounds revealed in meteorites. *P Natl Acad Sci USA* **2017**, 114(11), 2819-2824. https://doi.org/10.1073/pnas.1616019114
142. Smith, K.E.; House, C.H.; Arevalo Jr., R.D.; Dworking, J.P.; Callahan, M.P. Organometallic compounds as carriers of extraterrestrial cyanide in primitive meteorites. *Nature Communications* **2019**, 10, 2777. https://doi.org/10.1038/s41467-019-10866-x
143. Matzka, M.; Lucio, M.; Kanawati, B.; Quirico, E.; Bonal, L.; Loehle, S.; Schmitt-Kopplin, P. Thermal history of asteroid parent bodies is reflected in their metalorganic chemistry. *ApJL* **2021**, 915, L7.
144. Lunine, J.I. Origin of water ice in the Solar System. In *Meteorites and the Early Solar System II*, Lauretta, D.S., McSween, H.Y., Eds.; University of Arizona Press, Arizona, United States, 2006, pp. 309-319.
145. Slade, M.A.; Butler, B.J.; Muhleman, D.O. Mercury radar imaging: Evidence for polar ice. *Science* **1992**, 258, 635-640. https://doi.org/10.1126/science.258.5082.635
146. Ingersoll, A.P.; Svitek, T.; Murray, B.C. Stability of polar frosts in spherical bowl-shaped craters on the Moon, Mercury, and Mars. *Icarus* **1992**, 100(1), 40-47. https://doi.org/10.1016/0019-1035(92)90016-Z
147. Paige, D.A.; Wood, S.E.; Vasavada, A.R. The thermal stability of water ice at the poles of Mercury. *Science* **1992**, 258, 643-646. https://doi.org/10.1126/science.258.5082.643
148. Namur, O.; Collinet, M.; Charlier, B.; Grove, T.L.; Holtz, F.; McCammon, C. Melting processes and mantle sources of lavas on Mercury. *Earth & Planetary Science Letters* **2016**, 439, 117-128. https://doi.org/10.1016/j.epsl.2016.01.030
149. Namur, O.; Charlier, B. Silicate mineralogy at the surface of Mercury. *Nature Geoscience* **2017**, 10, 9-13. https://doi.org/10.1038/ngeo2860
150. Khodakovsky, I.L.; Volkov, V.P.; Sidorov, Y.I.; Borisov, M.V. Venus: Preliminary prediction of the mineral composition of surface rocks. *Icarus* **1979**, 39(3), 352-363. https://doi.org/10.1016/0019-1035(79)90146-5
151. Fegley, B.; Treiman, A.H.; Sharpton, V.L. Venus surface mineralogy: Observational and theoretical constraints. *Proceedings of Lunar and Planetary Science* **1992**, 22, 3-19.
152. Buffet, B.; Archer, D. Global inventory of methane clathrate: sensitivity to changes in the deep ocean. *Earth Planet Sci Lett* **2004**, 227, 185-199. https://doi.org/10.1016/j.epsl.2004.09.005
153. Prockter, L.M. Ices in the Solar System. *Johns Hopkins APL Technical Digest* **2005**, 26(2).
154. Reimold, W. U.; Gibson, R. L. Processes on the early Earth. *Geological Society of America* **2006**, 405. https://doi.org/10.1130/SPE405
155. Westall, F.; Brack, A. The importance of water for life. *Space Sci Rev* **2018**, 214, 50. https://doi.org/10.1007/s11214-018-0476-7
156. Taylor, S.R.; Jakes, P. The geochemical evolution of the Moon. *Proc. Lunar Sci. Conf.* **1974**, 5, 1287-1305.
157. Li, S.; Lucey, P.G.; Milliken, R.E.; Hayne, P.O.; Fisher, E.; Williams, J.-P.; Hurley, D.M.; Elphic, R.C. Direct evidence of surface exposed water ice in the lunar polar regions. *Proceedings of the National Academy of Sciences.* **2018**, 115(36), 8907-8912. https://doi.org/10.1073/pnas.1802345115
158. Gendrin, A.; Mangold, N.; Bibring, J.-P.; Langevin, Y.; Gondet, B.; Poulet, F.; Bonello, G.; Quantin, C.; Mustard, J.; Arvidson, R.; LeMouélic, S. Sulfates in martian layered terrains: The OMEGA/Mars Express view. *Science* **2005**, 307, 1587–91. https://doi.org/10.1126/science.1109087
159. Bibring, J.-P.; Langevin, Y.; Mustard, J.F.; Poulet, F.; Arvidson, R.; Gendrin, A.; Gondet, B.; Mangold, N.; Pinet, P.; Forget, F.; Berthé, M.; Bibring, J.-P.; Gendrin, A.; Gomez, C.; Gondet, B.; Jouglet, D.; Poulet, F.; Soufflot, A.; Vincendon, M.; Comes, M.; Drossart, P.; Encrenaz, T.; Fouchet, T.; Merchiorri, R.; Belluci, G.; Altieri, F.; Formisano, V.; Capaccioni, F.; Cerroni, P.; Coradini, A.; Fonti, S.; Korablev, O.; Kottsov, V.; Ignatiev, N.; Moroz, V.; Titov, D.; Zasova, L.; Loiseau, D.; Mangold, N.; Pinet, P.; Douté, S.; Schmitt, B.; Sotin, C.; Hauber, E.; Hoffmann, H.; Jaumann, R.; Keller, U.; Arvidson, R.; Mustard, J.F.; Duxbury, T.; Forget, F.; Neukum, G. Global mineralogical and aqueous Mars history derived from OMEGA/Mars Express data. *Science* **2006**, 312(5772), 400-404. https://doi.org/10.1126/science.1122659
160. Lasue, J.; Mangold, N.; Hauber, E.; Clifford, S.; Feldmann, W.; Gasnault, O.; Grima, C.; Maurice, S.; Mousis, O. Quantitative assessments of the Martian hydrosphere. *Space Sci Rev* **2013**, 174,155-212. https://doi.org/10.1007/s11214-012-9946-5

161. Mousis O.; Chassefière, E.; Holm, N.G.; Bouquet, A.; Hunter Waite, J.; Geppert, W.D.; Picaud, S.; Aikawa, Y.; Ali-Dib, M.; Charlou, J-L., Rousselot, P. Methane clathrates in the Solar System. *Astrobiology* **2015**, 15(4), 308-326. https://doi.org/10.1089/ast.2014.1189
162. Owen, T.C.; Roush, T.L.; Cruikshank, D.P.; Elliot, J.L.; Young, L.A.; de Bergh, C.; Schmitt, B.; Geballe, T.R.; Brown, R.H.; Bartholomew, M.J. Surface ices and the atmospheric composition of Pluto. *Science* **1993**, 261(5122), 745-748. https://doi.org/10.1126/science.261.5122.745
163. Mousis, O.; Gautier, D.; Coustenis, A. The D/H ratio in methane in Titan: Origin and history. *Icarus* **2002**, 159,156-165. https://doi.org/10.1006/icar.2002.6930
164. Rivkin A. S., Howell E. S., Vilas F., and Lebofsky L. A. Hydrated minerals on asteroids: The astronomical record. In *Asteroids III*, Bottke Jr., W.F. et al., Eds.; University of Arizona Press: Arizona, United States, 2002, pp. 235-253.
165. Fujiwara, A.; Kawaguchi, J.; Yeomans, D.K.; Abe, M.; Okada, T.; Saito, J.; Yano, H.; Yoshikawa, M.; Scheeres, D.J.; Barnouin-Jha, O.; Cheng, A.F.; Demura, H.; Gaskell, R.W.; Hirata, N.; Ikdea, H.; Kominato, T.; Miyamoto, H.; Nakamura, A.M.; Nakamura, R.; Sasaki, S.; Uesugi, K. The rubble-pile asteroid Itokawa as observed by Hayabusa. *Science* **2006**, 312, 1330-1334. https://doi.org/10.1126/science.1125841
166. Waite, J.H.; Jr., Lewis, W.S.; Magee, B.A.; Lunine, J.I.; McKinnon, W.B.; Glein, C.R.; Mousis, O.; Young, D.T.; Brockwell, T.; Westlake, J.; Nguyen, M.-J.; Teolis, B.D.; Niemann, H.B.; McNutt, R.L.; Perry, M.; Ip, W.-H. Liquid water on Enceladus from observations of ammonia and ^{40}Ar in the plume. *Nature* **2009**, 460,487-490. https://doi.org/10.1038/nature08153
167. Schwartz, A.W. Did minerals perform prebiotic combinatorial chemistry? *Chemistry & Biology* **1996**, 3, 515-518. https://doi.org/10.1016/s1074-5521(96)90140-4
168. Walton, C.R.; Shorttle, O.; Jenner, F.E.; Williams, H.M.; Golden, J.; Morrison, S.M.; Downs, R.T.; Zerkle, A.; Hazen, R.M.; Pasek, M. Phosphorus mineral evolution and prebiotic chemistry: From minerals to microbes. *Earth-Science Reviews* **2021**, 221, 103806. https://doi.org/10.1016/j.earscirev.2021.103806
169. Bass, M.N. Montmorillonite and serpentine in Orgueil meteorite. *Geochimica et Cosmochimica Acta* **1971**, 35(2), 139-147. https://doi.org/10.1016/0016-7037(71)90053-6
170. Tomeoka, K.; Buseck, P.R. Intergrown mica and montmorillonite in the Allende carbonaceous chondrite. *Nature* **1982**, 299, 326-327. https://doi.org/10.1038/299326a0
171. Pinnavaia, T.J. Intercalated clay catalysts. *Science* **1983**, 220(4595), 365-371. https://doi.org/10.1126/science.220.4595.365
172. Herschy, B.; Whicher, A.; Camprubí, E.; Watson, C.; Dartnell, L.; Ward, J.; Evans, J.R.G.; Lane, N. An origin-of-life reactor to simulate alkaline hydrothermal vents. *Journal of Molecular Evolution* **2014**, 79, 213-227. https://doi.org/10.1007/s00239-014-9658-4
173. Sojo, V.; Herschy, B.; Whicher, A.; Camprubí, E.; Lane, N. The origin of life in alkaline hydrothermal vents. *Astrobiology* **2016**, 16(2), 181-197. https://doi.org/10.1089/ast.2015.1406
174. Kitadai, N.; Maruyama, S. Origins of building blocks of life: A review. *Geoscience Frontiers* **2018**, 9(4), 1117-1153. https://doi.org/10.1016/j.gsf.2017.07.007
175. Mompeán, C.; Marín-Yaseli, M.R.; Espigares, P.; González-Toril, E.; Zorzano, M-P.; Ruiz-Bermejo, M. Prebiotic chemistry in neutral/reduced-alkaline gas-liquid interfaces. *Scientific Reports* **2019**, 9, 1916. https://doi.org/10.1038/s41598-018-36579-7
176. Kadoya, S.; Krissansen-Totton, J.; Catling, D.C. Probable cold and alkaline surface environment of the Hadean Earth caused by impact ejecta weathering. *Geochemistry, Geophysics, Geosystems* **2020**, 21(1), e2019GC008734. https://doi.org/10.1029/2019GC008734
177. Hazen, R.M.; Sverjensky, D.A. Mineral surfaces, geochemical complexities, and the origins of life. *Cold Spring Harbor Perspectives in Biology* **2010**, 2, A002162. https://doi.org/10.1101/cshperspect.a002162
178. Bernal, J.D. The physical basis of life. *Proceedings of the Physical Society. Section B* **1951**, 62(10), 597.
179. Paecht-Horowitz, M.; Eirich, F.R. The polymerization of amino-acid adenylates on sodium montmorillonite with preadsorbed polypeptides. *Orig. Life Evol. Biosph.* **1988**, 18, 359-387. https://doi.org/10.1007/BF01808216
180. Ferris, J.P.; Ertem, G. Oligomerization of ribonucleosides on montmorillonite: reaction of the 5′-phosphoimidazolide of adenosine. *Science* **1992**, 257(5075), 1387-1389. https://doi.org/10.1126/science.1529338
181. Pitsch, S.; Eschenmoser, A.; Gedulin, B.; Hui, S.; Arrhenius, G. Mineral-induced formation of sugar phosphates. *Orig. Life Evol. Biosph.* **1995**, 25, 297-334. https://doi.org/10.1007/BF01581773
182. Jiang, W.; Pacella, M.S.; Athanasiadou, D.; Nelea, V.; Vali, H.; Hazen, R.M.; Gray, J.J.; McKee, M.D. Chiral acidic amino acids induce chiral hierarchical structure in calcium carbonate. *Nature Communications* **2017**, 8, 15066. https://doi.org/10.1038/ncomms15066
183. Addadi, L.; Weiner, S. Crystals, asymmetry and life. *Nature* **2001**, 411, 753-755. https://doi.org/10.1038/35081227
184. Grande, C.; Patel, N.H. Nodal signalling is involved in left-right asymmetry in snails. *Nature* **2009**, 457(7232), 1007-1011. https://doi.org/10.1038/nature07603
185. Hazen, R.M. Chiral crystal faces of common rock-forming minerals. In *Progress in biological chirality*, Palyi, G., Zucchi, C., Caglioti, L., Eds.; Oxford: Elsevier, 2004, pp.137-151.
186. Hazen, R.M.; Filley, T.R.; Goodfriend, G.A. Selective adsorption of L- and D-amino acids on calcite: Implications for biochemical homochirality. *Proceedings of the National Academy of Sciences of the United States of America* **2001**, 98(10), 5487-5490. https://doi.org/10.1073/pnas.101085998
187. Hazen, R.M.; Sholl, D.S. Chiral selection on inorganic crystalline surfaces. *Nature Materials* **2003**, 2, 367-374. https://doi.org/10.1038/nmat879

188. Hazen, R.M. Mineral surfaces and the prebiotic selection and organization of biomolecules. *American Mineralogist* **2006**, 91, 1715-1729. https://doi.org/10.2138/am.2006.2289
189. Cody, A.M.; Cody, R.D. Chiral habit modifications of gypsum from epitaxial-like adsorption of stereospecific growth inhibitors. *Journal of Crystal Growth* **1991**, 113(3-4), 508-519. https://doi.org/10.1016/0022-0248(91)90086-K
190. Bortnovsky, O.; Sobafik, Z.; Wichterlová, B.; Bastl, Z. Structure of Al-Lewis site in beta zeolite active in the Meerwein-Ponndorf-Verley reduction of ketone to alcohol. *J. Catal.* **2002**, 210, 171-182. https://doi.org/10.1006/jcat.2002.3661
191. Ponnamperuma C.; Shimoyama, A.; Friebele, E. Clay and the origin of life. *Origins of Life* **1982**, 12, 9-40. https://doi.org/10.1007/BF00926908
192. Siffert. B.; Naidja, A. Stereoselectivity of montmorillonite in the adsorption and deamination of some amino acids. *Clay Minerals* **1992**, 27(1), 109-118. https://doi.org/10.1180/claymin.1992.027.1.11
193. Ikeda, T.; Amoh, H.; Yasunaga, T. Stereoselective exchange kinetics of L- and D-histidines for chloride in the interlayer of a hydrotalcite-like compound by the chemical relaxation method. *J. Am. Chem. Soc.* **1984**, 106(20), 5772-5775. https://doi.org/10.1021/ja00332a002
194. Fraser, D.G.; Fitz, D.; Jakschitz, T.; Rode, B.M. Selective adsorption and chiral amplification of amino acids in vermiculite clay-implications for the origin of biochirality. *Physical Chemistry Chemical Physics* **2011a**, 13(3), 831-838. https://doi.org/10.1039/C0CP01387K
195. Fraser, D.G.; Greenwell, H.C.; Skipper, N.T.; Smalley, M.V.; Wilkinson, M.A.; Deme, B.; Heenan, R. K. Chiral interactions of histidine in a hydrated vermiculite clay. *Physical Chemistry Chemical Physics* **2011b**, 13(3), 825-830. https://doi.org/10.1039/C0CP01387K
196. Downs, R.T.; Hazen, R.M. Chiral indices of crystalline surfaces as a measure of enantioselective potential. *Journal of Molecular Catalysis A: Chemical* **2004**, 216(2), 273-285. https://doi.org/10.1016/j.molcata.2004.03.026
197. Garcia, A.D.; Meinert, C.; Finger, F.; Meierheinrich, U.J.; Hejl, E. Racemate resolution of alanine and leucine on homochiral quartz, and its alteration by strong radiation damage. *Life (Basel)* **2021**, 11(11), 1222. https://doi.org/10.3390/life11111222
198. Thompson, R.M.; Downs, R.T. Quantifying distortion from ideal closest-packing in a crystal structure with analysis and application. *Acta Crystallographica Section B* **2001**, 57, 119-127. https://doi.org/10.1107/S0108768100016979
199. Amariglio, A.; Amariglio, H.; Duval, X. Asymmetric reactions on optically active quartz. *Helv. Chim. Acta* **1968**, 51, 2110-2115.
200. Bonner, W.A.; Kavasmaneck, P.R.; Martin, F.S.; Flores, J.J. Asymmetric adsorption of alanine by quartz. *Science* **1974**, 186(4159), 143-144. https://doi.org/10.1126/science.186.4159.143
201. Bonner, W.A.; Kavasmaneck, P.R.; Martin, F.S.; Flores, J.J. Asymmetric adsorption by quartz: a model for the prebiotic origin of optical activity. *Orig. Life* **1975**, 6(3), 367-376. https://doi.org/10.1007/BF01130338
202. Kahr, B.; Chittenden, B.; Rohl, A. Robert Boyle's chiral crystal chemistry: Computational re-evaluation of enantioselective adsorption on quartz. *Chirality* **2006**, 18(2), 127-133. https://doi.org/10.1002/chir.20229
203. Easson, L.H.; Stedman, E. Molecular dissymmetry and physiological activity. *Journal of the Chemical Society* **1933**, 1094-1098. https://doi.org/10.1039/JR9330001094
204. Ogston, A.G. Interpretation of experiments on metabolic processes, using isotopic tracer elements. *Nature* **1984**, 162, 963. https://doi.org/10.1038/162963b0
205. Davankov, V.A. The nature of chiral recognition: Is it a three-point interaction? *Chirality* **1997**, 9(2), 99-102. https://doi.org/10.1002/(SICI)1520-636X(1997)9:2<99::AID-CHIR3>3.0.CO;2-B
206. Asthagiri, A.; Hazen, R.M. An ab initio study of adsorption of alanine on the chiral calcite (213) surface. *Molecular Simulation* **2007**, 33(4-5), 343-351. https://doi.org/10.1080/08927020601155485
207. Booth, T.D.; Wahnon, D. Wainer, I.W. Is chiral recognition a three-point process? *Chirality* **1997**, 9(2), 96-98. https://doi.org/10.1002/(SICI)1520-636X(1997)9:2<96::AID-CHIR2>3.0.CO;2-E
208. Mesecar, A.D.; Koshland Jr., D.E. A new model for protein stereospecificity. *Nature* **2000**, 403, 614-615. https://doi.org/10.1038/35001144
209. Berthod, A. Chiral recognition mechanisms. *Anal. Chem.* **2006**, 78(7), 2093-2099. https://doi.org/10.1021/ac0693823
210. Goldberg, S.I. Enantiomeric enrichment on the prebiotic earth. *Orig. Life Evol. Biosph.* **2007**, 37, 55-60. https://doi.org/10.1039/C0CP01387K
211. Bada, J.L. Racemization of amino acids. In *Chemistry and Biochemistry of the Amino Acids*.; Barrett G.C., Ed.; Springer, Dordrecht, Germany, 1985; pp 399-414. https://doi.org/10.1007/978-94-009-4832-7_13
212. Soai, K.; Matsumoto, A.; Kawasaki, T. Asymmetric autocatalysis as a link between crystal chirality and highly enantioenriched organic compounds. *Israel Journal of Chemistry* **2021**, 61(9-10), 507-516. https://doi.org/10.1002/ijch.202100047
213. Sato, I.; Kadowaki, K.; Soai, K. Asymmetric synthesis of an organic compound with high enantiomeric excess induced by inorganic ionic sodium chlorate. *Angew Chem Int Ed Engl* **2000**, 39(8), 1510-1512. https://doi.org/10.1002/(sici)1521-3773(20000417)39:8<1510::aid-anie1510>3.0.co;2-r
214. Sato, I.; Kadowaki, K.; Ohgo, Y.; Soai, K. Highly enantioselective asymmetric autocatalysis induced by chiral ionic crystals of sodium chlorate and sodium bromate. *Journal of Molecular Catalysis A: Chemical* **2004**, 216(4), 209-214. https://doi.org/10.1016/j.molcata.2004.03.010
215. Shindo, H.; Shirota, Y.; Niki, K.; Kawasaki, T.; Suzuki, K.; Araki, Y.; Matsumoto, A.; Soai, K. Asymmetric autocatalysis induced by cinnabar: Observation of the enantioselective adsorption of a 5-pyrimidyl alkanol on the crystal surface. *Angew. Chem. Int. Ed.* **2013**, 52(35), 9135-9138. https://doi.org/10.1002/anie.201304284

216. Matsumoto, A.; Ozawa, H.; Inumaru, A.; Soai, K. Asymmetric induction by retgersite, nickel sulfate hexahydrate, in conjunction with asymmetric autocatalysis. *New J. Chem.* **2015**, 39(9), 6742-6745. https://doi.org/10.1039/C5NJ01459J
217. Matsumoto, A.; Kaimori, Y.; Uchida, M.; Omori, H.; Kawasaki, T.; Soai, K. Achiral inorganic gypsum acts as an origin of chirality through Its enantiotopic surface in conjunction with asymmetric autocatalysis. *Angew. Chem. Int. Ed.* **2017**, 56(2), 545-548. https://doi.org/10.1002/anie.201610099
218. Kondepudi, D.K.; Kaufman, R.J.; Singh, N. Chiral symmetry breaking in sodium chlorate crystallization. *Science* **1990**, 16, 975-976. https://doi.org/10.1126/science.250.4983.975
219. McBride, J.M.; Carter, R.L. Spontaneous resolution by stirred crystallization. *Angew Chem Intl Ed* **1991**, 30, 293-295. https://doi.org/10.1002/anie.199102931
220. Shinitzky, M.; Nudelman, F.; Barda, Y.; Haimovitz, R.; Chen, E.; Deamer, D.W. Unexpected differences between D- and L-tyrosine lead to chiral enhancement in racemic mixtures. *Origins of Life and Evolution of the Biosphere* **2002**, 32, 285-297. https://doi.org/10.1023/A:1020535415283
221. Lahav, M.; Weissbuch, I.; Shavit, E.; Reiner, C.; Nicholson, G.J.; Schurig, V. Parity violating energetic difference and enantiomorphous crystals - caveats; reinvestigation of tyrosine crystallization. *Orig Life Evol Biosph.* **2006**, 36(2),151-170. https://doi.org/10.1007/s11084-005-9000-7
222. Goldberg, S.I. Experimental evidence leading to an alternative explanation of why D-tyrosine sometimes crystallizes faster than its L-enantiomer. *Orig Life Evol Biosph*. **2008**, 38(2),149-153. https://doi.org/10.1007/s11084-008-9123-8
223. Shinitzky, M.; Deamer, D. Comments in a discussion: Differential rates of D- and L-tyrosine crystallization. *Origins of Life and Evolution of Biospheres* **2008**, 38, 271-275. https://doi.org/10.1007/s11084-008-9129-2
224. Wu, C.; Wang, X.; Zhao, K.; et al. Molecular modulation of calcite dissolution by organic acids. *Cryst. Growth Des.* **2011**, 11, 3153-3162. https://doi.org/10.1021/cg200403t
225. Frondel, C. Characters of quartz fibers. *American Mineralogist* **1978**, 63, 17-27.
226. Evgenii, K; Wolfram, T. The role of quartz in the origin of optical activity on Earth. *Origins of Life and Evolution of the Biosphere* **2000**, 30, 431–434. https://doi.org/10.1023/A:1006766311211
227. Ulbricht, T.L.V. Asymmetry: The non-conservation of parity and optical activity. *Q. Rev. Chem. Soc.* **1959**, 13, 48-60. https://doi.org/10.1039/qr9591300048
228. Ulbricht T.; Vester F. Attempts to induce optical activity with polarized β-radiation. *Tetrahedron*. **1962**, 18, 629-637. https://doi.org/10.1016/S0040-4020(01)92714-0
229. Myrgorodska, I.; Meinert, C.; Hoffmann, S.; Jones, N.; Nahon, L.; Meierhenrich, U. Light on chirality: Absolute asymmetric formation of chiral molecules relevant in prebiotic evolution. *ChemPlusChem* **2017**, 82 (1), 74-87. https://doi.org/10.1002/CPLU.201600214
230. Nair, N.N.; Schreiner, E.; Marx, D. Glycine at the pyrite-water interface: The role of surface defects. *J. Am. Chem. Soc.* **2006**, 128(42), 13815-13826. https://doi.org/10.1021/ja063295a
231. Xue, N.; Chen, X.; Nie, L.; Guo, X.; Ding, W.; Chen, Y.; Gu, M.; Xie, Z. Understanding the enhancement of catalytic performance for olefin cracking: Hydrothermally stable acids in P/HZSM-5. *J. Catal.* **2007**, 248, 20–28. https://doi.org/10.1016/j.jcat.2007.02.022
232. Fleming, G.J.; Adib, K.; Rodriguez, J.A.; Barteau, M.; White, J.; Idriss, H. The adsorption and reactions of the amino acid proline on rutile TiO2(1 1 0) surfaces. *Surface Science* **2008**, 602, 2029-2038. https://doi.org/10.1016/j.susc.2008.04.010
233. Wu, J.; Buseck, P. Carbon storage at defect sites in mantle mineral analogues. *Nature Geoscience* **2013**, 6, 875–878. https://doi.org/10.1038/ngeo1903
234. Yang, G.; Zhou, L. Zwitterionic versus canonical amino acids over the various defects in zeolites: A two-layer ONIOM calculation. *Sci. Rep.* **2014**, 4, 6594. https://doi.org/10.1038/srep06594
235. Li, X.; Li, H.; Yang, G. Promoting the adsorption of metal ions on kaolinite by defect sites: A molecular dynamics study. *Sci. Rep.* **2015**, 5, 14377. https://doi.org/10.1038/srep14377
236. Zaia, D.A.M.; Zaia, C.T.B.V. A few experimental suggestions using minerals to obtain peptides with a high concentration of L-amino acids and protein amino acids. *Symmetry* **2020**, 12, 2046. https://doi.org/10.3390/sym12122046
237. Tosca, N. J.; McLennan, S. M. Chemical divides and evaporite assemblages on Mars. *Earth and Planet. Sci. Lett.* **2006**, 241(1-2), 21-31. https://doi.org/10.1016/j.epsl.2005.10.021
238. Vaniman, D. T.; Martinez, G. M.; Rampe, E. B., Bristow, T.F.; Blake, D.F.; Yen, A.S.; Ming, D.W.; Rapin, W.; Meslin, P-Y.; Morookian, J.M.; Downs, R.T.; Chipera, S.J.; Morris, R.V.; Morrison, S.M.; Treiman, A.H.; Achilles, C.N.; Robertson, K.; Grotzinger, J.P.; Hzaen, R.M.; Wiens, R.C.; Sumner, D.Y. Gypsum, bassanite, and anhydrite at Gale crater, Mars. *American Mineralogist* **2018**, 103(7), 1011-1020. https://doi.org/10.2138/am-2018-6346
239. Samotoin, N.D. Enantiomorphism of kaolinite: Manifestation at the levels of elementary layer and microcrystals. *Crystallography Reports* **2011**, 56(2), 327-334. https://doi.org/10.1134/S1063774511010202
240. Wray, J.J.; Milliken, R.E.; Dundas, C.M.; Swayze, G.A.; Andrews-Hanna, J.C.; Baldridge, A.M.; Chojnacki, M.; Bishop, J.L.; Ehlmann, B.L.; Murchie, S.L.; Clark, R.N.; Seelos, F.P.; Tornabene, L.L.; Squyers, S.W. Columbus crater and other possible groundwater-fed paleolakes of Terra Sirenum, Mars. *JGR Planets* **2011**, 116, E01001, 1-41. https://doi.org/10.1029/2010JE003694
241. Cuadros, J.; Michalski, J. R. Investigation of Al-rich clays on Mars: Evidence for kaolinite–smectite mixed-layer versus mixture of end-member phases. *Icarus* **2013**, 222(1), 296-306. https://doi.org/10.1016/j.icarus.2012.11.006

242. Cairns-Smith, A.G.; Hall, A.J.; Russell, M.J. Mineral theories of the origin of life and an iron sulfide example. In *Marine Hydrothermal Systems and the Origin of Life*; Holm, N.G., Ed.; Springer: Dordrecht, Germany, 1992; pp. 161-180. https://doi.org/10.1007/978-94-011-2741-7_9
243. Zamaraev, K.I.; Romannikov, V.N.; Salganik, R.I.; Wlassoff, W.A.; Khramtsov, V.V. Modelling of the prebiotic synthesis of oligopeptides: Silicate catalysts help to overcome the critical stage. *Origins of Life and Evolution of the Biosphere* **1997**, 27, 325-337. https://doi.org/10.1023/a:1006571800690
244. Ruff, S.W. Spectral evidence for zeolite in the dust on Mars. *Icarus* **2004**, 168(1), 131-143. https://doi.org/10.1016/j.icarus.2003.11.003
245. Carter, J.; Poulet, F.; Bibring, J.P.; Mangold, N.; Murchie, S. Hydrous minerals on Mars as seen by the CRISM and OMEGA imaging spectrometers: Updated global view. *Journal of Geophysical Research: Planets* **2013**, 118, 831-858. https://doi.org/10.1029/2012JE004145
246. Christensen, P.R.; Wyatt, M.B.; Glotch, T.D.; Rogers, A.D.; Anwar, S.; Arvidson, R.E.; Banfield, J.L.; Blaney, D.L.; Budney, C.; Calvin, W.M.; Fallacaro, A.; Fergason, R.L.; Gorelick, N.; Graff, T.G.; Hamilton, V.E.; Hayes, A.G.; Johnson, J.R.; Knudson, A.T.; McSween Jr, H.Y.; Mehall, G.L.; Moersch, J.E.; Morris, R.V.; Smith, M.D.; Squyers, S.W.; Ruff, S.W.; Wolff, M.J. Mineralogy at Meridiani Planum from the mini-TES experiment on the Opportunity rover. *Science* **2004**, 306(5702),1733-1739. https://doi.org/10.1126/science.1104909
247. Stromberg, J. M.; Applin, D. M.; Cloutis, E. A.; et al. The persistence of a chlorophyll spectral biosignature from Martian evaporite and spring analogues under Mars-like conditions. *Int. J. Astrobiology*. **2013**, 13(3), 203-223. https://doi.org/10.1017/S1473550413000402
248. Cockell, C.S.; Wilhelm, M.B.; Perl, S.; Wadsworth, J.; Payler, S.; McMahon, S.; Paling, S.; Edwards, T. 0.25 Ga salt deposits preserve signatures of habitable conditions and ancient lipids. *Astrobiology* **2020**, 20(7), 864-877. http://doi.org/10.1089/ast.2019.2053
249. De Sanctis, M. C.; Raponi, A.; Ammannito, E.; Ciarniello, M.; Toplis, M.J.; McSween, H.Y.; Castillo-Rogez, J.C.; Ehlmann, B.L.; Carrozzo, F.G.; Marchi, S.; Tosi, F.; Zambon, F.; Capaccioni, F.; Capria, M.T.; Fonte, S.; Formisano, M.; Frigeri, A.; Giardino, M.; Longobardo, A.; Magni, G.; Palomba, E.; McFadden, L.A.; Pieters, C.M.; Jaumann, R.; Schenk, P.; Mugnuolo, R.; Raymond, C.A.; Russell, C.T. Bright carbonate deposits as evidence of aqueous alteration on (1) Ceres. *Nature* **2016**, 536, 54–57. https://doi.org/10.1038/nature18290
250. Raponi, A.; De Sanctis, M. C.; Carrozzo, F. G.; Ciarniello, M.; Castillo-Rogez, J.C.; Ammannito, E.; Frigeri, A.; Longobardo, A.; Palomba, E.; Tosi, F.; Zambon, F.; Raymond, C.A.; Russell, C.T. Mineralogy of Occator crater on Ceres and insight into its evolution from the properties of carbonates, phyllosilicates, and chlorides. *Icarus* **2019**, 320, 83-96. https://doi.org/10.1016/j.icarus.2018.02.001
251. Banin, A.; Ben-Shlomo, T.; Margulies, L.; Blake, D.F.; Mancinelli, R.L.; Gehring, A.U. The nanophase iron mineral(s) in Mars soil. *J. Geophys. Res*. **1993**, 98, 20831-20853.
252. Madsen, M.B.; Hviid, S.F.; Gunnlaugsson, H.P.; Knudsen, J.M.; Goetz, W.; Pedersen, C.T.; Dinesen, A.R.; Mogensen, C.T.; Olsen, M.; Hargraves, R.B. The magnetic properties experiments on Mars Pathfinder. *J. Geophys. Res.* **1999**, 104, 8761-8779. https://doi.org/10.1029/1998JE900006
253. Morris, R.V.; Golden, D.C.; Bell III, J.F.; Shelfer, T.D.; Scheinost, A.C.;. Hinman, N.W.; Furniss, G.;. Mertzman, S.A.; Bishop, J.L.; Ming, D.W.; Allen, C.C.; Britt, D.T. Mineralogy, composition, and alteration of Mars Pathfinder rocks and soils: Evidence from multispectral, elemental, and magnetic data on terrestrial analogue, SNC meteorite, and Pathfinder samples. *J. Geophys. Res.* **2000**, 105, 1757-1817. https://doi.org/10.1029/1999JE001059
254. Barrn, V.; Torrent, J. Evidence for a simple pathway to maghemite in Earth and Mars soils. *Geochim. Cosmochim. Acta* **2002**, 66(15), 2801-2806. https://doi.org/10.1016/S0016-7037(02)00876-1
255. Ricardo, A.; Carrigan, M.A.; Olcott, A.; Benner, S.A. Borate minerals stabilize ribose. *Science* **2004**, 303 ,196. https://doi.org/10.1126/science.1092464
256. Scorei, R.; Cimpoiaşu, V.M. Boron enhances the thermostability of carbohydrates. *Orig Life Evol Biosph* **2006**, 36, 1-11. https://doi.org/10.1007/s11084-005-0562-1
257. Furukawa, Y.; Horiuchi, M.; Kakegawa, T. Selective stabilization of ribose by borate. *Orig Life Evol Biosph* **2013**, 43, 353–361. https://doi.org/10.1007/s11084-013-9350-5
258. Gasda, P.J.; Haldeman, E.B.; Wiens, R.C.; Rapin, W.; Bristow, T.F.; Bridges, J.C.; Schwenzer, S.P.; Clark, B.; Herkenhoff, K.; Frydenvang, J.; Lanza, N.L.; Maurice, S.; Clegg, S.; Delapp, D.M.; Sanford, V.L.; Bodine, M.R.; McInroy, R. In situ detection of boron by ChemCam on Mars. *Geophysical Research Letters* **2017**, 44(17), 8739-9748. https://doi.org/10.1002/2017GL074480
259. Stephenson, J. D.; Hallis, L. J.; Nagashima, K.; Freeland, S. J. Boron enrichment in Martian clay. *PLOS One* **2013**, 8(6), e64624. https://doi.org/10.1371/journal.pone.0064624
260. Das, D.; Gasda, P.J.; Wiens, R.C.; Berlo, K.; Leveille, R.J.; Frydenvang, J.; Mangold, N.; Kronyak, R.E.; Schwenzer, S.P.; Forni, O.; Cousin, A.; Maurice, S.; Gasnault, O. Boron and lithium in calcium sulfate veins: Tracking precipitation of diagenetic materials in Vera Rubin ridge, Gale crater. *JGR Planets* **2020**, 125(8), e2019JE006301. https://doi.org/10.1029/2019JE006301
261. Eglinton, G.; Logan, G.A.; Ambler, R.P.; Boon, J.J.; Perizonius, W.R.K. Molecular preservation [and discussion]. *Philosophical Transactions: Biological Sciences* **1991**, 333(1268), 315-328.
262. Castañeda, I.S.; Schouten, S. A review of molecular organic proxies for examining modern and ancient lacustrine environments. *Quat. Sci. Rev.* **2011**, 30, 2851-2891. https://doi.org/10.1016/j.quascirev.2011.07.009

263. Sollai, M.; Villanueva, L.; Hopmans, E.C.; Keil, R.G.; Sinninghe Damsté, J.S. Archaeal sources of intact membrane lipid biomarkers in the oxygen deficient zone of the Eastern Tropical South Pacific. *Front. Microbiol.* **2019**, 10, 765. https://doi.org/10.3389/fmicb.2019.00765
264. Lee, C.; Brocks, J.J. Identification of carotane breakdown products in the 1.64 billion year old Barney Creek Formation, McArthur Basin, northern Australia. *Organic Geochemistry* **2011**, 42(4), 425-430. https://doi.org/10.1016/j.orggeochem.2011.02.006
265. Summons, R.E.; Welander, P.V.; Gold, D.A. Lipid biomarkers: molecular tools for illuminating the history of microbial life. *Nature Reviews Microbiology* **2021**, https://doi.org/10.1038/s41579-021-00636-2
266. Burgos, C.; Ayer, D.; Johnson, R.A. A new, asymmetric synthesis of lipids and phospholipids. *J. Org. Chem.* **1987**, 52(22), 4973-4977. https://doi.org/10.1021/JO00231A025
267. Listunov, D.; Fabing, I.; Saffon-Merceron, N.; Gaspard, H.; Volovenko, Y.; Maraval, V.; Chauvin, R.; Génnison, Y. Asymmetric synthesis and biological evaluation of natural or bioinspired cytotoxic C2-symmetrical lipids with two terminal chiral alkynylcarbinol pharmacophores. *J. Org. Chem.* **2015**, 80(11), 5386-5394. https://doi.org/10.1021/acs.joc.5b00494
268. Mountanea, O.G.; Limnios, D.; Kokotou, M.G.; Bourboula, A.; Kokotos, G. Asymmetric synthesis of saturated hydroxy fatty acids and fatty acid esters of hydroxy fatty acids. *European Journal of Organic Chemistry* **2019**, 2019(10), 2010-2019. https://doi.org/10.1002/ejoc.201801881
269. Altamura, E.; Comte, A.; D'Onofrio, A.D.; Roussillon, C.; Fayolle, D.; Buchet, R.; Mavelli, F.; Stano, P.; Fiore, M.; Strazewski, P. Racemic phospholipids for origin of life studies. *Symmetry* **2020**, 12(7), 1108. https://doi.org/10.3390/sym12071108
270. Des Marais, D.J. Isotopic evolution of the biogeochemical carbon cycle during the Precambrian. *Reviews in Mineralogy and Geochemistry* **2001**, 43, 555-578. https://doi.org/10.2138/gsrmg.43.1.555
271. Tegelaar, E.W.; Derenne, S.; Largeau, C;, de Leeuw, J.W. A reappraisal of kerogen formation. *Geochimica Cosmochimica Acta* **1989**, 3, 3103-3107. https://doi.org/10.1016/0016-7037(89)90191-9
272. Burdige, D. Preservation of organic matter in marine sediments: Controls, mechanisms, and an imbalance in sediment organic carbon budgets? *Chem. Rev.* **2007**, 107(2), 467-485. https://doi.org/10.1021/cr050347q
273. Brocks, J.J.; Summons, R.E. Sedimentary hydrocarbons, biomarkers for early life. In *Treatise on Geochemistry*, 2nd ed.; Holland, D.H.; Turekian, K.K., Eds.; Elsevier: 2003; Volume 8, pp. 61-103.
274. Lee, C.; Love, G.D.; Jahnke, L.L.; Kubo, M.D.; Des Marais, D.J. Early diagenetic sequestration of microbial mat lipid biomarkers through covalent binding into insoluble macromolecular organic matter (IMOM) as revealed by sequential chemolysis and catalytic hydropyrolysis. *Organic Geochemistry* **2019**, 132, 11-22. https://doi.org/10.1016/j.orggeochem.2019.04.002
275. Lee, C.; Love, G.D.; Jahnke, L.L.; Kubo, M.D.; Des Marais, D.J. Diagenetic transformations and preservation of free and bound lipids in a hypersaline microbial mat from Guerrero Negro, Baja California Sur, Mexico. *Org. Geochem.* **2021**, 153, 104196. https://doi.org/10.1016/j.orggeochem.2021.104196
276. Bishop, A.N.; Love, G.D.; McAulay, A.D.; Snape, C.E.; Farrimond, P. Release of kerogen bound hopanoids by hydropyrolysis. *Org. Geochem.* **1998**, 29, 989-1001. https://doi.org/10.1016/S0146-6380(98)00140-5
277. Farrimond, P.; Love, G.D.; Bishop, A.N.; Innes, H.E.; Watson, D.F.; Snape, C.E. Evidence for rapid incorporation of hopanoids into kerogen. *Geochimica et Cosmochimica Acta* **2003**, 67, 1383-1394. https://doi.org/10.1016/S0016-7037(02)01287-5
278. Peters, K.E., Walters, C.C., Moldowan, J.M., *The Biomarker Guide: Biomarkers and Isotopes in Petroleum Exploration and Earth History, Volume 2*, 2nd ed.; Cambridge University Press, Cambridge, United Kingdom, 2005.
279. Horsfield, B.; Rullkötter, J. Diagenesis, catagenesis, and metagenesis of organic matter. In *The Petroleum System—From Source to Trap*, Magoon, L.B., Dow, W.G., Eds.; American Association of Petroleum Geologists, 1994, Volume 60. https://doi.org/10.1306/M60585C10
280. Durand, B. Sedimentary organic matter and kerogen: Definition and quantitative importance of kerogen. In *Kerogen: Insoluble organic matter from sedimentary rocks*; Durand, B., Ed.; Editions Technip: Paris, France, 1980, pp. 13-33.
281. Tissot, B.P.; Welte, D.H. *Petroleum formation and occurrence*, 1st ed.; Springer Berlin Heidelberg: Berlin, Germany, 1984. https://doi.org/10.1007/978-3-642-87813-8
282. Vandenbroucke, M.; Largeau, C. Kerogen origin, evolution and structure. *Org. Geochem.* **2007**, 38, 719-833. https://doi.org/10.1016/j.orggeochem.2007.01.001
283. Keil, R.G.; Montluçon, D.B.; Prahl, F.G.; Hedges, J.I. Sorptive preservation of labile organic matter in marine sediments. *Nature* **1994**, 370, 549-552. https://doi.org/10.1038/370549a0
284. Keil, R.G.; Mayer, L.M. Mineral matrices and organic matter. In *Treatise on Geochemistry*, 2nd ed.; Holland, D.H., Turekian, K.K., Eds.; Elsevier: 2014, Volume 12, pp. 337-359. https://doi.org/10.1016/B978-0-08-095975-7.01024-X
285. Fox, A.C.; Eigenbrode, J.L.; Freeman, K.H. Radiolysis of macromolecular organic material in Mars-relevant mineral matrices. *JGR Planets* **2019**, 124, 3257-3266. https://doi.org/1029/2019JE006072
286. Salmon, V.; Derenne, S.; Lallier-Vergès, E.; Largeau, C.; Beaudoin, B. Protection of organic matter by mineral matrix in a Cenomanian black shale. *Org. Geochem.* **2000**, 31, 463-474. https://doi.org/10.1016/S0146-6380(00)00013-9
287. Love, G.D.; Stalvies, C.; Grosjean, E.; Meredith, W.; Snape, C.E. Analysis of molecular biomarkers covalently bound within Neoproterozoic sedimentary kerogen. In *From Evolution to Geobiology: Research Questions Driving Paleontology at the Start of a New Century, Paleontological Society Short Course, Paleontological Society Papers*, Kelley, P.H., Bambach, R.K., Eds.; 2008, Vol. 14, pp. 67-83. https://doi.org/10.1017/S1089332600001613
288. Petsch S. Kerogen. In *Encyclopedia of Geochemistry. Encyclopedia of Earth Sciences Series*, White, W.M., Ed.; Springer, Cham; 2018 https://doi.org/10.1007/978-3-319-39312-4_163

289. Kerridge, J.F. Formation and processing of organics in the early Solar System. *Space Science Reviews* **1999**, 290, 275-288. https://doi.org/10.1023/A:1005222804192
290. Tsuchiya, H.; Mizogami, M. Discrimination of stereoisomers by their enantioselective interactions with chiral cholesterol-containing membranes. *Molecules* **2018**, 23(1), 49. https://doi.org/10.3390/molecules23010049
291. Gerst, N.; Ruan, B.; Pang, J.; Wilson, W.K.; Schroepfer Jr, G.J. An updated look at the analysis of unsaturated C27 sterols by gas chromatography and mass spectrometry. *Journal of Lipid Research* **1997**, 38, 1685-1701. https://doi.org/10.1016/S0022-2275(20)37187-X
292. Maxwell, J.R.; Mackenzie, A.S. Volkman, J.K. Configuration at C-24 in steranes and sterols *Nature* **1980**, 286, 694-697. https://doi.org/10.1038/286694a0
293. vaan Kaam-Peters, H.M.E.; Köster, J.; van der Gaast, S.J.; Dekker, M.; de Leeuw, J.W.; Sinninghe Damsté, J.S. The effect of clay minerals on diasterane/sterane ratios. *Geochimica et Cosmochimica Acta* **1998**, 62, 2923-2929. https://doi.org/10.1016/S0016-7037(98)00191-4
294. Elie, M.; Nogueira, A.C.R.; Nedlec, A.; Trindale, R.I.F.; Kenig, F. A red algal bloom in the aftermath of the Marinoan Snowball Earth. *Terra Nova* **2007**, 19, 303-308. https://doi.org/10.1111/j.1365-3121.2007.00754.x
295. Tannenbaum E.; Huizinga B.J.; Kaplan I.R. Role of minerals in thermal alteration of organic matter--II: A material balance. *Amer. Assoc. Petrol. Geol Bull* **1986**, 70, 1156-1165. https://doi.org/10.1306/94886A92-1704-11D7-8645000102C1865D
296. Soldan, A.L.; Cerqueira, J.R. Effects of thermal maturation on geochemical parameters obtained by simulated generation of hydrocarbons. *Org. Geochem.* **1986**, 10(1-3), 339-345. https://doi.org/10.1016/0146-6380(86)90034-3
297. Love, G.D.; Snape, C.E.; Carr, A.D.; Houghton, R.C. Release of covalently-bound alkane biomarkers in high yields from kerogen via catalytic hydropyrolysis. *Org. Geochem.* **1995**, 23(10), 981-986. https://doi.org/10.1016/0146-6380(95)00075-5
298. Love, G.D.; Snape, C.E.; Carr, A.D.; Houghton, R.C. Changes in molecular biomarker and bulk carbon skeletal parameters of vitrinite concentrates as a function of rank. *Energy Fuels* **1996**, 10(1), 149-157. https://doi.org/10.1021/ef950026p
299. Love, G.D.; McAulay, A.; Snape, C.E.; Bishop, A.N. Effect of process variables in catalytic hydropyrolysis on the release of Covalently bound aliphatic hydrocarbons from sedimentary organic matter. *Energy Fuels* **1997**, 11(3), 522-531. https://doi.org/10.1021/ef960194x
300. Love, G.D.; Snape, C.E.; Fallick, A.E. Differences in the mode of incorporation and biogenicity of the principal aliphatic constituents of a Type I oil shale. *Org. Geochem.* **1998**, 28(12), 797-811. https://doi.org/10.1016/S0146-6380(98)00050-3
301. Love, G.D.; Bowden, S.A.; Summons, R.E.; Jahnke, L.L.; Snape, C.E.; Campbell, C.N.; Day, J.G. An optimised catalytic hydropyrolysis method for the rapid screening of microbial cultures for lipid biomarkers. *Org. Geochem.* **2005**, 36, 63-82. https://doi.org/10.1016/j.orggeochem.2004.07.010
302. Sudgen, M.A.; Abbott, G.D. The stereochemistry of bound and extractable pentacyclic triterpenoids during closed system pyrolysis. *Org. Geochem.* **2002**, 33(12), 1515-1521. https://doi.org/10.1016/S0146-6380(02)00114-6
303. Krot, A.N.; Amelin, Y.; Bland, P.; Ciesla, F.J.; Connelly, J.; Davis, A.M.; Huss, G.R.; Hutcheon, I.D.; Makide, K.; Nagashima, K.; Nyquist, L.E.; Russell, S.S.; Scott, E.R.D.; Thrane, K.; Yurimoto, H.; Yin, Q-Z. Origin and chronology of chondritic components: A review. *Geochim Cosmochim Ac* **2009**, 73(17), 4963-4997. https://doi.org/10.1016/j.gca.2008.09.039
304. Cloutis, E.A.; Izawa, M.R.M.; Beck, P. Chapter 4 - Reflectance Spectroscopy of Chondrites. In *Primitive Meteorites and Asteroids Physical, Chemical and Spectroscopic Observations Paving the Way to Exploration*; Abreu, N., Ed.; Elsevier, pp. 273-343. https://doi.org/10.1016/B978-0-12-813325-5.00004-5
305. Krot, A.N.; Keil, K.; Scott, E.R.D.; Goodrich, C.A.; Weisberg, M.K. Classification of meteorites and their genetic relationships. In *Treatise on Geochemistry*; Holland, D.H.; Turekian, K.K., Eds.; Elsevier, 2014, vol. 1, pp. 1-63.
306. Maurel, C.; Bryson, J.F.J.; Lyons, R.J.; Ball, M.R.; Chopdekar, R.V.; Scholl, A.; Ciesla, F.J.; Bottke, W.F.; Wiess, B.P. Meteorite evidence for partial differentiation and protracted accretion of planetesimals. *Sci. Adv.* **2014**, 6(30), eaba1303. https://doi.org/10.1126/sciadv.aba1303
307. Weisberg, M.K.; McCoy, T.J.; Krot, A.N. Systematics and evaluation of meteorite classification. In *Meteorites and the early Solar System II*; Lauretta, D.S.; McSween Jr., H.Y., Eds.; University of Arizona Press, Arizona, United States, 2006, pp. 19-52.
308. Wood, J.A. Chondritic meteorites and the solar nebula. *Annu Rev Earth Pl Sc* **1988**, 16, 53-72. https://doi.org/10.1146/annurev.ea.16.050188.000413
309. Braukmüller, N.; Wombacher, F.; Hezel, D.C.; Escoube, R.; Münker, C. The chemical composition of carbonaceous chondrites: Implications for volatile element depletion, complementarity and alteration. *Geochim Cosmochim Ac* **2018**, 239, 17-48. https://doi.org/10.1016/j.gca.2018.07.023
310. Van Schmus, W.R.; Wood, J.A. A chemical-petrologic classification for the chondritic meteorites. *Geochimica et Cosmochimica Acta* **1967**, 31(5), 747-754. https://doi.org/10.1016/S0016-7037(67)80030-9
311. Grimm, R.E.; McSween Jr., H.Y. Water and the thermal evolution of carbonaceous chondrite parent bodies. *Icarus* **1989**, 82(2), 244-280. https://doi.org/10.1016/0019-1035(89)90038-9
312. Brearley, A.J.; Jones, R.H. Chondritic meteorites. In *Planetary Materials*; Papike, J.J., Ed.; De Gruyter, 1998, 36, 3.1-3.398. https://doi.org/10.1515/9781501508806-018
313. Scott, E.R.D.; Krot, A.N. Chondrites and their components. In *Meteorites, comets and planets: Treatise on geochemistry*; Davis, A.M.; Holland, H.D.; Turekian, K.K., Eds. Elsevier B. V.: Amsterdam, The Netherlands, 2005; Vol. 1, p 143.
314. Scott, E.R. Chondrites and the protoplanetary disk. *Annu. Rev. Earth Planet. Sci.* **2007**, 35, 577-620. https://doi.org/10.1146/annurev.earth.35.031306.140100

315. Hiroi, T.; Pieters, C.M.; Zolensky, M.; Lipschutz, M.E. Evidence of thermal metamorphism on the C, G, B, and F asteroids. *Science* **1993**, 261(5124), 1016-1018. https://doi.org/10.1126/science.261.5124.1016
316. Huss, G.R.; Rubin, A.E.; Grossman, J.N. Thermal metamorphism in chondrites. In *Meteorites and the early Solar System II*, Lauretta, D.S., McSween Jr., H.Y., Eds.; University of Arizona Press, Arizona, United States, **2006**, pp. 567-586.
317. Gyollai, I.; Bérczi, S.; Fintor, K.; Nagy, S.; Gucsik, A. Thermal metamorphism of the Mócs meteorite (L6) revealed by optical microscopy and BSE imaging. *Central European Geology* **2015**, 58(4), 321-333. https://doi.org/10.1556/24.58.2015.4.3
318. King, A.J.; Schofield, P.F.; Russell, S.S. Thermal alteration of CM carbonaceous chondrites: Mineralogical changes and metamorphic temperatures. *Geochimica et Cosmochimica Acta* **2021**, 298, 167-190. https://doi.org/10.1016/j.gca.2021.02.011
319. Yesiltas, M.; Young, J.; Glotch, T.D. Thermal metamorphic history of Antarctic CV3 and CO3 chondrites inferred from the first- and second-order Raman peaks of polyaromatic organic carbon. *American Mineralogist* **2021**, 106(4), 506-517. https://doi.org/10.2138/am-2021-7507
320. Kallemeyn, G.W.; Rubin, A.E.; Wasson, J.T. The compositional classification of chondrites: VI. The CR carbonaceous chondrite group. *Geochimica et Cosmochimica Acta* **1994**, 58(13), 2873-2888. https://doi.org/10.1016/0016-7037(94)90121-X
321. Amelin, Y.; Ghosh, A.; Rotenberg, E. Unraveling the evolution of chondrite parent asteroids by precise U-Pb dating and thermal modeling. Geochim Cosmochim Ac 2005, 69(2), 505-518. https://doi.org/10.1016/j.gca.2004.05.047
322. Goldstein, J.I.; Scott, E.R.D.; Chabot, N.L. Iron meteorites: Crystallization, thermal history, parent bodies, and origin. *Chemie der Erde* **2009**, 69, 293-325. https://doi.org/10.1016/j.chemer.2009.01.002
323. Yang, J.; Goldstein, J.I.; Michael, J.R.; Kotula, P.G.; Scott, E.R.D. Thermal history and origin of the IVB iron meteorites and their parent body. *Geochimica et Cosmochimica Acta* **2010**, 74, 4493-4506. https://doi.org/10.1016/j.gca.2010.04.011
324. Henke, S.; Gail, H.-P.; Trieloff, M.; Schwarz, W.H.; Kleine, T. Thermal history modelling of the H chondrite parent body. *Astronomy & Astrophysics* **2012**, 545, A135. https://doi.org/10.1051/0004-6361/201219100
325. Gail, H-P.; Trieloff, M. Thermal history modelling of the L chondrite parent body. *Astronomy & Astrophysics* **2019**, 628, 1-21. https://doi.org/10.1051/0004-6361/201936020
326. Brearley, A.J. The action of water. In *Meteorites and the early Solar System II*; Lauretta, D.S.; McSween Jr., H.Y., Eds.; University of Arizona Press: Arizona, United States, 2006, pp. 587-624.
327. Doyle, P.M.; Jogo, K.; Nagashima, K.; Krot, A.N.; Wakita, S.; Ciesla, F.J. Early aqueous activity on the ordinary and carbonaceous chondrite parent bodies recorded by fayalite. *Nature Communications* **2015**, 6, 7444. https://doi.org/10.1038/ncomms8444
328. Endress, M.; Bischoff, A. Carbonates in CI chondrites: Clues to parent body evolution. *Geochimica et Cosmochimica Acta* **1996**, 60(3), 489-507. https://doi.org/10.1016/0016-7037(95)00399-1
329. Endress, M.; Zinner, E.; Bischoff, A. Early aqueous activity on primitive meteorite parent bodies. *Nature* **1996**, 379, 701-703. https://doi.org/10.1038/379701a0
330. Berger, E.L.; Zega, T.L.; Keller, L.P.; Lauretta, D.S. Evidence for aqueous activity on comet 81P/Wild 2 from sulfide mineral assemblages in Stardust samples and CI chondrites. *Geochimica et Cosmochimica Acta* **2011**, 75(12), 3501-3513. https://doi.org/10.1016/j.gca.2011.03.026
331. Berger, E.L.; Keller, L.P.; Lauretta, D.S. An experimental study of the formation of cubanite ($CuFe_2S_3$) in primitive meteorites. *Meteoritics & Planetary Science* **2015**, 50(1), 1-14. https://doi.org/10.1111/maps.12399
332. Sarafian, A.R.; Nielsen, S.G.; Marshall, H.R.; Gaetani, G.A.; Righter, K.; Berger, E.L. The water and fluorine content of 4 Vesta. *Geochimica et Cosmochimica Acta* **2019**, 266, 568-581. https://doi.org/10.1016/j.gca.2019.08.023
333. Kojima, T.; Tomeoka, K. Indicators of aqueous alteration and thermal metamorphism on the CV parent body: Microtextures of a dark inclusion from Allende. *Geochimica et Cosmochimica Acta* **1996**, 60(14), 2651-2666. https://doi.org/10.1016/0016-7037(96)00116-0
334. Kikuchi, S.; Shibuya, T.; Abe, M.; Uematsu, K. Experimental chondrite–water reactions under reducing and low-temperature hydrothermal conditions: Implications for incipient aqueous alteration in planetesimals. *Geochimica et Comsochimica Acta* **2021**, *In press* https://doi.org/10.1016/j.gca.2021.11.006
335. Dyl, K.A.; Bischoff, A.; Ziegler, K.; Young, E.D.; Wimmer, K.; Bland, P.A. Early Solar System hydrothermal activity in chondritic asteroids on 1–10-year timescales. *Proc Natl Acad Sci U S A*. **2012**, 109(45), 18306-18311. https://doi.org/10.1073/pnas.1207475109
336. Putnis, A.; Austrheim, H. Fluid-induced processes: metasomatism and metamorphism. *Geofluids* **2010**, 10, 245-269. https://doi.org/10.1111/j.1468-8123.2010.00285.x
337. Yasui, M.; Tazawa, T.; Hashimoto, R.; Arakawa, M.; Ogawa, K. Impacts may provide heat for aqueous alteration and organic solid formation on asteroid parent bodies. *Communications Earth & Environment* **2021**, 2, 95. https://doi.org/10.5281/zenodo.4626228
338. Hirakawa, N.; Kebukawa, Y.; Furukawa, Y.; Kondo, M.; Nakano, H.; Kobayashi, K. Aqueous alteration without initial water: possibility of organic-induced hydration of anhydrous silicates in meteorite parent bodies. *Earth, Planets, and Space* **2021**, 73, 16. https://doi.org/10.1186/s40623-020-01352-6
339. Scott, E.R.D.; Keil, K.; Stoffler, D. Shock metamorphism of carbonaceous chondrites. *Geochimica et Cosmochimica Acta* **1992**, 56(12), 4281-4293. https://doi.org/10.1016/0016-7037(92)90268-N
340. Sharp, T.G.; DeCarli, P.S. Shock effects in meteorites. In *Meteorites and the early Solar System II*, Lauretta, D.S., McSween Jr., H.Y., Eds.; University of Arizona Press: Arizona, United States, 2006, pp. 653-677.
341. Bischoff, A.; Scott, E.R.D.; Metzler, K.; Goodrich, C.A. Nature and origins of meteoritic breccias. In *Meteorites and the early Solar System II*; Lauretta, D.S.; McSween Jr., H.Y., Eds.; University of Arizona Press, Arizona, United States, 2006, pp. 679-712.

342. Glavin, D.P.; Alexander, C.M'OD.; Aponte, J.C.; Dworkin, J.P.; Elsila, J.E., Yabuta, H. Chapter 3: The origin and evolution of organic matter in carbonaceous chondrites and links to their parent bodies. In *Primitive meteorites and asteroids: Physical, chemical and spectroscopic observations paving the way to exploration*, Abreu, N., Ed.; Elsevier; 2018, pp. 205-271. https://doi.org/10.1016/B978-0-12-813325-5.00003-3
343. Callahan, M.P.; Smith, K.E.; Cleaves II, J.; Ruzicka, J.; Stern, J.C.; Glavin, D.P.; House, C.H.; Dworkin, J.P. Carbonaceous meteorites contain a wide range of extraterrestrial nucleobases. *Proceedings of the National Academy of Sciences of the United States of America* **2011**, 108(34), 13995-13998. https://doi.org/10.1073/pnas.1106493108
344. Burton, A.S.; Stern, J.C.; Elsila, J.E.; Glavin, D.P.; Dworkin, J.P. Understanding prebiotic chemistry through the analysis of extraterrestrial amino acids and nucleobases in meteorites. *Chemical Society Reviews* **2012**, 41, 5459-5472. https://doi.org/10.1039/c2cs35109a
345. Elsila, J.E.; Aponte, J.C.; Blackmond, D.G.; Burton, A.S.; Dworkin, J.P.; Glavin, D.P. Meteoritic amino acids: Diversity in compositions reflects parent body histories. *ACS Central Science* **2016**, 2(6), 370-379. https://doi.org/10.1021/acscentsci.6b00074
346. Glavin, D.P.; McLain, H.L.; Dworkin, J.P.; Parker, E.T.; Elsila, J.E.; Aponte, J.C.; Simkus, D.N.; Pozarycki, C.I.; Graham, H.V.; Nittler, L.R.; Alexander, C.M.O'D. Abundant extraterrestrial amino acids in the primitive CM carbonaceous chondrite Asuka 12236. *Meteoritics & Planetary Science* **2020b**, 55(9), 1979-2006. https://doi.org/10.1111/maps.13560
347. Sephton, M.A. Organic compounds in carbonaceous chondrites. *Nat. Prod. Rep.* **2002**, 19, 292-311. https://doi.org/10.1039/b103775g
348. Ehrenfreund, P.; Glavin, D.P.; Botta, O.; Cooper, G.; Bada, J.L. Extraterrestrial amino acids in Orgueil and Ivuna: Tracing the parent body of CI type carbonaceous chondrites. *Proc Natl Acad Sci U S A* **2001**, 98(5), 2138-2141. https://doi.org/10.1073/pnas.051502898
349. Wächtershäuser, G. Pyrite formation, the first energy source for life: A hypothesis. *Systematic and Applied Microbiology* **1988**, 10(3), 207-210. https://doi.org/10.1016/S0723-2020(88)80001-8
350. Wächtershäuser, G. Groundworks for an evolutionary biochemistry: The iron-sulphur world. *Progress in Biophysics and Molecular Biology* **1992**, 58(2), 85-201. https://doi.org/10.1016/0079-6107(92)90022-X
351. Huber, C.; Wächtershäuser, G. α-hyydroxy and α-amino acids under possible Hadean, volcanic origin-of-life conditions. *Science* **2006**, 314(5799), 630-632. https://doi.org/10.1126/science.1130895
352. Yadav, M.; Kumar, R.; Krishnamurthy, R. Chemistry of abiotic nucleotide synthesis. *Chem. Rev* **2020**, 120(11), 4766-4805. https://doi.org/10.1021/acs.chemrev.9b00546
353. Weber, J.M.; Henderson, B.L.; LaRowe, D.E.; Goldman, A.D.; Perl, S.M.; Billings, K.; Barge, L.M. Testing abiotic reduction of NAD+ directly mediated by iron/sulfur minerals. *Astrobiology* **2021**, 22(1), 25-34. https://doi.org/10.1089/ast.2021.0035
354. Nguyen, L.A.; He, H.; Pham-Huy, C. Chiral drugs: An overview. *Int J Biomed Sci.* **2006**, 2(2), 85-100.
355. Bruylants, G.; Wouters, J.; Michaux, C. Differential scanning calorimetry in life science: Thermodynamics, stability, molecular recognition and application in drug design. *Curr Med Chem.* **2005**, 12, 2011–2020. https://doi.org/10.2174/0929867054546564
356. Gil-Av, E.; Feibush, B.; Charles-Sigler, R. Separation of enantiomers by gas liquid chromatography with an optically active stationary phase. *Tetrahedron Letters* **1966**, 7(10), 1009-1015. https://doi.org/10.1016/S0040-4039(00)70231-0
357. Grybinik, S.; Bosakova, Z. An overview of chiral separations of pharmaceutically active substances by HPLC (2018–2020). *Monatshefte für Chemie - Chemical Monthly* **2021**, 152, 1033-1043. https://doi.org/10.1007/s00706-021-02832-5
358. Labuta, J.; Ishihara, S.; Šikorský, T.; Futera, Z.; Shundo, A.; Hanyková, L.; Burda, J.V.; Ariga, K.; Hill, J.P. NMR spectroscopic detection of chirality and enantiopurity in referenced systems without formation of diastereomers. *Nature Communications* **2013**, 4, 2188. https://doi.org/10.1038/ncomms3188
359. Gottarelli, G.; Osipov, M.A.; Spada, G.P. A study of solvent effect on the optical rotation of chiral biaryls. *J. Phys. Chem.* **1991**, 95(9), 3879-3884. https://doi.org/10.1021/j100162a080
360. Langeveld-Voss, B.M.W.; Christiaans, M.P.T.; Janssen, R.A.J.; Meijer, E.W. Inversion of optical activity of chiral polythiophene aggregates by a change of solvent. *Macromolecules* **1998**, 31(19), 6702-6704. https://doi.org/10.1021/ma980813w
361. Thiemann, W.H-P.; Rosenbauer, H.; Meierhenrich, U.J. Conception of the 'chirality-experiment' on ESA's mission ROSETTA to comet P46/Wirtanen. *Advances in Space Research* **2001**, 27(2), 323-328. https://doi.org/10.1016/S0273-1177(01)00064-3
362. Freissinet, C.; Buch, A.; Sternberg, R.; Szopa, C.; Geffroy-Rodier, C.; Jelinek, C.; Stambouli, M. Search for evidence of life in space: analysis of enantiomeric organic molecules by N,N-dimethylformamide dimethylacetal derivative dependant gas chromatography-mass spectrometry. *J Chromatogr A* **2010**, 1217(5), 731-740. https://doi.org/10.1016/j.chroma.2009.11.009
363. Mahaffy, P.R.; Webster, C.R.; Cabane, M.; Conrad, P.G.; Coll, P., Atreya, S.K.; Arvey, R.; Barciniak, M.; Benna, M.; Bleacher, L.; Brinckerhoff, W.B.; Eigenbrode, J.L.; Carignan, D.; Cascia, M.; Chalmers, R.A.; Dworkin, J.P.; Errigo, T.; Everson, P.; Franz, H.; Farley, R.; Feng, S.; Frazier, G.; Freissinet, C.; Glavin, D.P.; Harpold, D.N.; Hawk, D.; Holmes, V.; Johnson, C.S.; Jones, A.; Jordan, P.; Kellogg, J.; Lewis, J.; Lyness, E.; Malespin, C.A.; Martin, D.K.; Maurer, J.; McAdam, A.C.; McLennan, D.; Nolan, T.J.; Noriega, M.; Pavlov, A.A.; Prats, B.; Raaen, E.; Sheinman, O.; Ming, D.W.; Morris, R.V.; Jones, J.; Gundersen, C.; Steele, A.; Wray, J.; Botta, O.; Leshin, L.A.; Owen, T.; Battel, S.; Jakosky, B.M.; Manning, H.; Squyers, S.; Navarro-González, R.; McKay, C.P.; Raulin, F.; Sternberg, R.; Buch, A.; Sorenson, P.; Kline-Schroder, R.; Coscia, D.; Szopa, C.; Teinturier, S.; Baffes, C.; Feldman, J.; Flesch, G.; Forouhar, S.; Garcia, R.; Keymeulen, D.; Woodward, S.; Block, B.P.; Arnett, K.; Miller, R.; Edmonson, C.; Gorevan, S.; Mumm, E. The Sample Analysis at Mars Investigation and Instrument Suite. *Space Science Reviews* **2012**, 170, 401–478. https://doi.org/10.1007/s11214-012-9879-z

364. Goesmann, F.; Brinckerhoff, W.B.; Raulin, F.; Goetz, W.; Danell, R.M.; Getty, S.A.; Siljeström, S.; Mißbach, H.; Steininger, H.; Arevalo Jr., R.D.; Buch, A.; Freissinet, C.; Grubisic, A.; Meierhenrich, U.J.; Pinnick, V.T.; Stalport, F.; Szopa, C.; Vago, J.L.; Lindner, R.; Schulte, M.D.; Brucato, J.R.; Glavin, D.P.; Grand, N.; Li, X.; van Amerom, F.H.W. The Mars Organic Molecule Analyzer (MOMA) instrument: Characterization of organic material in Martian sediments. *Astrobiology* **2017**, 17(6-7), 655-685. https://doi.org/10.1089/ast.2016.1551
365. Ulamec, S.; Goesmann, F.; Meierhenrich, U.J. Philae landing on comet 67P/Churyumov-Gerasimenko – Planned chirality measurements and ideas for the future. *Journal of Interdisciplinary Methodologies and Issues in Science* **2018**, 4, 1-11. https://doi.org/10.18713/JIMIS-230718-4-2
366. Sousa, E.P.; Tiritan, M.E.; Oliveira, R.; Afonso, C.M.M.; Cass, Q.B.; Pinto, M.M.M. Enantiomeric resolution of kielcorin derivatives by HPLC on polysaccharide stationary phases using multimodal elution. *Chirality* **2004**, 16(5), 279-285. https://doi.org/10.1002/chir.20031
367. Dossou, K.S.S.; Chiap, P.; Servais, A.C.; Fillet, M.; Crommen, J. Evaluation of chlorine containing cellulose-based chiral stationary phases for the LC enantioseparation of basic pharmaceuticals using polar non-aqueous mobile phases. *J. Sep Sci.* **2011**, 34(6), 617-622. https://doi.org/10.1002/jssc.201000774
368. Ianni, F.; Saluti, G.; Galarini, R.; Fiorito, S.; Sardella, R.; Natalini, B. Enantioselective high-performance liquid chromatography analysis of oxygenated polyunsaturated fatty acids. *Free Radic Biol Med*. **2019**, 144, 35-54. https://doi.org/10.1016/j.freeradbiomed.2019.04.038
369. Mangelings, D.; Vander Heyden, Y. Chiral separations in sub- and supercritical fluid chromatography. *J. Sep Sci* **2008**, 31(8), 1252-1273. https://doi.org/10.1002/jssc.200700564
370. West, C. Enantioselective separations with supercritical fluids - review. *Current Anal. Chem*. **2014**, 10, 99-120. https://doi.org/10.2174/1573411011410010009
371. Gübitz, G.; Schmid, M.G. Chiral separation principles in capillary electrophoresis. *Journal of Chromatography A* **1997**, 792(1-2), 179-225. https://doi.org/10.1016/S0021-9673(97)00871-6
372. Mathies, R.A.; Razu, M.E.; Kim, J.; Stockton, A.M.; Turin, P.; Butterworth, A. Feasibility of detecting bioorganic compounds in Enceladus plumes with the Enceladus Organic Analyzer. *Astrobiology* **2017**, 17(9), 902-912. https://doi.org/10.1089/ast.2017.1660
373. Zamuruyev, K.; Santos, M.S.F.; Mora, M.F.; Kurfman, E.A.; Noell, A.C.; Willis, P.A. Automated capillary electrophoresis system compatible with multiple detectors for potential in situ spaceflight missions. *Anal. Chem.* **2021**, 93(27), 9647-9655. https://doi.org/10.1021/acs.analchem.1c02119
374. Gübitz, G.; Schmid, M.G. Chiral separation by capillary electrochromatography. *Enantiomer* **2000**, 5(1), 5-11.
375. Wistuba, D.; Schurig, V. Recent progress in enantiomer separation by capillary electrochromatography. *Electrophoresis* **2000**, 21(18), 4136-4158. https://doi.org/10.1002/1522-2683(200012)21:18<4136::AID-ELPS4136>3.0.CO;2-1
376. Fanali, C.; Della Posta, S.; Fanali, S. Capillary electrochromatography applied to drug analysis. *Journal of Chromatography Open* **2021**, 1, 100015. https://doi.org/10.1016/j.jcoa.2021.100015
377. Kodama, S.; Yamamoto, A.; Iio, R.; Sakamoto, K.; Matsunaga, A.; Hayakawa, K. Chiral ligand exchange capillary electrophoresis using borate anion as a central ion. *Analyst* **2004**, 129(12),1238-1242. https://doi.org/10.1039/B406875K
378. Mu, X.; Qi, L.; Shen, Y.; Zhang, H.; Qiao, J.; Ma, H. A novel chiral ligand exchange capillary electrophoresis system with amino acid ionic liquid as ligand and its application in screening d-amino-acid oxidase inhibitors. *Analyst* **2012**, 137(18), 4235-4240. https://doi.org/10.1039/C2AN35753D
379. Liu, L.; Bao, P.; Qiao, J.; Zhang, H.; Qi, L. Chiral ligand exchange capillary electrophoresis with L-dipeptides as chiral ligands for separation of Dns-D,L-amino acids. *Talanta* **2020**, 217, 121069. https://doi.org/10.1016/j.talanta.2020.121069
380. Wang, F.; Khaledi, M.G. Chiral separations by nonaqueous capillary electrophoresis. *Anal. Chem.* **1996**, 68(19), 3460-3467. https://doi.org/10.1021/ac960537o
381. Limero, T.; Reese, E.; Trowbridge, J.; Hohman, R.; James, J.T. The Volatile Organic Analyzer (VOA) aboard the International Space Station. *SAE Technical Paper 2002-01-2407*, **2002**, https://doi.org/10.4271/2002-01-2407
382. Dwivedi, P.; Wu, C.; Matz, L.M.; Clowers, B.H.; Siems, W.F.; Hill Jr., H.H. Gas-phase chiral separations by ion mobility spectrometry. *Anal. Chem.* **2006**, 78(24), 8200-8206. https://doi.org/10.1021/ac0608772
383. Mie, A.; Jörntén-Karlsson, M.; Axelsson, B-O.; Ray, A.; Reimann, C.T. Enantiomer separation of amino acids by complexation with chiral reference compounds and high-field asymmetric waveform ion mobility spectrometry: Preliminary results and possible limitations. *Anal. Chem.* **2007**, 79(7), 2850-2858. https://doi.org/10.1021/ac0618627
384. Will, J.M.l; Behrens, A.; Macke, M.; Derrick Quales Jr., C.; Karst, U. Automated chiral analysis of amino acids based on chiral derivatization and trapped ion mobility–mass spectrometry. *Anal. Chem.* **2021**, 93(2), 878-885. https://doi.org/10.1021/acs.analchem.0c03481
385. Brodbelt, J.S. Photodissociation mass spectrometry: new tools for characterization of biological molecules. *Chemical Society Reviews* **2014**, 43(8), 2757-2783. https://doi.org/10.1039/C3CS60444F
386. Fujihara, A.; Maeda, N.; Doan, T.N.; Hayakawa, S. Enantiomeric excess determination for monosaccharides using chiral transmission to cold gas-phase tryptophan in ultraviolet photodissociation. *Journal of The American Society for Mass Spectrometry* **2017**, 28(2), 224-228. https://doi.org/10.1007/s13361-016-1519-5
387. Shi, Y.; Zhou, M.; Zhang, K.; Ma, L.; Kong, X. Chiral differentiation of non-covalent diastereomers based on multichannel dissociation induced by 213-nm ultraviolet photodissociation. *Journal of The American Society for Mass Spectrometry* **2019**, 30, 2297-2305. https://doi.org/10.1007/s13361-019-02302-7

388. Koehbach, J.; Gruber, C.W.; Becker, C.; Kreil, D.P.; Jilek, A. MALDI TOF/TOF-based approach for the identification of D-amino acids in biologically active peptides and proteins. *J. Proteome Res*. **2016**, 15(5). 1497-1496. https://doi.org/10.1021/acs.jproteome.5b01067
389. Casy, A.F.; Mercer, A.D. Application of cyclodextrins to chiral analysis by 1H NMR spectroscopy. *Magnetic Resonance in Chemistry* **1988**, 26(9), 765-774. https://doi.org/10.1002/mrc.1260260908
390. Kubo, Y.; Maeda, S.; Tokita, S.; Kubo, M. Colorimetric chiral recognition by a molecular sensor. *Nature* **1996**, 382, 522-524. https://doi.org/10.1038/382522a0
391. Tsubaki, K.; Nuruzzaman, M.; Kusumoto, T.; Hayashi, N.; Bin-Gui, W.; Fuji, K. Visual enantiomeric recognition using chiral phenolphthalein derivatives. *Org. Lett*. **2001**, 3(25), 4071-4073. https://doi.org/10.1021/ol016825a
392. Wirz, R.; Bürgi, T.; Baiker, A. Probing enantiospecific interactions at chiral solid−liquid interfaces by absolute configuration modulation infrared spectroscopy. *Langmuir* **2003**, 19(3), 785-792. https://doi.org/10.1021/la026568y
393. Hinsmann, P.; Arce, L.; Svasek, P.; Lämmerhofer, M.; Lendl, B. Separation and on-line distinction of enantiomers: a non-aqueous capillary electrophoresis Fourier transform infrared spectroscopy study. *Appl Spectrosc.* **2004**, 58(6), 662-666. https://doi.org/10.1366/000370204873042
394. Giorgio, E.; Viglione, R.G.; Zanasi, R.; Rosini, C. Ab initio calculation of optical rotatory dispersion (ORD) curves: A simple and reliable approach to the assignment of the molecular absolute configuration. *J. Am. Chem. Soc.* **2004**, 126(40), 12968-12976. https://doi.org/10.1021/ja046875l
395. Qiu, S.; De Gussem, E.; Tehrani, K.A.; Sergeyev, S.; Bultinck, P.; Herrebout, W. Stereochemistry of the Tadalafil diastereoisomers: A critical assessment of vibrational circular dichroism, electronic circular dichroism, and optical rotatory dispersion. *J. Med. Chem.* **2013**, 56(21), 8903-8914. https://doi.org/10.1021/jm401407w
396. Beaulieu, S.; Comby, A.; Descamps, D.; Fabre, B.; Garcia, G.A.; Géneaux, R.; Harvey, A.G.; Légaré, F.; Mašín, Z.; Nahon, L.; Ordonez, A.F.; Petit, S.; Pons, B.; Mairesse, Y.; Smirnova, O.; Blanchet, B. Photoexcitation circular dichroism in chiral molecules. *Nature Physics* **2018**, 14, 484-489. https://doi.org/10.1038/s41567-017-0038-z
397. Kneer, L.M.; Roller, E-M.; Besteiro, L.V.; Schreiber, R.; Govorov, A.O.; Liedl, T. Circular dichroism of chiral molecules in DNA-assembled plasmonic hotspots. *ACS Nano* **2018**, 12(9), 9110-9115. https://doi.org/10.1021/acsnano.8b03146
398. Vestler, D.; Ben-Moshe, A.; Markovich, G. Enhancement of circular dichroism of a chiral Material by dielectric nanospheres. *J. Phys. Chem. C* **2019**, 123(8), 5017-5022. https://doi.org/10.1021/acs.jpcc.8b10975
399. Bégin, J-L.; Alsaawy, M.; Bhardwaj, R. Chiral discrimination by recollision enhanced femtosecond laser mass spectrometry. *Sci Rep* **2020**, 10, 14074. https://doi.org/10.1038/s41598-020-71069-9
400. Sparks, W.; Hough, J.H.; Germer, T.; Robb, F.; Kolokolova, L. Remote sensing of chiral signatures on Mars. *Planetary and Space Science* **2012**, 72(1),111-115. https://doi.org/10.1016/j.pss.2012.08.010
401. Sofikitis, D.; Bougas, L.; Katsoprinakis, G.E.; Spiliotis, A.K.; Loppinet, B.; Rakitzis, T.P. Evanescent-wave and ambient chiral sensing by signal-reversing cavity ringdown polarimetry. *Nature* **2014**, 514, 76-79. https://doi.org/10.1038/nature13680
402. Li, L.; Wang, J.; Kang, L.; Liu, W.; Yu, L.; Zheng, B.; Brongersma, M.L.; Werner, D.H.; Lan, S.; Shi, Y.; Xu, Y.; Wang, X. Monolithic full-Stokes near-infrared polarimetry with chiral plasmonic metasurface integrated graphene–silicon photodetector. *ACS Nano* **2020**, 14(12), 16634-16642. https://doi.org/10.1021/acsnano.0c00724
403. Risley, D.S.; Strege, M.A. Chiral separations of polar compounds by hydrophilic interaction chromatography with evaporative light scattering detection. *Anal Chem*. **2000**, 72(8),1736-1739. https://doi.org/10.1021/ac9911490
404. Zhang, T.; Nguyen, D.; Franco, P. Use of evaporative light scattering detector in the detection and quantification of enantiomeric mixtures by HPLC. *J. Sep Sci* **2006**, 29(10), 1517-1524. https://doi.org/10.1002/jssc.200600128
405. Bradshaw, D.S.; Andrews, D.L. Laser optical separation of chiral molecules. *Optics Letters* **2015**, 40(4), 677-680. https://doi.org/10.1364/OL.40.000677
406. Solomon, M.L.; Saleh, A.A.E.; Poulikakos, L.V.; Abendroth, J.M.; Tadesse, L.F.; Dionne, J.A. Nanophotonic platforms for chiral sensing and separation. *Acc. Chem. Res.* **2020**, 53, 588-598. https://doi.org/10.1021/acs.accounts.9b00460
407. Cook, C.; Bryne, S.; Drouet d'Aubigny, C.; Viola, D.; Mikucki, J.; Ellis, W. Detection limits for chiral amino acids using a polarization camera. *The Planetary Science Journal* **2020**, 1(2), 46. https://doi.org/10.3847/PSJ/abae57
408. Chiu, M.H.; Prenner, E.J. Differential scanning calorimetry: An invaluable tool for a detailed thermodynamic characterization of macromolecules and their interactions. *J. Pharm. Bioallied Sci*. **2011**, 3(1), 39-59. https://doi.org/10.4103/0975-7406.76463
409. Marcellos, C.F.C.; Durand, H.; Kwon, J.S., Barreto Jr., A.G.; da Cunha Lage, P.L.; de Souza Jr., M.B.; Secchi, A.R.; Christofides, P.D. Optimal enantiomer crystallization operation using ternary diagram information. *Computer Aided Chemical Engineering* **2018**, 44, 499-504. https://doi.org/10.1016/B978-0-444-64241-7.50078-1
410. Lam, W.H.; Ng, K.M. Diastereomeric salt crystallization synthesis for chiral resolution of ibuprofen. *AIChE Journal* **2007**, 53(2), 429-437. https://doi.org/10.1002/aic.11087
411. Pham, X-H.; Kim, J-M.; Chang, S-M.; Kim, I.; Sim, W.K. Enantioseparation of D/L-mandelic acid with L-phenylalanine in diastereomeric crystallization. *Journal of Molecular Catalysis B: Enzymatic* **2009**, 60(1-2), 87-92. https://doi.org/10.1016/j.molcatb.2008.12.023
412. Simon, M.; Wood, B.; Ferguson, S.; Glennon, B.; Jones, R.C. Diastereomeric salt crystallization of chiral molecules via sequential coupled-Batch operation. *AIChE Journal* **2018**, 65(2), 604-616. https://doi.org/10.1002/aic.16466
413. Robinson, D.E.J.E.; Bull, S.D. Kinetic resolution strategies using non-enzymatic catalysts. *Tetrahedron: Asymmetry* **2003**, 14(11), 1407-1446. https://doi.org/10.1016/S0957-4166(03)00209-X

414. Mousaw, P.; Saranteas, K.; Prytko, B. Crystallization improvements of a diastereomeric kinetic resolution through understanding of secondary nucleation. *Org. Process Res. Dev.* **2008**, 12(2), 243-248. https://doi.org/10.1021/op700276w
415. Imayoshi, A.; Lakshmi, B.V.; Ueda, Y.; Yoshimura, T.; Matayoshi, A.; Furuta, T.; Kawabata, T. Enantioselective preparation of mechanically planar chiral rotaxanes by kinetic resolution strategy. *Nature Communications* **2021**, 12, 404. https://doi.org/10.1038/s41467-020-20372-0
416. Skelley, A.M.; Mathies, R.A. Chiral separation of fluorescamine-labeled amino acids using microfabricated capillary electrophoresis devices for extraterrestrial exploration. *J. Chromatogr A* **2003**, 1021, 191-199. https://doi.org/10.1016/j.chroma.2003.08.096
417. Pu, L. Fluorescence of organic molecules in chiral recognition. *Chem Rev.* **2004**, 104(3), 1687-1716. https://doi.org/10.1021/cr030052h
418. Ohrui, H.; Kato, R.; Kodaira, T.; Shimizu, H.; Akasaka, K.; Kitahara, T. Development of highly potent D-glucosamine-based chiral fluorescent labeling reagents and a microwave-assisted beta-selective glycosidation of a methyl glycoside reagent. *Biosci Biotechnol Biochem.* **2005**, 69(5),1054-1057. https://doi.org/10.1271/bbb.69.1054
419. Wei, W.; Qu, K.; Ren, J.; Qu, X. Chiral detection using reusable fluorescent amylose-functionalized graphene. *Chem. Sci.* **2011**, 2, 2050-2056. https://doi.org/10.1039/C1SC00308A
420. Creamer, J.S.; Mora, M.F.; Noell, A.C.; Willis, P.A. Long-term thermal stability of fluorescent dye used for chiral amino acid analysis on future spaceflight missions. *Electrophoresis* **2019**, 40(23-24), 3117-3122. https://doi.org/10.1002/elps.201900268
421. Miller, S.L;, Van Trump, J.E. The Strecker synthesis in the primitive ocean. In *Origin of Life*, Wolman, Y., Ed.; Springer: Dordrecht, 1981, pp. 135-141. https://doi.org/10.1007/978-94-009-8420-2_18
422. Rodriguez, L.E.; Altari, T.; Hermis, N.Y.; Jia, T.Z.; Roche, T.P.; Steller, L.H.; Weber, J.M. Astrobiology Primer 3.0 Chapter 4: A geological and chemical context for the origins of life on early Earth. *Astrobiology* **2022,** *In review*
423. Butlerov, A. Bildung einer zuckerartigen Substanz durch Synthese. *Liebigs Ann Chem* **1861** 120(3),295-298. https://doi.org/10.1002/jlac.18611200308
424. Sharma, M.; Mangas-Sanchez, J.; Turner, N.J.; Grogan, G. NAD(P)H-dependent dehydrogenases for the asymmetric reductive amination of ketones: Structure, mechanism, evolution and application. *Advanced Synthesis & Catalysis* **2017**, 359(12), 2011-2025. https://doi.org/10.1002/adsc.201700356
425. Stubbs, R.T.; Yadav, M.; Krishnamurthy, R.; Springsteen, G. A plausible metal-free ancestral analogue of the Krebs cycle composed entirely of α-ketoacids. *Nature Chemistry* **2020**, 12, 1016-1022. https://doi.org/10.1038/s41557-020-00560-7
426. Kumar A.; Sharma, S.; Maurya, R.A. Single nucleotide-catalyzed biomimetic reductive amination. *Advanced Synthesis & Catalysis* **2010**, 352(13), 2227-2232. https://doi.org/10.1002/adsc.201000178
427. Storer, R.I.; Carrera, D.E.; Ni, Y.; MacMillan, D.W.C. Enantioselective organocatalytic reductive amination. *J. Am. Chem. Soc.* **2006**, 128(1), 84-86. https://doi.org/10.1021/ja057222n
428. Tripathi, R.P.; Verma, S.S.; Pandey, J.; Tiwari, V.K. Recent development on catalytic reductive amination and applications. *Current Organic Chemistry* **2008**, 12(13), 1092-1115. https://doi.org/10.2174/138527208785740283
429. Afanasyev, O.I.; Kuchuk, E.; Usanov, D.L.; Chusov, D. Reductive amination in the synthesis of pharmaceuticals. *Chem. Rev.* **2019**, 119(23), 11857-11911. https://doi.org/10.1021/acs.chemrev.9b00383
430. Strecker, A. Ueber einen neuen aus Aldehyd - Ammoniak und Blausäure entstehenden Körper. *Justus Liebigs Annalen der Chemie* **1854**, 91(3), 349-351. https://doi.org/10.1002/jlac.18540910309
431. Harada, K. Asymmetric synthesis of α-amino-acids by the Strecker synthesis. *Nature* **1963**, 200, 1201. https://doi.org/10.1038/2001201a0
432. Gröger, H. Catalytic enantioselective Strecker reactions and analogous syntheses. *Chem. Rev.* **2003**, 103(8), 2795-2828. https://doi.org/10.1021/cr020038p
433. Krishnamurthy, R.; Pulletikurti, S.; Yadav, M.; Springsteen, G. Prebiotic synthesis of α-amino acids and orotate from α-ketoacids potentiates transition to extant metabolic pathways. **2021** *In Review*. https://doi.org/10.21203/rs.3.rs-870237/v1
434. Davis, F.A.; Reddy, R.E.; Portonovo, P.S. Asymmetric strecker synthesis using enantiopure sulfinimines: A convenient synthesis of α-amino acids. *Tetrahedron Letters* **1994**, 35(50), 9351-9354. https://doi.org/10.1016/S0040-4039(00)78540-6
435. Iyer, M.S.; Gigstad, K.M.; Namdev, N.D.; Lipton, M. Asymmetric catalysis of the Strecker amino acid synthesis by a cyclic dipeptide. *Amino Acids* **1996**, 11, 259-268. https://doi.org/10.1007/BF00807935
436. Aiba, S.; Takamatsu, N.; Sasai, T.; Tokunaga, Y.; Kawasaki, T. Replication of α-amino acids via Strecker synthesis with amplification and multiplication of chiral intermediate aminonitriles. *Chemical Communications* **2016**, 52(72), 10834-10837. https://doi.org/10.1039/c6cc05544c
437. Miyagawa, S.; Yoshimura, K.; Yamazaki, Y.; Takamatsu, N.; Kuraish, T.; Aiba, S.; Tokunaga, Y.; Kawasaki, T. Asymmetric Strecker reaction arising from the molecular orientation of an achiral imine at the single-crystal face: Enantioenriched L- and D-amino acids. *Angew. Chem. Int. Ed.* **2016**, 56(4), 1055-1058. https://doi.org/10.1002/anie.201611128
438. Legnani, L.; Darù, A.; Jones, A.X.; Blackmond, D.G. Mechanistic insight into the origin of stereoselectivity in the ribose-mediated Strecker synthesis of alanine. *J. Am. Chem. Soc.* **2021**, 143(20), 7852-7858. https://doi.org/10.1021/jacs.1c03552
439. Jeilani, Y.A.; Nguyen, M.T. Autocatalysis in formose reaction and formation of RNA nucleosides. *J. Phys. Chem. B* **2020**, 124(50), 11324-11336. https://doi.org/10.1021/acs.jpcb.0c07070
440. Cleaves, H.J.; Formose reaction. In *Encyclopedia of Astrobiology*; Gargaud, M. et al. Eds.; Springer: Berlin, Heidelberg, Germany, 2011. https://doi.org/10.1007/978-3-642-11274-4_587

441. Fialho, D.M.; Clarke, K.C.; Moore, M.K.; Schuster, G.B.; Krishnamurthy, R.; Hud, N.V. Glycosylation of a model proto-RNA nucleobase with non-ribose sugars: implications for the prebiotic synthesis of nucleosides. *Organic & Biomolecular Chemistry* **2018**, 16, 1263-1271. https://doi.org/10.1039/C7OB03017G
442. Omran, A.; Menor-Salvan, C.; Springsteen, G.; Pasek, M. The messy alkaline formose reaction and its link to metabolism. *Life (Basel)* **2020**, 10(8), 125. https://doi.org/10.3390/life10080125
443. Mizuno, T., Mori, T.; Shiomi, N.; Nakatsuji, H. Studies on synthesis and utilization of formose Part I. *J. Agr. Chem. Soc. Japan* **1970**, 44(7), 324-331. https://doi.org/10.1271/nogeikagaku1924.44.324
444. Shigemasa, Y.; Nagae, O.; Sakazawa, C.; Nakashima, R.; Matsuura, T. Formose reactions. 5. A selective formose reaction. *J. Am. Chem. Soc.* **1978**, 100(4), 1309-1310. https://doi.org/10.1021/ja00472a056
445. SMatsumoto, T.; Inoue, S. Formose reactions. Part 3. Selective formose reaction catalyzed by organic bases. *Journal of the Chemical Society, Perkin Transactions 1* **1982**, 1, 1975-1979. https://doi.org/10.1039/P19820001975
446. Kopetzki, D.; Antonietti, M. Hydrothermal formose reaction. *New Journal of Chemistry* **2011** 35, 1787-1794. https://doi.org/10.1039/C1NJ20191C
447. Lambert, J.B.; Gurusamy-Thangavelu, S.A.; Ma, K. The silicate-mediated formose reaction: Bottom-up synthesis of sugar silicates. *Science* **2010**, 327(5968), 984-986. https://doi.org/10.1126/science.1182669
448. Eschenmoser, A. On a hypothetical generational relationship between HCN and constituents of the reductive citric acid cycle. *Chem. Biodivers.* **2007**, 4(4),554-573. https://doi.org/10.1002/cbdv.200790050
449. Stovbun, S.V.; Skoblin, A.A.; Zanin, A.M.; Tverdislov, V.A.; Taran, O.P.; Parmon, V.N. Formation of chiral structures in UV-initiated formose reaction. *Physical Chemistry* **2018**, 479, 57-60. https://doi.org/10.1134/S001250161803003X
450. Breslow, R.; Cheng, Z-L. L-amino acids catalyze the formation of an excess of D-glyceraldehyde, and thus of other D sugars, under credible prebiotic conditions. *Proc Natl Acad Sci U S A* **2010**, 107(13), 5723-5725. https://doi.org/10.1073/pnas.1001639107
451. Burroughs, L.; Clarke, P.A.; Forintos, H.; Gilks, J.A.R.; Hayes, C.J.; Vale, M.E.; Wade, W.; Zbytniewski, M. Asymmetric organocatalytic formation of protected and unprotected tetroses under potentially prebiotic conditions. *Organic & Biomolecular Chemistry* **2012**, 10(8), 1565-1570. https://doi.org/10.1039/C1OB06798B
452. Bolm, C.; Mocci, R.; Schumacher, C.; Turberg, M.; Puccetti, F.; Hernández, J.G. Mechanochemical activation of iron cyano complexes: A prebiotic impact scenario for the synthesis of α-amino acid derivatives. *Angewandte Chemie* **2018**, 130(9), 2447-2450. https://doi.org/10.1002/ange.201713109
453. Eguaogie, O.; Vyle, J.S.; Conlon, P.F.; Gîlea, M.A.; Liang, Y. Mechanochemistry of nucleosides, nucleotides and related materials. *Beilstein J. Org. Chem.* **2018**, 14, 955-970. https://doi.org/10.3762/bjoc.14.81
454. Lamour, S.; Pallmann, S.; Haas, M.; Trapp, O. Prebiotic sugar formation under nonaqueous conditions and mechanochemical acceleration. *Life* **2019**, 9, 52. https://doi.org/10.3390/life9020052
455. Stolar, T.; Grubešić, S.; Cindro, N.; Meštrović, E.; Užarević, K.; Hernández, J.G. Mechanochemical prebiotic peptide bond formation. *Angew. Chem. Int. Ed.* **2021**, 60(23), 12727-12731. https://doi.org/10.1002/ange.202100806
456. Porcheddu, A.; Colacino, E.; De Luca, L.; Delogu, F. Metal-mediated and metal-catalyzed reactions under mechanochemical conditions. *ACS Catal.* **2020**, 10(15), 8344-8394. https://doi.org/10.1021/acscatal.0c00142
457. Goldanskii, V.I. Nontraditional pathways of extraterrestrial formation of prebiotic matter. *J. Phys. Chem. A* **1997**, 101(19), 3424-3432. https://doi.org/10.1021/jp970042i
458. Rodríguez, B.; Bruckmann, A.; Bolm, C. A highly efficient asymmetric organocatalytic Aldol reaction in a ball mill. *Chemistry A European Journal* **2007**, 13(17), 4710-4722. https://doi.org/10.1002/chem.200700188
459. Mateti, S.; Mathesh, M.; Liu, Z.; Tao, T.; Ramireddy, T.; Glushenkov, A.M.; Yang, W,; Chen, Y.I. Mechanochemistry: A force in disguise and conditional effects towards chemical reactions. *Chemical Communications* **2021**, 57(9), 1080-1092. https://doi.org/10.1039/D0CC06581A
460. Fiss, B.G.; Richard, A.J.; Friščić, T.; Moores, A. Mechanochemistry for sustainable and efficient dehydrogenation/hydrogenation. *Canadian Journal of Chemistry* **2020**, 99(2), 93-112. https://doi.org/10.1139/cjc-2020-0408
461. Baig, R.B.N.; Varma, R.S. Alternative energy input: mechanochemical, microwave and ultrasound-assisted organic synthesis. *Chem. Soc. Rev.* **2012**, 41(4), 1559-1584. https://doi.org/10.1039/C1CS15204A
462. Jiménez-González, C.; Constable, D.J.C.; Ponder, C.S. Evaluating the "Greenness" of chemical processes and products in the pharmaceutical industry—a green metrics primer. *Chem. Soc. Rev*. **2012**, 41(4), 1485-1498. https://doi.org/10.1039/C1CS15215G
463. Do, J-L.; Friščić, T. Mechanochemistry: A force of synthesis. *ACS Cent. Sci.* **2017**, 3(1), 13-19. https://doi.org/10.1021/acscentsci.6b00277
464. Achar, T.K.; Bose, A.; Mal, P. Mechanochemical synthesis of small organic molecules. *Beilstein J. Org. Chem.* **2017** 13, 1907-1931. https://doi.org/10.3762/bjoc.13.186
465. Baláž, P.; Baláž M.; Achimovičová, M.; Bujňáková, Z.; Dutková, E. Chalcogenide mechanochemistry in materials science: insight into synthesis and applications (a review). *Journal of Materials Science* **2017**, 52, 11851-11890. https://doi.org/10.1007/s10853-017-1174-7
466. Chyba, C.F.; Thomas, P.J.; Brookshaw, L.; Sagan, C. Cometary delivery of organic molecules to the early Earth. *Science* **1990**, 249(4967), 366-373. https://doi.org/10.1126/science.11538074
467. Chyba, C.; Sagan, C. Endogenous production, exogenous delivery and impact-shock synthesis of organic molecules: an inventory for the origins of life. *Nature* **1992**, 355, 125-132. https://doi.org/10.1038/355125a0

468. Bernstein, M. Prebiotic materials from on and off the early Earth. *Philos Trans R Soc Lond B Biol Sci*. **2006**, 361(1474), 1689-1702. https://doi.org/10.1098/rstb.2006.1913
469. Pierazzo, E.; Chyba, C. Impact delivery of prebiotic organic matter to planetary surfaces. In *Comets and the origin and evolution of life. Advances in astrobiology and biogeophysics*, Thomas P.J., Hicks R.D., Chyba C.F., McKay C.P., Eds.; Springer, Berlin, Heidelberg; 2006, pp. 137-168. https://doi.org/10.1007/3-540-33088-7_5
470. Hörz, F.; Cintala, M.J. Impact experiments related to the evolution of planetary regoliths. *Meteoritics & Planetary Science* **1997**, 32, 179-209. https://doi.org/10.1111/J.1945-5100.1997.TB01259.X
471. Hörz, F.; Basilevsky, A.T.; Head, J.W.; Cintala, M.J. Erosion of lunar surface rocks by impact processes: A synthesis. *Planet Space Sci.* **2020**, 194, 105105. https://doi.org/10.1016/j.pss.2020.105105
472. Peterson, E.; Hörz, F.; Chang, S. Modification of amino acids at shock pressures of 3.5 to 32 GPa. *Geochim Cosmochim Ac* **1997**, 61(18), 3937-3950. https://doi.org/10.1016/s0016-7037(97)00192-0
473. Martins, Z.; Price, M.C.; Goldman, N.; Sephton, M.A.; Burchell, M.J. Shock synthesis of amino acids from impacting cometary and icy planet surface analogues. *Nature Geoscience* **2013**, 6, 1045-1049. https://doi.org/10.1038/ngeo1930
474. McCaffrey, V.P.; Zellner, N.E.B.; Waun, C.; Bennett, E.R.; Karl, E.K. Reactivity and survivability of glycolaldehyde in simulated meteorite impact experiments. *Orig Life Evol Biosph*. **2014**, 44(1), 29-42. https://doi.org/10.1007/s11084-014-9358-5
475. Sugahara, H.; Mimura, K. Shock-induced pyrolysis of amino acids at ultra high pressures ranged from 3.2 to 35.3 GPa. *Journal of Analytical and Applied Pyrolysis* **2014a**, 108, 170-175. https://doi.org/10.1016/j.jaap.2014.05.003
476. Sugahara, H.; Mimura, K. Glycine oligomerization up to triglycine by shock experiments simulating comet impacts. *Geochemical Journal* **2014b**, 48, 51-62. https://doi.org/10.2343/GEOCHEMJ.2.0285
477. Sugahara, H.; Mimura, K. Peptide synthesis triggered by comet impacts: A possible method for peptide delivery to the early Earth and icy satellites. *Icarus* **2015**, 257, 103-112. https://doi.org/10.1016/j.icarus.2015.04.029
478. Frantseva, K.; Mueller, M.; ten Kate, I.L.; van der Tak, F.F.S.; Greenstreet, S. Delivery of organics to Mars through asteroid and comet impacts. *Icarus* **2018**, 309, 125-133. https://doi.org/10.1016/j.icarus.2018.03.006
479. Jaramillo-Botero, A.; Cable, M.L.; Hofmann, A.E.; Malaska, M.; Hodyss, R.; Lunine, J. Understanding hypervelocity sampling of biosignatures in space missions. Astrobiology 2020, 21(4), 421-442. http://doi.org/10.1089/ast.2020.2301
480. Klenner, F.; Postberg, F.; Hillier, J.; Khawaja, N.; Cable, M.L.; Abel, B.; Kempf, S.; Glein, C.R.; Lunine, J.I.; Hodyss, R.; Reviol, R.; Stolz, F. Discriminating abiotic and biotic fingerprints of amino acids and fatty acids in ice grains relevant to ocean worlds. *Astrobiology* **2020**, 20(10), 1168-1184. http://doi.org/10.1089/ast.2019.2188
481. Des Marais, D.J.; Nuth III, J.A.; Allamandola, L.J.; Boss, A.P.; Farmer, J.D.; Hoehler, T.M.; Jakosky, B.M.; Meadows, V.S.; Pohorille, A.; Runnegar, B.; Spormann, A.M. The NASA Astrobiology Roadmap. *Astrobiology* **2008**, 8(4), 715-730. https://doi.org/10.1089/ast.2008.0819
482. Beegle, L.W.; Bhartia, R.; White, M.; DeFlores, L.; Abbey, W.; Wu, Y-H.; Cameron, B.; Moore, J.; Fries, M.; Burton, A.; Edgett, K.S.; Ravine, M.A.; Hug, W.; Reid, R.; Nelson, T.; Clegg, S.; Wiens, R.; Asher, S.; Sobron, P. SHERLOC: Scanning Habitable Environments with Raman & Luminescence for Organics & Chemicals. Proceedings of the IEEE Aerospace Conference, Big Sky, Montana, USA, 2015, https://doi.org/10.1109/AERO.2015.7119105
483. Bhartia, R.; Beegle, L.W.; DeFlores, L.; Abbey, W.; Razzell Hollis, J.; Uckert, K.; Monacelli, B.; Edgett, K.S.; Kennedy, M.R.; Sylvia, M.; Aldrich, D.; Anderson, M.; Asher, S.A.; Bailey, Z.; Boyd, K.; Burton, A.S.; Caffrey, M.; Calaway, M.J.; Calvert, R.; Cameron, B.; Caplinger, M.A.; Carrier, B.L.; Chen, N.; Chen, A.; Clark, M.J.; Clegg, S.; Conrad, P.G.; Cooper, M.; Davis, K.N.; Ehlmann, B.; Facto, L.; Fries, M.D.; Garrison, D.H.; Gasway, D.; Ghaemi, F.T.; Graff, T.G.; Hand, K.P.; Harris, C.; Hein, J.D.; Heinz, N.; Herzog, H.; Hochberg, E.; Houck, A.; Hug, W.F.; Jensen, E.H.; Kah, L.C.; Kennedy, J.; Krylo, R.; Lam, J.; Lindeman, M.; McGlown, J.; Michel, J.; Miller, E.; Mills, Z.; Minitti, M.E.; Mok, F.; Moore, J.; Nealson, K.H.; Nelson, A.; Newell, R.; Nixon, B.E.; Nordman, D.A.; Nuding, D.; Orellana, S.; Pauken, M.; Peterson, G.; Pollock, R.; Quinn, H.; Quinto, C.; Ravine, M.A.; Reid, R.D.; Riendeau, J.; Ross, A.J.; Sackos, J.; Schnaffer, J.A.; Schwochert, M.; Shelton, M.O.; Simon, R.; Smith, C.L.; Sobron, P.; Steadman, K.; Steele, A.; Thiessen, D.; Tran, V.D.; Tsai, T.; Tuite, M.; Tung, E.; Wehbe, R.; Weinberg, R.; Wiener, R.H.; Wiens, R.C.; Williford, K.; Wollonciej, C.; Wu, Y-H.; Yingst, R.A.; Zan, J. Perseverance's Scanning Habitable Environments with Raman and Luminescence for Organics and Chemicals (SHERLOC) Investigation. *Space Sci Rev* **2021**, 217, 58. https://doi.org/10.1007/s11214-021-00812-z
484. Meierhenrich, U.J.; Thiemann, W.H.; Goesmann, F.; Roll, R.; Rosenbauer, H. Enantiomer separation of hydrocarbons in preparation for ROSETTA's "chirality-experiment". *Chirality* **2001**, 13(8), 454-457. https://doi.org/10.1002/chir.1061
485. Szopa, C.; Sternberg, R.; Coscia, D.; Raulin, F.; Vidal-Madjar, C.; Rosenbauer, H. Gas chromatography for in situ analysis of a cometary nucleus III. Multi-capillary column system for the cometary sampling and composition experiment of the Rosetta lander probe. *J. Chromatogr A*. **2002**, 953(1-2), 165-173. https://doi.org/10.1016/s0021-9673(02)00104-8
486. Bibring, J.-P.; Rosenbauer, H.; Boehnhardt, H.; Ulamec, S.; Biele, H.; Espinasees, S.; Feuerbacher, B.; Gaudon, P.; Hemmerich, P.; Kletzkine, P.; Moura, D.; Mugnuolo, R.; Nietner, G.; Pätz, B.; Roll, R.; Scheuerle, H.; Szegö, K.; Wittmann, K.; Philae Project Office; The Entire Philae Team9. The Rosetta lander ("Philae") investigations. *Space Science Reviews* **2007**, 128, 205-220. https://doi.org/10.1007/s11214-006-9138-2
487. Goesmann, F.; Rosenbauer, H.; Bredehöft, J.H.; Cabane, M.; Ehrenfreund, P.; Gautier, T.; Giri, C.; Krüger, H.; Le Roy, L.; MacDermott, A.J.; McKenna-Lawlor, S.; Meierhenrich, U.J.; Muñoz Caro, G.M.; Raulin, F.; Roll, R.; Steele, A.; Steininger, H.; Sternberg, R.; Szopa, C.; Thiemann, W.; Ulamec, S. Organic compounds on comet 67P/Churyumov-Gerasimenko revealed by COSAC mass spectrometry. *Science* **2015**, 349(6247). https://doi.org/10.1126/science.aab0689

488. Sephton, M.A.; Carter, J.N. The chances of detecting life on Mars. *Planetary and Space Science* **2015**, 112, 15-22. https://doi.org/10.1016/j.pss.2015.04.002
489. Fairén, A.G.; Parro, V.; Schulze-Makuch, D.; Whyte, L. Is searching for Martian life a priority for the Mars community? *Astrobiology* **2018**, 18(2), 101-107. https://doi.org/10.1089/ast.2017.1772
490. Carrier, B.L.; Beaty, D.W.; Meyer, M.A.; Blank, J.G.; Chou, L.; DasSharma, S.; Des Marais, D.J.; Eigenbrode, J.L.; Grefenstette, N.; Lanza, N.L.; Schuerger, A.C.; Schwender, P.; Smith, H.D.; Stoker, C.R.; Tarnas, J.D.; Webster, K.D.; Bakermans, C.; Baxter, B.K.; Bell, M.S.; Benner, S.A.; Bolivar Torres, H.H.; Boston, P.J.; Bruner, R.; Clark, B.C.; DasSharma, P.; Engelhart, A.E.; Gallegos, Z.E.; Garvin, Z.K.; Gasda, P.J.; Green, J.H.; Harris, R.L.; Hoffman, M.E.; Tieft, T.; Koeppel, A.H.D.; Lee, P.A.; Li, X.; Lynch, K.L.; Mackelprang, R.; Mahaffy, P.R.; Matthies, L.H.; Nellessen, M.A.; Newsom, H.E.; Northup, D.E.; O'Connor, B.R.W.; Perl, S.M.; Quinn, R.C.; Rowe, L.A.; Sauterey, B.; Schneegurt, M.A.; Schulze-Makuch, D.; Scuderi, L.A.; Spilde, M.N.; Stamenković, V.; Torres Celis, J.A.; Wade, V.B.D.; Walker, C.J.; Wiens, R.C.; Williams, A.J.; Williams, J.M.; Xu, J. Mars extant life: What's next? Conference Report. *Astrobiology* **2020**, 20(6), 785-814. https://doi.org/10.1089/ast.2020.2237
491. Steele, A.; McCubbin, F.M.; Fries, M.; Kater, L.; Boctor, Z.; Fogel, M.L.; Conrad, P.G.; Glamocija, M.; Spencer, M.; Morrow, A.L.; Hammond, M.R.; Zare, R.N.; Vicenzi, E.P.; Siljeström, S.; Bowden, R.; Herd, C.D.K.; Mysen, B.O.; Shirey, S.B.; Amudsen, H.E.F.; Treiman, A.H.; Bullock, E.S.; Jull, A.J.T. A reduced organic carbon component in Martian basalts. *Science* **2012**, 337(6091), 212-215. https://doi.org/10.1126/science.1220715
492. Steele, A.; McCubbin, F.M.; Fries, M.D. The provenance, formation, and implications of reduced carbon phases in Martian meteorites. *Meteoritics & Planetary Science* **2016**, 51(11), 2203-2225. https://doi.org/10.1111/maps.12670
493. Steele, A.; Benning, L.G.; Wirth, R.; Schreiber, A.; Araki, T.; McCubbin, F.M.; Fries, M.D.; Nittler, L.R.; Wang, J.; Hallis, L.J.; Conrad, P.G.; Conley, C.; Vitale, S.; O'Brien, A.C.; Riggi, V.; Rogers, K. Organic synthesis associated with serpentinization and carbonation on early Mars. *Science* **2022**, 375(6577), 172-177. https://doi.org/10.1126/science.abg7905
494. Grotzinger, J.P.; Crisp, J.; Vasavada, A.R.; Anderson, R.C.; Baker, C.J.; Barry, R.; Blake, D.F.; Conrad, P.; Edgett, K.S.; Ferdowski, B.; Gellert, R.; Gilbert, J.B.; Golombek, M.; Gómez-Elvira, J.; Hassler, D.M.; Jandura, L.; Litvak, M.; Mahaffy, P.; Maki, J.; Meyer, M.; Malin, M.C.; Mitrofanov, I.; Simmonds, J.J.; Vaniman, D.; Welch, R.V.; Wiens, R.C. Mars Science Laboratory mission and science investigation. *Space Science Reviews* **2012**, 170, 5-56. https://doi.org/10.1007/s11214-012-9892-2
495. Farley, K.A.; Williford, K.H.; Stack, K.M.; Bhartia, R.; Chen, A.; de la Torre, M.; Hand, K.; Goreva,Y.; Herd, C.D.K.; Hueso, R.; Liu, Y.; Maki, J.N.; Martinez, G.; Moeller, R.C.; Nelessen, A.; Newman, C.E.; Nunes, D.; Ponce, A.; Spanovich, N.; Willis, P.A.; Beegle, L.W.; Bell III, J.F.; Brown, A.J.; Hamran, S-E.; Hurowitz, J.A.; Maurice, S.; Paige, D.A.; Rodriguez-Manfredi, J.A.; Schulte, M.; Wiens, R.C. Mars 2020 mission overview. *Space Sci. Rev.* **2020**, 216, 142. https://doi.org/10.1007/s11214-020-00762-y
496. Millan, M.; Szopa, C.; Buch, A.; Cabane, M.; Teinturier, S.; Mahaffy, P.; Johnson, S.S. Performance of the SAM gas chromatographic columns under simulated flight operating conditions for the analysis of chlorohydrocarbons on Mars. *J Chromatogr A* **2019**, 1598, 183-195. https://doi.org/10.1016/j.chroma.2019.03.064
497. Quantin-Nataf, C.; Carter, J.; Mandon, L.; Thollot, P.; Balme, M.; Volat, M.; Pan, L.; Loizeau, D.; Millot, C.; Breton, S.; Dehouck, E.; Fawdon, P.; Gupta, S.; Davis, J.; Grindrod, P.M.; Pacifici, A.; Bultel, B.; Allemand, P.; Ody, A.; Lozach, L.; Broyer, J. Oxia Planum: The landing site for the ExoMars "Rosalind Franklin" rover mission: Geological context and prelanding interpretation. *Astrobiology* **2021,** 21(3), 345-366. http://doi.org/10.1089/ast.2019.2191
498. Vago, J.L.; Westall, F.; Pasteur Instrument Teams, Landing Site Selection Working Group, and Other Contributors, Coates, A.J.; Jaumann, R.; Korablev, O.; Ciarletti, V.; Mitrofanov, I.; Josset, J-L.; De Sanctis, M.C.; Bibring, J-P.; Rull, F.; Goesmann, F.; Steininger, H.; Goetz, W.; Brinckerhoff, W.; Szopa, C.; Raulin, F.; Westall, F.; Edwards, H.G.M.; Whyte, L.G.; Fairén, A.G.; Bibring, J-P.; Bridges, J.; Hauber, E.; Ori, G.G.; Werner, S.; Loizeau, D.; Kuzmin, R.O.; Williams, R.M.E.; Flahaut, J.; Forget, F.; Vago, J.L.; Rodionov, D.; Korablev, O.; Svedhem, H.; Sefton-Nash, E.; Kminek, G.; Lorenzoni, L.; Joudrier, L.; Mikhailov, V.; Zashchirinskiy, A.; Alexashkin, S.; Calantropio, F.; Merlo, A.; Poulakis, P.; Witasse, O.; Bayle, O.; Bayón, S.; Meierhenrich, U.; Carter, J.; García-Ruiz, J.M.; Baglioni, P.; Haldemann, A.; Ball, A.J.; Debus, A.; Lindner, R.; Haessig, F.; Monteiro, D.; Trautner, R.; Voland, C.; Rebeyre, P.; Goulty, D.; Didot, F.; Durrant, S.; Zekri, E.; Koschny, D.; Toni, A.; Visentin, G.; Zwick, M.; van Winnendael, M.; Azkarate, M.; Carreau, C.; and the ExoMars Project Team. Habitability on early Mars and the search for biosignatures with the ExoMars rover. *Astrobiology* **2017**, 17(6-7), 471-510. http://doi.org/10.1089/ast.2016.1533
499. Razzell Hollis, J.; Ireland, S.; Abbey, W.; Bhartia, R.; Beegle, L.W. Deep-ultraviolet Raman spectra of Mars-relevant evaporite minerals under 248.6 nm excitation. *Icarus* **2021**, 357, 114067. https://doi.org/10.1016/j.icarus.2020.114067
500. Abrahamsson, V.; Henderson, B.L.; Herman, J.; Zhong, F.; Lin, Y.; Kanik, I.; Nixon, C.A. Extraction and separation of chiral amino acids for life detection on ocean worlds without using organic solvents or derivatization. *Astrobiology* **2021**, 21(5), 575-586. https://doi.org/10.1089/ast.2020.2298
501. Foroughbakhshfasaei, M.; Dobó, M.; Boda, F.; Szabó, Z.; Tóth, G. Comparative chiral separation of thalidomide class of drugs using polysaccharide-type stationary phases with emphasis on elution order and hysteresis in polar organic mode. *Molecules* **2022**, 27(1), 111. https://doi.org/10.3390/molecules27010111
502. Gao, L.; Zhao, X.; Qin, S.; Dong, Q.; Hu, X.; Chu, H. A covalent organic framework for chiral capillary electrochromatography using a cyclodextrin mobile phase additive. *Chirality* **2022**, https://doi.org/10.1002/chir.23405
503. Li, X-L.; Han, Y.; Huang, Y.; Sun, X.; Xiao, S.; Min, J.Z. Highly sensitive novel fluorescent chiral probe possessing (S)-2-methylproline structures for the determination of chiral amino compounds by ultra-performance liquid chromatography with fluorescence: An application in the saliva of healthy volunteer. *Journal of Chromatography A* **2022**, 1661, 462672. https://doi.org/10.1016/j.chroma.2021.462672

504. Niu, X.; Yan, S.; Chen, J.; Li, H.; Wang, K. Enantioselective recognition of L/D-amino acids in the chiral nanochannels of a metal-organic framework. *Electrochimica Acta* **2022**, 405, 139809. https://doi.org/10.1016/j.electacta.2021.139809
505. Arevalo Jr., R.; Ni, Z.; Danell, R.M. Mass spectrometry and planetary exploration: A brief review and future projection. *Journal of Mass Spectrometry* **2020**, 55, e4454. https://doi.org/10.1002/jms.4454
506. Chou, L.; Mahaffy, P.; Trainer, M.; Eigenbrode, J.; Arevalo, R.; Brinckerhoff, W.; Getty, S.; Grefenstette, N.; Da Poian, V.; Fricke, G.M.; Kempes, C.R.; Marlow, J.; Sherwood Lollar, B.; Graham, H.; Stewart Johnson, S. Planetary mass spectrometry for agnostic life detection in the Solar System. *Front. Astron. Space Sci* **2021**, 8, 755100. https://doi.org/10.3389/fspas.2021.755100
507. Willis, P.A.; Creamer, J.S.; Mora, M.F. Implementation of microchip electrophoresis instrumentation for future spaceflight missions. *Anal. Bioanal. Chem.* **2015**, 407(23), 6939-6963. https://doi.org/10.1007/s00216-015-8903-z
508. Creamer, J.S.; Mora, M.F.; Willis, P.A. Enhanced resolution of chiral amino acids with capillary electrophoresis for biosignature detection in extraterrestrial samples. *Anal. Chem.* **2017**, 89(2), 1329-1337. https://doi.org/10.1021/acs.analchem.6b04338
509. Creamer, J.S.; Mora, M.F.; Willis, P.A. Stability of reagents used for chiral amino acid analysis during spaceflight missions in high-radiation environments. *Electrophoresis* **2018**, 39(22),2864-2871. https://doi.org/10.1002/elps.201800274
510. Dong, Z.; Ma, Y. Atomic-level handedness determination of chiral crystals using aberration-corrected scanning transmission electron microscopy. *Nature Communications* **2020**, 11, 1588. https://doi.org/10.1038/s41467-020-15388-5
511. Eigenbrode, J.L.; Gold, R.; Canham, J.S.; Schulze, E.; Davila, A.F.; Seas, A.; Errigo, T.; Kujawa, F.; Kusnierkiewicz, D.; Lorentson, C.; McKay, C. Contamination control for ultra-sensitive life-detection missions. *Front. Space Technol.* **2021**, 2, 734423. https://doi.org/10.3389/frspt.2021.734423
512. Spiers, E.M.; Weber, J.M.; Venigalla, C.; Annex, A.M.; Chen, C.P.; Lee, C.; Gray, P.C.; McIntyre, K.J.; Berdis, J.R.; Carberry Mogan, S.R.; do Vale Pereira, P.; Kumar, S.; O'Neill, W.; Czajka, E.A.; Johnson, P.E.; Pascuzzo, A.; Tallapragada, S.; Phillips, D.; Mitchell, K.; Nash, A.; Scully, J.; Lowes, L. Tiger: Concept study for a New Frontiers Enceladus habitability mission. *The Planetary Science Journal* **2021**, 2(5), 195. https://doi.org/10.3847/PSJ/ac19b7
513. Hendrickson, R.; Urbaniak, C.; Minich, J.J.; Aronson, H.S.; Martino, C.; Stepanauskas, R.; Knight, R.; Venkateswaran, K. Clean room microbiome complexity impacts planetary protection bioburden. *Microbiome* **2021**, 9, 238.
514. Glavin, D.P..; Dworkin, J.P.; Lupisella, M.; Kminek, G.; Rummel, J.D. Biological contamination studies of lunar landing sites: implications for future planetary protection and life detection on the Moon and Mars. International Journal of *Astrobiology* **2005**, 3(3), 265-271. https://doi.org/10.1017/S1473550404001958
515. Glavin, D.P.; Freissinet, C.; Miller, K.E.; Eigenbrode, J.L.; Brunner, A.E.; Buch, A.; Sutter, B.; Archer, P.D.; Atreya, S.K.; Brinckerhoff, W.B.; Cabane, M.; Coll, P.; Conrad, P.G.; Coscia, D.; Dworkin, J.P.; Franz, H.B.; Grotzinger, J.P.; Leshin, L.A.; Martin, M.G.; McKay, C.; Ming, D.W.; Navarro-González, R.; Pavlov, A.; Steele, A.; Summons, R.E.; Szopa, C.; Teinturier, S.; Mahaffy, P.R. Evidence for perchlorates and the origin of chlorinated hydrocarbons detected by SAM at the Rocknest aeolian deposit in Gale Crater. *JGR Planets* **2013**, 118(10), 1955-1973. https://doi.org/10.1002/jgre.20144
516. Miller, K.E.; Kotrc, B.; Summons, R.E.; Belmahdi, I.; Buch, A.; Eigenbrode, J.L.; Freissinet, C.; Glavin, D.P.; Szopa, C. Evaluation of the Tenax trap in the Sample Analysis at Mars instrument suite on the Curiosity rover as a potential hydrocarbon source for chlorinated organics detected in Gale Crater. *JGR Planets* **2015**, 120(8), 1446-1459. https://doi.org/10.1002/2015JE004825
517. Craven, E.; Winters, M.; Smith, A.L.; Lalime, E.; Mancinelli, R.; Shirey, B.; Schubert, W.; Schuerger, A.; Burgin, M.; Seto, E.P.; Hendry, M.; Mehta, A.; Bendarini, J.N.; Ruvkun, G. Biological safety in the context of backward planetary protection and Mars Sample Return: conclusions from the Sterilization Working Group. *International Journal of Astrobiology* **2021**, 20(1), 1-28. https://doi.org/10.1017/S1473550420000397
518. Longo, A.; Damer, B. Factoring origin of life hypotheses into the search for life in the Solar System and beyond. *Life (Basel)* **2020**, 10(5), 52. https://doi.org/10.3390/life10050052